Volume 10(4)
4th Quarter 1995

ISSN: 0127-7065

35

JOURNAL OF NATURAL RUBBER RESEARCH

Price

Malaysia:	*RM30 per Issue* *RM100 per Volume*
Other countries:	*US$15 per Issue* *US$50 per Volume*

JOURNAL OF NATURAL RUBBER RESEARCH

EDITORIAL BOARD

EDITORIAL COMMITTEE

Rubber Research Institute of Malaysia (RRIM)
Malaysian Rubber Research and Development Board (MRRDB)
Malaysian Rubber Producers' Research Association (MRPRA)

First published as the *Journal of the Rubber Research Institute of Malaya* in 1929.
Each volume of the *Journal of Natural Rubber Research* constitutes four issues published quarterly in March, June, September and December each year.

Published by the Rubber Research Institute of Malaysia
Printed by Cetaktama Sdn. Bhd.
1996

Contents

J. nat. Rubb. Res.
Volume 10(4), 1995

J. nat. Rubb. Res. **10(4)**, 218–227

The Friction of Various Rubber Articles Lubricated with Acid and Alkaline Water

S.C. RICHARDS* AND A.D. ROBERTS*#

Friction coefficients have been measured for commonly encountered uses of rubber, involving practical formulations and real surfaces. The aim was to see whether the water lubricated friction was sensitive to the acidity or alkalinity of the water. Measurements were made on fully compounded black- and silica-filled test sheets rubbed against glass, concrete and tarmac. Measurements were also made for windscreen wipers, running shoes and bicycle tyres. Results show that the friction in the presence of alkaline water (pH 11) is noticeably lower than for slightly acid water (pH 6). Observations indicate that it is possible to detect an influence of water pH on friction in practical situations as well as under laboratory conditions.

The purpose of this work was to measure the coefficient of friction for commonly encountered uses of rubber, involving practical formulations and real surfaces. The aim was to see whether under idealised conditions laboratory findings[1,2] on the effect of water pH on friction would be borne out in practice.

EXPERIMENTAL

The coefficient of sliding friction was measured using apparatus described in earlier communications[1,3]. Unless otherwise stated, measurements were made for the contact between a plane surface and a hemispherical rubber surface of diameter 37.5 mm (see *Figure 1*).

To find the coefficient of sliding friction between rubber and a hard substrate in lubricated contact, the bending of the leaf springs due to the frictional force was measured by a four-part strain gauge bridge, the output of which was amplified and recorded. The coefficient of friction, μ, is found from

$$\mu = \frac{Fd_2}{Wd_1}$$

where F is the friction force, W is the applied load, d_1 is the distance from the pivot to the point of loading, and d_2 is the distance from the pivot to the point of application of the load, as shown in *Figure 1* (in this work $d_1 = 0.1$ m, $d_2 = 0.23$ m).

The liquids used as lubricants were distilled water (pH 6) and buffer solutions at pH 6 and pH 11. The effect of friction reduction seen previously[1] occurred between pH 8 and pH 9, so the buffer solutions at pH 6 and pH 11 were chosen to be equally above and below this transition. The surfaces used in these tests were as described in *Table 1*. Details for the formulation and vulcanisation of BLACK, SILICA, TR and other rubbers are given in *Table 2*.

RESULTS

Friction Tests at Constant Speed

Friction measurements were made in dry contact, and lubricated with distilled water and the two buffer solutions. The sliding speed was 5.0 mms^{-1}, and the contact loads were 0.25 N, 0.5 N and 1 N.

The dry friction, for each contact pair tested, is shown in *Table 3*. Also shown in *Table 3* is the roughness of the rubber surface(s) of the contact pair. These roughness values were obtained using a Talysurf 10 surface texture measuring

*Malaysian Rubber Producers' Research Association Brickendonbury, Hertford, SG13 8NL, United Kingdom
#Corresponding author

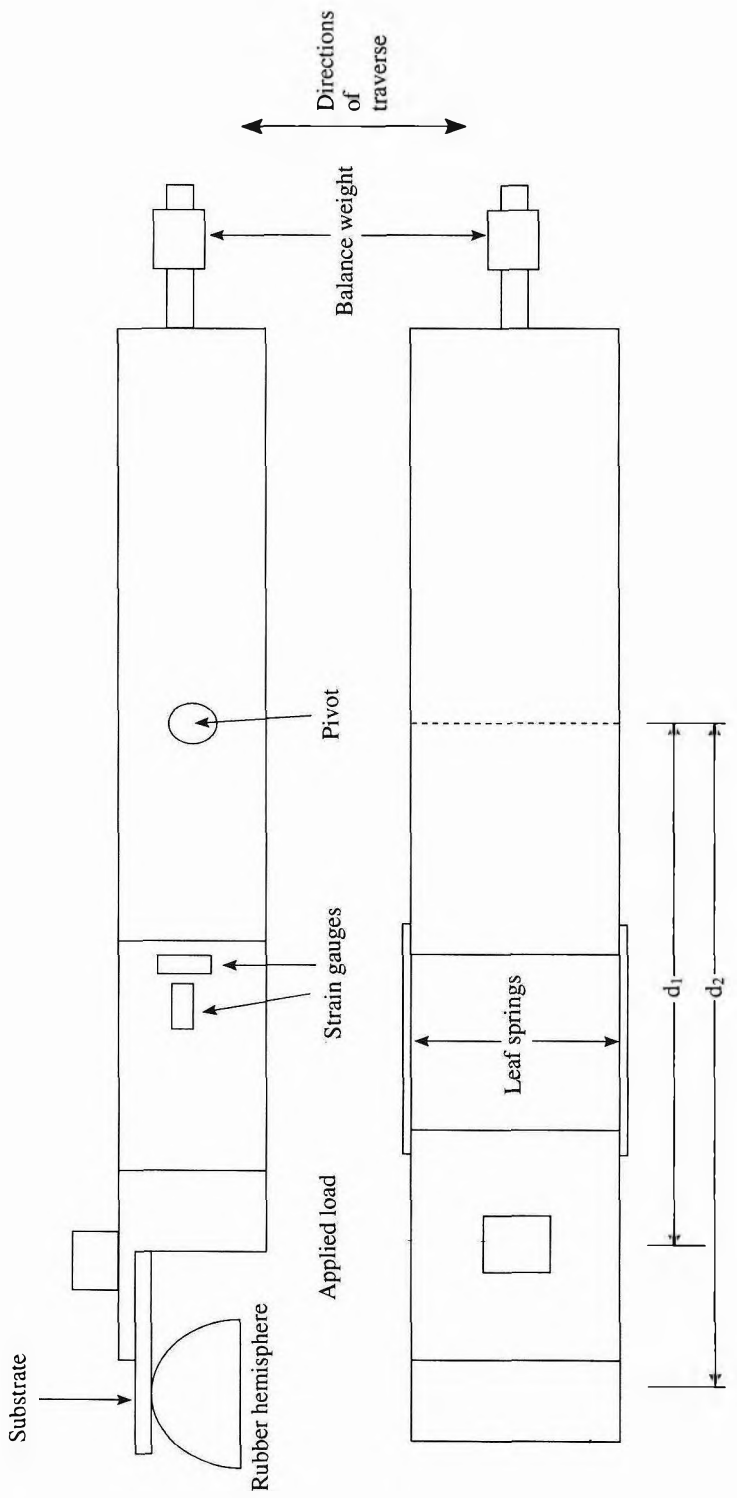

Figure 1. The friction apparatus.

instrument (Rank Taylor Hobson), Leicester, UK). This machine measures the average roughness (centre line average, CLA) over three horizontal distances; V_h = 0.08 mm, 0.25 mm and 0.8 mm.

The surface roughness of CONCRETE and TAR are 1.0 μm – 2.0 μm and 0.5 μm – 0.8 μm, respectively.

As a way of comparing the data for different contact pairs the lubricated friction values were divided by the dry friction value to give a 'relative lubricated friction'. The data are shown in *Figure 2*. The vertical lines joining the points show the variation in relative friction with contact load.

Friction at Constant Load

Using a contact load of 0.5 N, measurements of friction were made at sliding speeds from 0.05 mms^{-1} – 5.0 mms^{-1}, for the lubricated contact of IR, OENR, and TR with CONCRETE and TAR. The results are shown in *Figures 3* to *5*.

Friction Measurements Using a Windscreen Wiper Blade, a Running Shoe, and Bicycle Tyres

Measurements of friction were made for the following systems:

- A windscreen wiper blade in contact with a soda-glass plate. The applied load was 0.01 N/mm, a typical in-service load.

TABLE 1. THE VARIOUS SURFACES USED IN THE TESTS

GLASS	:	Optically smooth soda glass track.
CONCRETE	:	Concrete, cast against glass, to form a track.
TAR	:	Bitumen (as used in roof repairs) to form a track.
BLACK	:	A carbon black-filled rubber sheet.
SILICA	:	A silica-filled rubber sheet.
IR	:	2% dicup cured *Cariflex 305* sheet.
NR	:	2% dicup cured SMR L sheet.
OENR	:	An oil-extended black-filled natural rubber sheet.
TR	:	A black-filled sheet of a compound used as a tyre retreading material.
TUBING	:	Natural rubber tubing (Red).
GLOVES	:	Household washing-up gloves.
WIPER	:	A windscreen wiper blade, based on natural rubber.
SHOE	:	A running shoe tread, based on natural rubber.
TYRES	:	Three bicycle tyres, based on natural rubber.

Tyres A and B have carbon black as filler, and Tyre C has silica as filler.

TABLE 2. FORMULATIONS FOR RUBBER COMPOUNDS

Compound/Cure condition	Silica	Black	TR	NR	IR	OENR
Natural Rubber (SMR L)	100	100	–	100	–	–
Cariflex 305	–	–	–	–	100	–
Natural Rubber (SMR 20)	–	–	80	–	–	–
Oil extended Natural Rubber (25% aromatic oil)	–	–	–	–	–	85
Polybutadiene (Europrene *cis*)	–	–	20	–	–	15
Zinc oxide	5	5	4	–	–	5
Stearic acid	2	2	2	–	–	2
Sulphur	2.5	2.5	1.2	–	–	1.2
Dicumyl peroxide	–	–	–	2	2	–
Nonox ZA (Permanax IPPD)	1	1	–	–	–	2
Santocure NS	–	0.5	–	–	–	–
Struktol A.82	–	–	1.2	–	–	–
Aromatic oil	–	–	8	–	–	–
Santoflex 13	–	–	2	–	–	–
Santocure MOR	–	–	1.2	–	–	–
P.E.G. 1500	1.5	–	–	–	–	–
SI 69	3.0	–	–	–	–	–
CBS	1	–	–	–	–	1.2
N339 Black	–	–	55	–	–	–
HAF N330 Black	–	50	–	–	–	–
ISAF Black (N220)	–	–	–	–	–	55
VN3 Silica	40	–	–	–	–	–
Cure time (min)	60	60	25	60	60	15
Cure temp (°C)	150	150	150	160	160	150

TABLE 3. DRY FRICTION COEFFICIENT AND SURFACE ROUGHNESS VALUES

Contact pair	Dry friction			Rubber surface roughness, CLA (μm)		
	25 g	50 g	100 g	V_h = 0.08 mm	V_h = 0.25 mm	V_h = 0.8 mm
BLACK/BLACK	5.20	5.20	4.30	.007 ± .002	.011 ± .005	.035 ± .007
BLACK/BLACK(R)	5.00	4.40	3.90	.084 ± .009	.14 ± .01	.29 ± .04
BLACK/GLASS	3.20	2.80	2.35	.007 ± .002	.011 ± .005	.035 ± .007
BLACK/GLASS (R)	3.60	3.30	2.95	.084 ± .009	.14 ± .01	.29 ± .04
SILICA/SILICA	4.80	4.50	3.80	.002 ± .001	.009 ± .004	.027 ± .006
SILICA/SILICA(R)	3.80	3.90	3.63	.006 ± .004	.017 ± .006	.061 ± .015
SILICA/GLASS	3.00	2.90	2.95	.002 ± .001	.009 ± .004	.027 ± .006
SILICA/GLASS (R)	2.60	2.60	2.55	.006 ± .004	.017 ± .006	.061 ± .015
TUBING/TUBING	3.80	3.30	3.00	.005 ± .002	.021 ± .009	.056 ± 0.16
TUBING/GLASS	3.40	2.90	2.45	.005 ± .002	.021 ± .009	.056 ± 0.16
GLOVES/GLOVES	1.20	1.13	1.21	.009 ± .003	.055 ± .003	.24 ± .01
GLOVES/GLASS	0.90	0.65	0.55	.009 ± .003	.055 ± .003	.24 ± .01
IR/GLASS	3.20	3.10	2.50	.003 ± .001	.010 ± .004	.029 ± .005
IR/GLASS(R)	2.80	3.00	2.65	.13 ± .05	*	*
NR/GLASS	3.60	2.90	2.55	.004 ± .001	.012 ± .003	.024 ± .005
NR/GLASS(R)	3.60	3.10	2.65	.16 ± .07	*	*
IR/CONCRETE(R)	1.60	1.40	1.35	.13 ± .05	*	*
IR/TAR(R)	2.60	2.20	2.35	.13 ± .05	*	*
OENR/CONCRETE(R)	0.85	0.88	0.84	.07 ± .02	*	*
OENR/TAR(R)	2.20	1.70	1.85	.07 ± .02	*	*
TR/CONCRETE(R)	1.50	1.45	1.35	.03 ± .01	*	*
TR/TAR(R)	2.10	2.20	1.80	.03 ± .01	*	*

(R) Rubber surfaces roughened using glass paper.

* Roughness values unobtainable due to curvature of surface.

Note: For BLACK and SILICA, rubber/rubber friction is substantially greater than rubber/GLASS friction. Hertz theory[4] predicts a difference of about 60%, if it is assumed that the frictional stress per unit area is the same in rubber/rubber and rubber/GLASS contacts.

- A running shoe in contact with a plastic floor tile, and with concrete and tar road surfaces.

- Three different bicycle tyres in contact with concrete and tar road surfaces.

The friction of the wiper blade was found using the friction apparatus (*Figure 1*) at 5 mms^{-1} sliding speed. For the running shoe and bicycle tyres a spring balance was used to record the force required to cause tangential movement from stationary contact.

Values for friction coefficient were found in dry contact and for contacts lubricated with distilled water (pH 6) and buffer solutions at pH 6 and pH 11.

The results (averages of three measurements) are shown in *Table 4*. In contact with concrete and tarmac surfaces, the lubricated friction is almost the same for the three lubricants. However, in the contact of the running shoe with the floor tile there is a 35% reduction in friction between pH 6 and pH 11, and with the wiper blade against glass there is a 45% reduction between pH 6 and pH 11. These observations show that it is possible to detect the influence of lubricant pH on friction in practical situations as well as under laboratory conditions.

DISCUSSION

The measurements made at constant speed (*Figure 2*) show that, apart from the contact pairs which include CONCRETE or TAR, the friction at a lubricant pH of 11 is noticeably lower than the friction with the solution at pH 6. The contact pairs in which the effect is most pronounced are BLACK/BLACK and SILICA/SILICA.

With GLASS as one of the contact pair the relative friction is generally lower than with two rubber surfaces in contact, for all lubricated conditions. There is still a definite reduction in friction from the pH 6 solution to the pH 11 solution.

Film thickness measurements[2] on IR in contact with GLASS gave an increase in the equilibrium film thickness with increasing pH. With a solution at pH 6 there was no evidence for an equilibrium film, which means there is contact between the surfaces. However, with a solution at pH 11 there was film support at all pressures tested. This is probably the reason for the observed low friction for contacts involving GLASS and alkaline water as lubricant.

For contact between two rough surfaces, the difference in the relative friction at pH 6 and pH 11 is small, in the case of SILICA/SILICA(R) and BLACK/BLACK(R), or almost non-existent, as in the case of all contacts involving CONCRETE and TAR. For rough surfaces the area within the geometric contact periphery which is actually in contact is far smaller than for smooth surfaces. Rough surfaces will give higher contact pressures at the points where contact is made, so the ability to support a film is reduced.

By considering the coefficient of lubricated friction for the contacts involving CONCRETE and TAR (*Figures 3* to *5*), a feature of the system is revealed which is not apparent from the data of relative friction (*Figure 2*). Almost without exception, over the whole range of sliding speed, the friction of a lubricated Rubber/CONCRETE contact is lower than the lubricated friction of a Rubber/TAR contact.This cannot be attributed to the fact that the TAR surface is only half as rough as the CONCRETE surface, since that would be more likely to lead to higher lubricated friction for CONCRETE. There was very little evidence for an effect of lubricant pH on the friction but it is possible that the pH of the surface itself has some influence. The pH of a surface was found using a Phoenix PHM4 Antimony electrode (CP Instrument Co., Bishops Stortford, UK). The surface pH values for the materials used in these tests were:

TAR	pH 5.2 – 6.2
TR	pH 5.8 – 6.0
OENR	pH 5.8 – 6.2
IR	pH 7.0 – 7.2
BLACK	pH 7.4 – 7.6
SILICA	pH 7.8 – 8.0
CONCRETE	pH 8.7 – 11.0

If the pH of the surface is of consequence in the lubricated friction measurements then it would be expected that CONCRETE would give a lower friction than TAR, which was the observation made.

CONCLUSION

The effect of lubricant pH on sliding friction, as seen initially[1,2] in the contact of two optically smooth unfilled rubber surfaces, has been shown to be noticeable in contacts where the rubber is filled with carbon black or silica, when only one of the surfaces is rubber, and when the surfaces are rough.

In the contact of two surface-smooth, filled natural rubber compounds the difference in friction between lubrication at pH 6 and pH 11 is large, but when the surfaces are roughened the difference is greatly reduced. It would therefore seem that for rubber/rubber contact, smoothness of the surfaces is of far more importance than fillers.

In all rubber/GLASS contacts, the lubricated friction is lower than for the same rubber/rubber contact. Unless a high solution pH draws fatty acids from the rubber, to give a soapy solution, the rubber will not be readily wetted by the

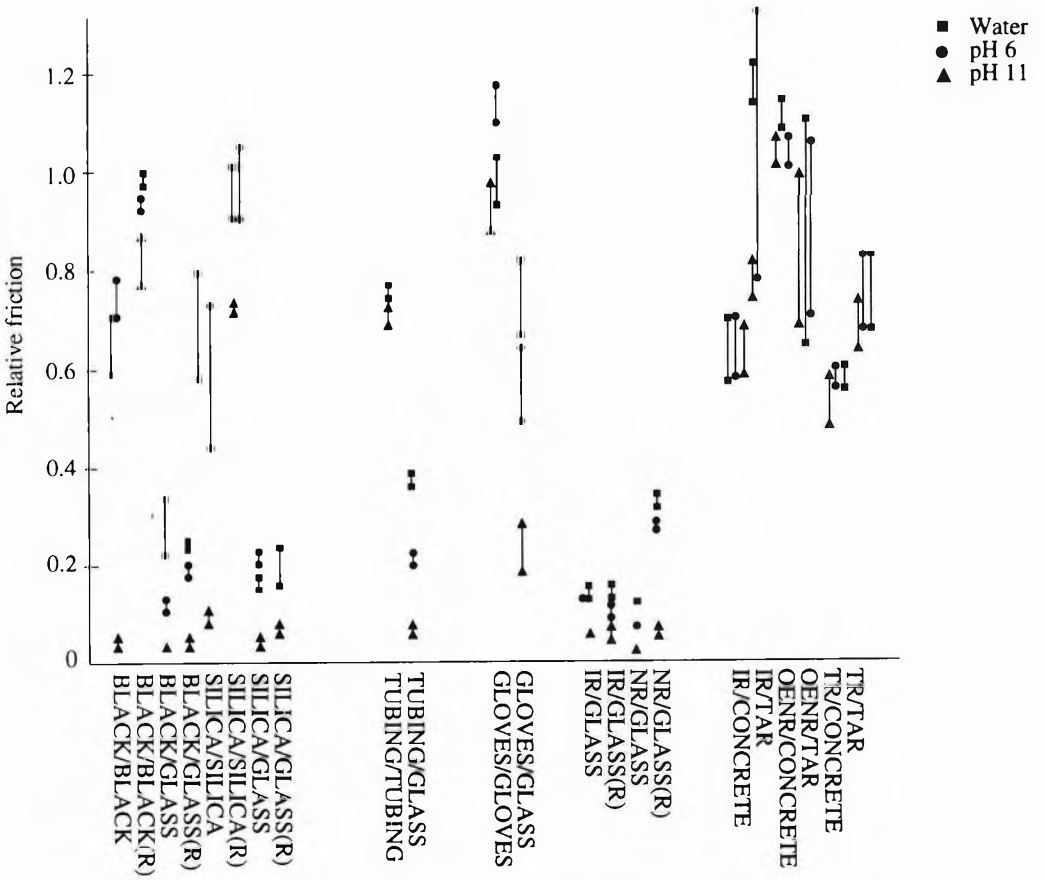

Figure 2. Relative friction in lubricated contact.

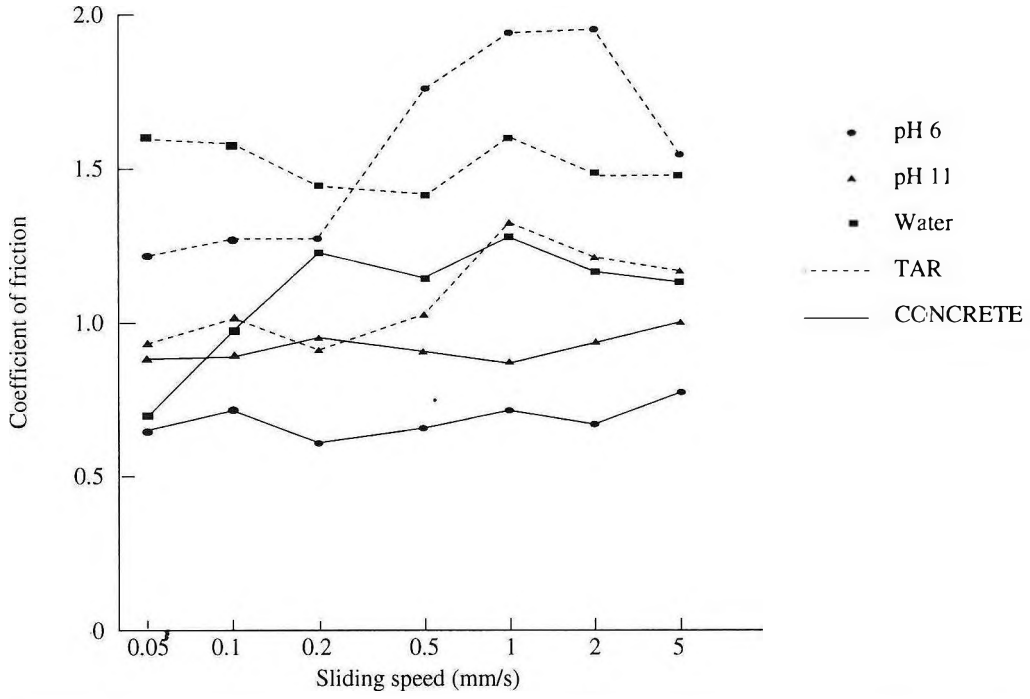

Figure 3. Friction of IR in lubricated contact with TAR and CONCRETE over a range of sliding speeds.

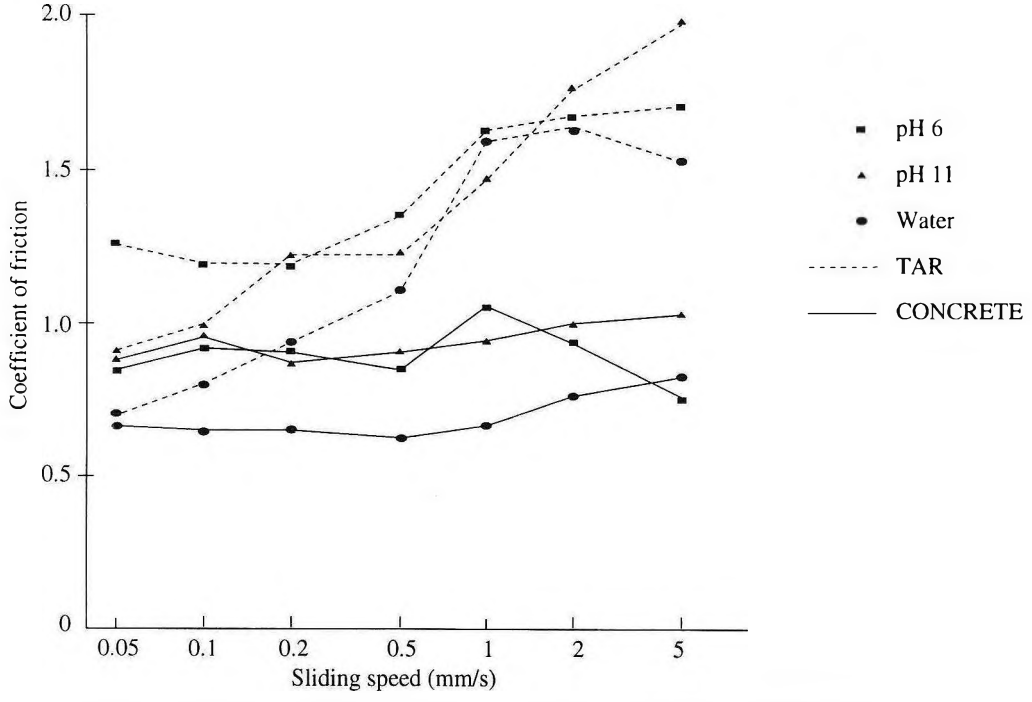

Figure 4. Friction of OENR in lubricated contact with TAR and CONCRETE over a range of sliding speeds.

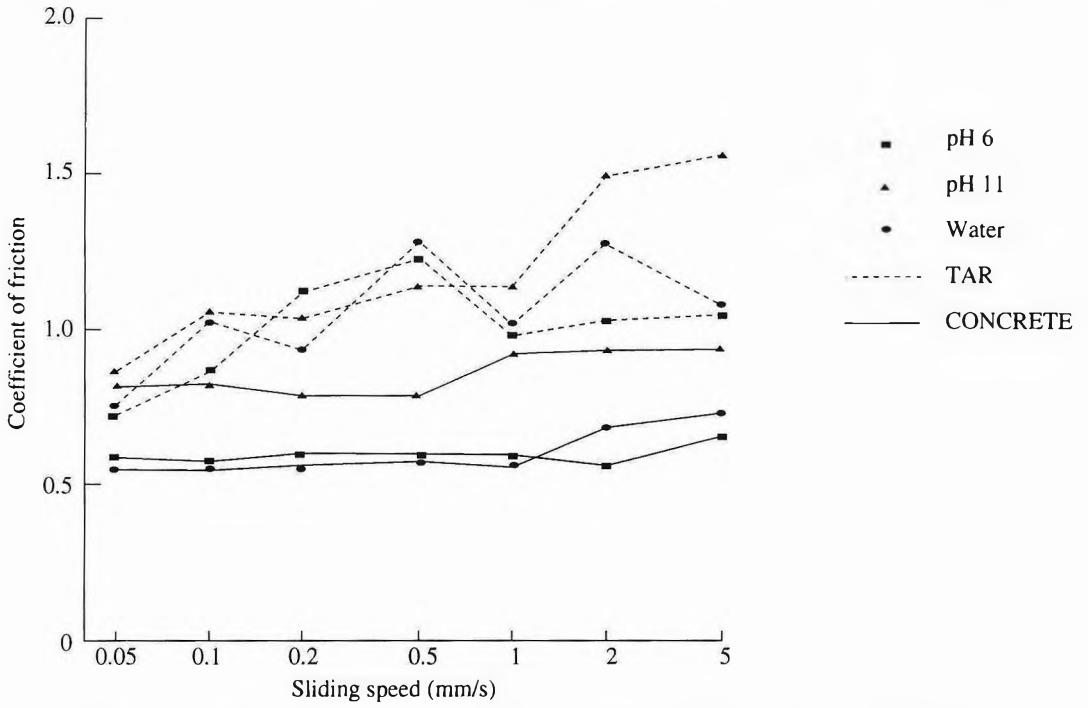

Figure 5. Friction of TR in lubricated contact with TAR and CONCRETE over a range of sliding speeds.

TABLE 4. FRICTION COEFFICIENT FOR WIPER BLADE, RUNNING SHOE, AND BICYCLE TYRES

Contact pair	Load	Coefficient of friction			
		Dry	Water	pH 6	pH 11
Wiper blade/glass	0.01 N/mm	1.15 ± .08	0.54 ± .04	0.40 ± .02	0.22 ± .01
Running shoe/floor tile	50 N	1.33 ± .08	1.10 ± .17	1.23 ± .08	0.80 ± .10
Running shoe/concrete	50 N	0.87 ± .08	0.60 ± .03	0.57 ± .03	0.52 ± .03
Running shoe/tarmac	50 N	0.57 ± .06	0.55 ± .05	0.57 ± .06	0.55 ± .05
Tyre A/concrete	16 N	1.19 ± .11	1.08 ± .04	0.92 ± .04	0.92 ± .04
Tyre A/tarmac	16 N	1.36 ± .10	1.15 ± .04	1.23 ± .04	1.13 ± .04
Tyre B/concrete	20 N	0.93 ± .04	1.04 ± .04	0.98 ± .04	0.84 ± .06
Tyre B/tarmac	20 N	1.27 ± .06	1.10 ± .05	1.22 ± .10	1.18 ± .08
Tyre C/concrete	26 N	0.95 ± .12	1.13 ± .09	1.01 ± .04	0.99 ± .04
Tyre C/tarmac	26 N	1.27 ± .04	1.23 ± .02	1.14 ± .02	1.08 ± .08

aqueous lubricants, whereas a cleaned glass surface, of hydrophilic nature, is wetted and more likely to give a low friction.

Wettability may relate to the difference in friction between CONCRETE and TAR since lower friction is seen on the hydrophilic CONCRETE than on the hydrophobic TAR.

The results for contacts involving CONCRETE and TAR show that, by having a rough rubber surface in contact with the rough non-rubber surfaces, the influence of lubricant pH on friction is noticeable, but is not as great as seen when the sliding surfaces are smooth.

It would seem that three conditions may be ranked in the following levels of importance, if the effect of friction reduction in alkaline water is to be observed:

Most important – Smooth surfaces in contact

Intermediate – Two rubber surfaces in contact (unless the non-rubber surface is glass)

Least important – Unfilled rubber.

Date of receipt: August 1995
Date of acceptance: October 1995

REFERENCES

1. RICHARDS S.C., AND ROBERTS A.D. (1994) Friction of Rubber Lubricated by Aqueous Solutions of Different Acidity/ Alkalinity. *J. nat. Rubb. Res.*, **9(3)**, 190.

2. RICHARDS S.C., ROBERTS A.D., AND BARNES. P, (1995) The Thickness of Aqueous Boundary Films in Static Rubber/ Glass and Rubber/Rubber Contacts. *J. nat. Rubb. Res.*, **9(3)**, 154.

3. ARNOLD, S.P.ROBERTS, A.D. AND TAYLOR, A.D. (1987) Rubber Friction Dependence on Roughness and Surface Energy. *J. nat. Rubb. Res.*, **2(1)**, 1.

4. HERTZ, H. (1896) *Miscellaneous Papers*. London: Macmillan.

J. nat. Rubb. Res. **10(4)**, 228–241

Drying of Granules from Natural Rubber Latex

B. NAON*, J.M. BENOIT*, G. BERTHOMIEU*# AND J.C. BENET*

A study was performed to analyse the convective drying of natural rubber in granule form. Matter and energy exchanges take place between the substance and the drying air in this kind of drying. To quantify these exchanges, a series of tests were carried out at a production site in Côte d'Ivoire using a portable laboratory drier. It was thus possible to work on rubber that had not been denatured by transport. Tests were performed at a range of temperatures from 40°C to 120°C with air velocity from 0.5 m/s to 2.5 m/s and relative humidity values varying from several percent to 90 percent according to the temperature. Analysis of the drying kinetics led to modelling the matter exchange coefficient. Energy exchange coefficient was determined using measurement of the temperature of air flowing between the grains and measurement of the temperature of the grains themselves.

INTRODUCTION

There has been less research on drying of natural rubber in granule form than as sheets. In the few studies available[1,2,3,4] the authors examined under experimental conditions the drying characteristics of a thick layer of granules under the effect of drying air parameter. Theoretical studies on internal transfer mechanisms during convection drying of granular materials have been carried out in the laboratory[5,6]. A mathematical model was developed to show the characteristics of the substance dried and of the air at any moment and at any point in the layer of granules.

The experimental determination of two coefficients — the drying rate and the energy exchange coefficient—is described here. Knowledge of these coefficients made it possible to activate a mathematical model[7,8,9] which, after validation, led to writing a simulation program. It was then possible to use a digital procedure to vary the parameters of the drying air, the thickness of the layer and flux direction as in industrial zone driers in order to seek optimal drying conditions.

EXPERIMENTAL APPARATUS AND OPERATING PROCEDURE

Natural rubber is a biological material and subject to numerous reactions that may denature its quality and physico-chemical characteristics unless it is stabilised by drying. In order to analyse drying mechanisms, a portable laboratory drier was designed, constructed and adjusted for performing tests immediately after collection of the rubber.

Drier

The design is similar to that of existing driers. Its originality lies in its dimensions (l:3 m; w:1m and h:2m). The drier is shown diagrammatically in *Figure 1*.

The test cell containing the material and ducting conveying the drying air are cylindrical and 200 mm in diameter.

The ranges of drying air characteristics were:

Velocity (V): 0–5m/s
Temperature (T): 20°C–150°C
Relative humidity (RH): 0%–100% according to temperature.

*Laboratoire de Mécanique et Génie Civil, Université Montpellier II – Sciences et Techniques du Languedoc, Case 034 – Place Eugéne Bataillon, 34095 MONTPELLIER CEDEX 5, FRANCE
#Corresponding author

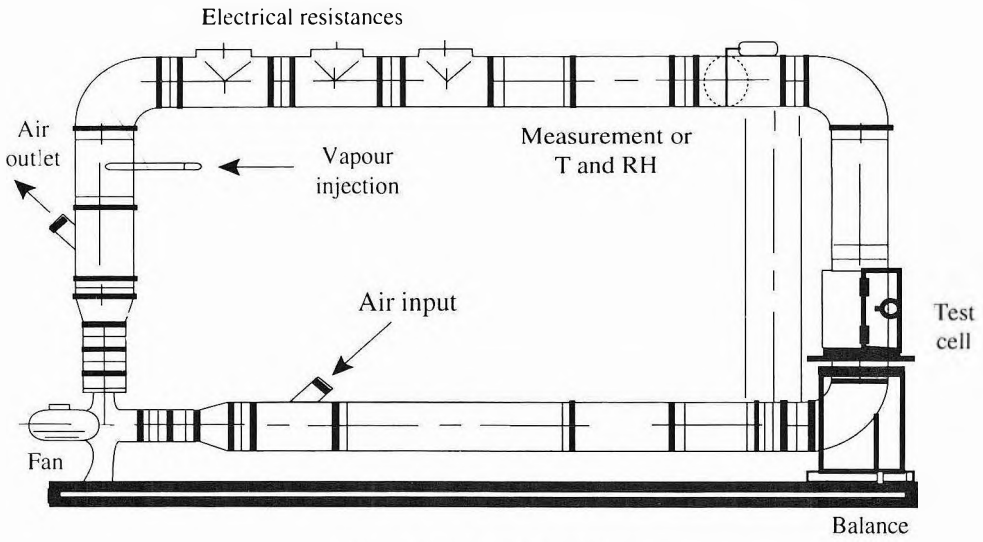

Figure 1. Laboratory drier.

Regulation of the different parameters and frequency of weighing of the material to be dried was performed by a controller connected to a computer. The drier was run from a mimic supervision monitor. The air was diverted during weighing. The size of the equipment and details of the functioning of the drier have been described elsewhere[7,10,11].

Test Procedure

The tests were performed in Côte d'Ivoire at an estate at Thoupa operated by Société Africaine de Plantation d'Hévéas.

To limit causes of variability, the latex used (GT 1) was from the same trees tapped at the same time.

After collection, the latex was subjected to the following sequence of treatments:

- dilution to a dry rubber content (DRC) of 30%
- coagulation at pH 4.8
- maturation of the coagulum for 18 h
- granulation by using a rotary-cutter fitted with a 1.3 cm screen, and
- drainage for 30 min to 45 min.

Granules approximately 1 cm in diameter placed in the test cell were weighed at predetermined intervals. The test was considered to end when the variation of weight in time was no longer significant.

Several granules were removed at the end of each test and further dried to determine the anhydrous mass of rubber and to plot drying kinetics.

DETERMINATION OF THE MATTER EXCHANGE COEFFICIENT

The mass of rubber particles was traversed by hot air. Matter exchange resulted in a loss of water from the material. The variation of water content (drying rate R) for certain values of T, V and RH was given by derivation of the thin-layer (a few centimetres) drying kinetics[7,8].

Modelling the industrial drying of a mass of granules requires knowledge of R in as broad a range as possible of temperature, velocity and relative humidity of the air.

The tests were performed with different values of V and RH within two temperature ranges as follows:

$40°C < T < 80°C$ with $20\% < RH < 95\%$ and $0.5m/s < V < 2.5m/s$ and $80°C < T < 120°C$ with $5\% < RH < 20\%$ and $0.5m/s < V < 2.5m/s$.

Test Results

A series of 64 tests was performed[7,12] with different combinations of parameters T, V and RH.

Kinetics and drying rates. The drying kinetics showing variation in the water content (w) as a function of time (t) obtained during the tests were of the same form. One of these kinetics is shown below (*Figure 2*) together with the variation in the drying rate ($R = -dw/dt$) according to w.

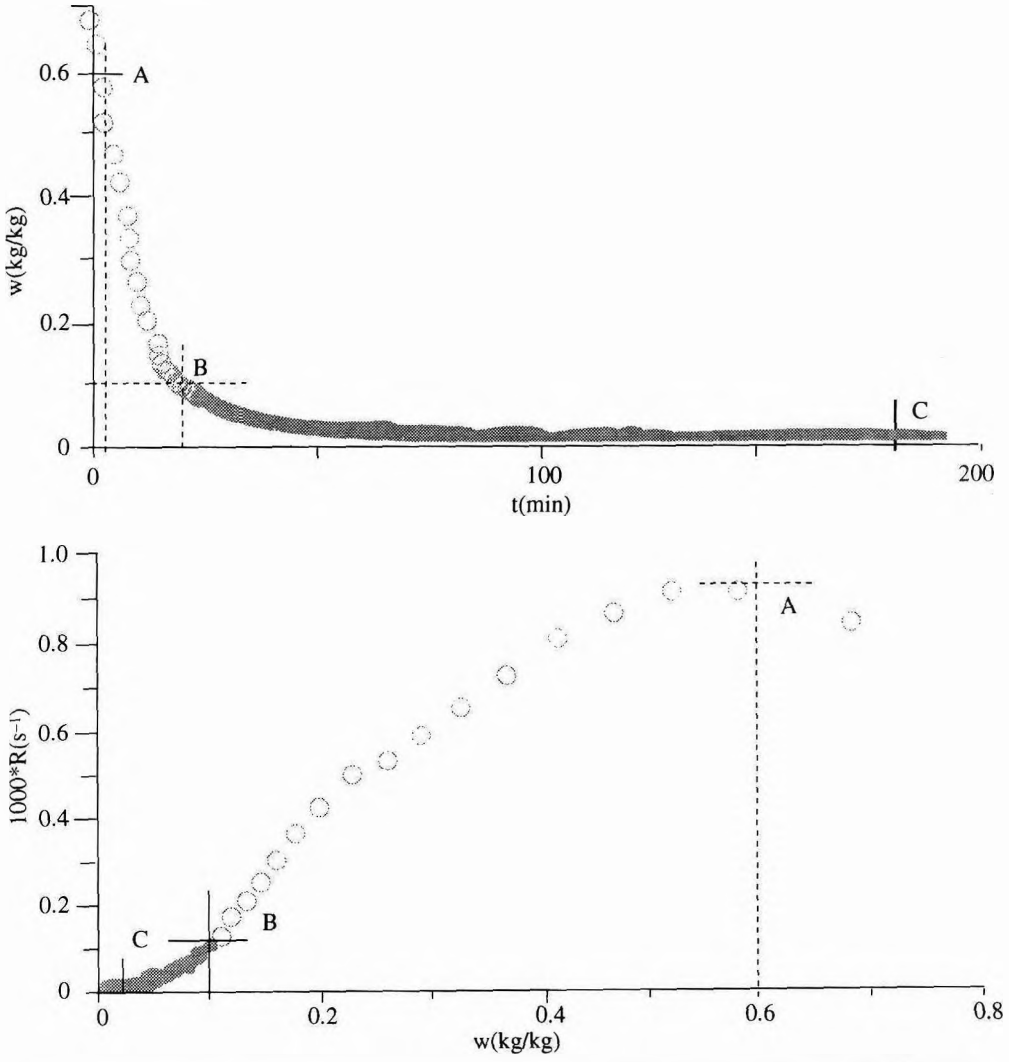

Figure 2. An example of kinetics and drying rate (T = 100°C; V = 1.5 m/s; RH = 10%).

Analysis of the drying rate curves reveals three zones: $w > 60\%$, $10\% < w < 60\%$ (zone AB) and $w < 10\%$ (zone BC), that are examined separately below.

Variability of the material and dispersion of the measurements. Variations in drying speed in an experiment repeated three times under the same conditions is shown in *Figure 3.*

Dispersion was observed at the beginning of the measurements. This was caused mainly by:

- the variability of latex, a particularly unstable natural substance which, in spite of precautions during collection and preparation, may not always have the same initial characteristics.
- the instability of the characteristics of the air and especially the relative humidity; this varies at the start of drying because of substantial surface evaporation that tends to disturb the regulation of relative humidity at the beginning of drying.

Modelling of the Drying Rate *R*

First phase of drying (w>*60%*). It was assumed for all kinetics that the constant drying rate phase occurred with a water content of over 60%.

The drying rate during this phase depends on the three drying parameters *T*, *V* and *RH*. Study of the results of tests led to modelling this phase by a function with the following form:

$$R_{60} = 6 \times 10^{-6} (1-RH)\, T\, V \qquad \ldots 1$$

The drying rate measured according to that calculated using the approximation above is shown in *Figure 4*. Comparison with the first bisectrix shows that in most cases there is good agreement between measurements and the equation proposed. The points that deviate substantially from the first bisectrix are for ongoing experiments during which a crusting phenomenon has been observed.

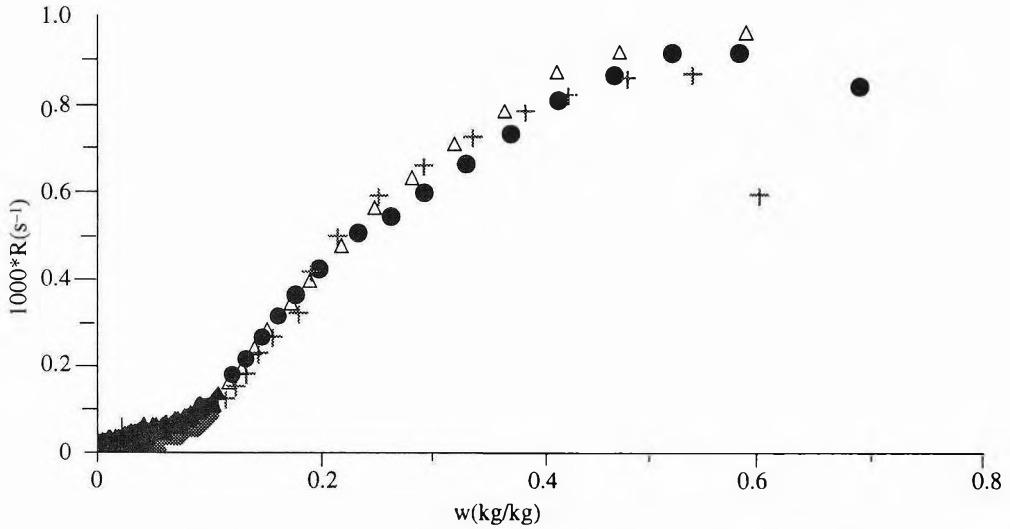

Figure 3. Example of measurement dispersion in thin-layer tests.

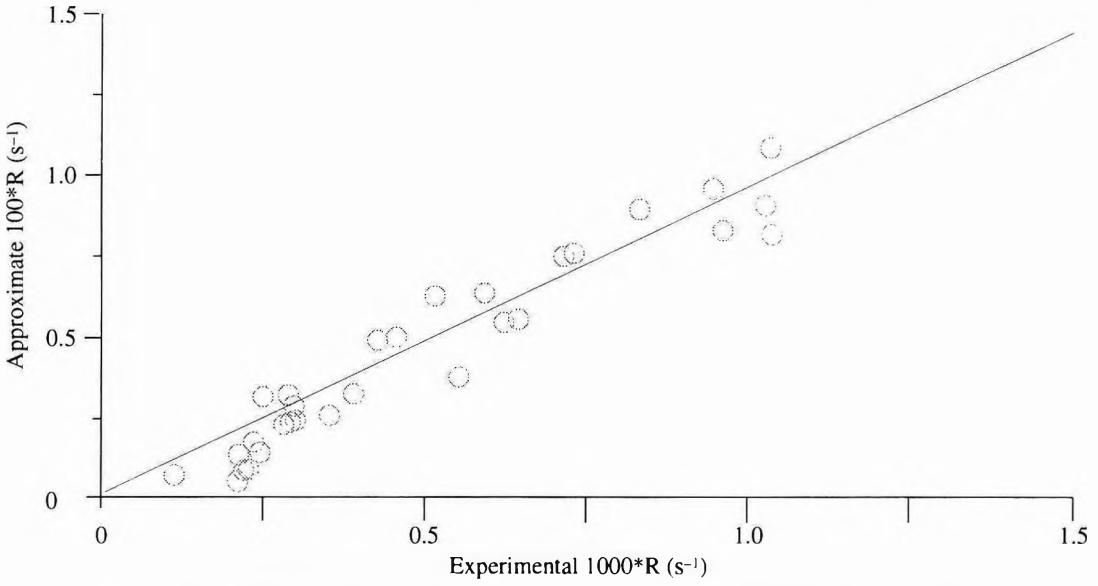

Figure 4. Variations in approximate drying rate according to the rate measured for water contents greater than 60%.

Falling rate phase (w < *10%*). During the falling rate period, the drying rate appears to vary parabolically with the water content and depends essentially on the temperature. This is in agreement with the results found in the literature[5,6,13,14,15,16]. The following procedure is used to find the rate during this phase:

- The variation in drying at transition point B (w = 10%) can be modelled by the following function (*Figure 5*):

$$R_{10} = 2.4 \times 10^{-5} - 1.3 \times 10^{-6}\, T + 1.9 \times 10^{-8}\, T^2 \quad \ldots 2$$

- Point C is the equilibrium water content calculation from the desorption isotherm. The latter was approximated from data in the literature and especially the work of Auria[5] (*Figure 6*).

Approximation of this curve gives the following:

- when $RH \leq 0.6$: $w = 5.10^{-3} + 0.49RH$
- when $RH > 0.6$: $w = \dfrac{-5.48 * 0.427 * RH}{1 + 5.48 * RH} + \dfrac{0.996 * 0.092 * RH}{1 - 0.996 * RH} + 0.733 * RH$

Intermediate phase (*10%* < w < *60%*). The intermediate phase from 10% to 60% is approximated by a third degree function in w taking into account the continuity at the two transition points A and B. The approximation also takes into account the continuity of the derivative at point B (w = 10%) and assumes a horizontal tangent at point A (w = 60%) to take into account the constant rate drying phase.

Validity of the Approximation of the Drying Rate

Several examples of measured and approximated drying rates are shown in *Figures 7a*, *7b* and *7c*. At first sight, there are substantial divergences, but this impression should be modulated.

There is good agreement in all cases when the water content is lower than 10% and this part of

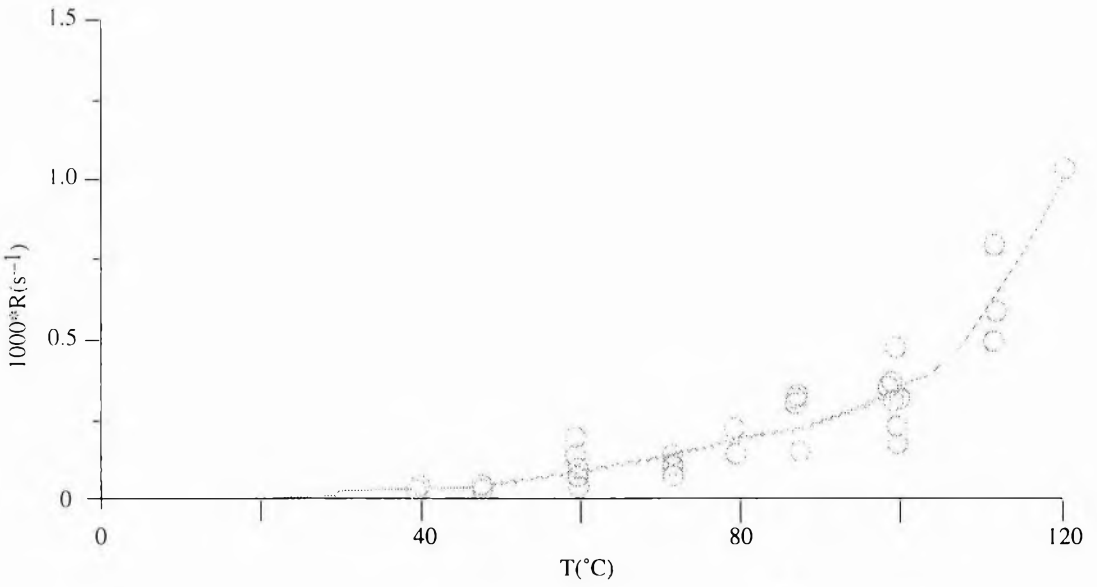

Figure 5. Variation in the drying rate at transition point B (w = 10%) according to the temperature of the drying air.

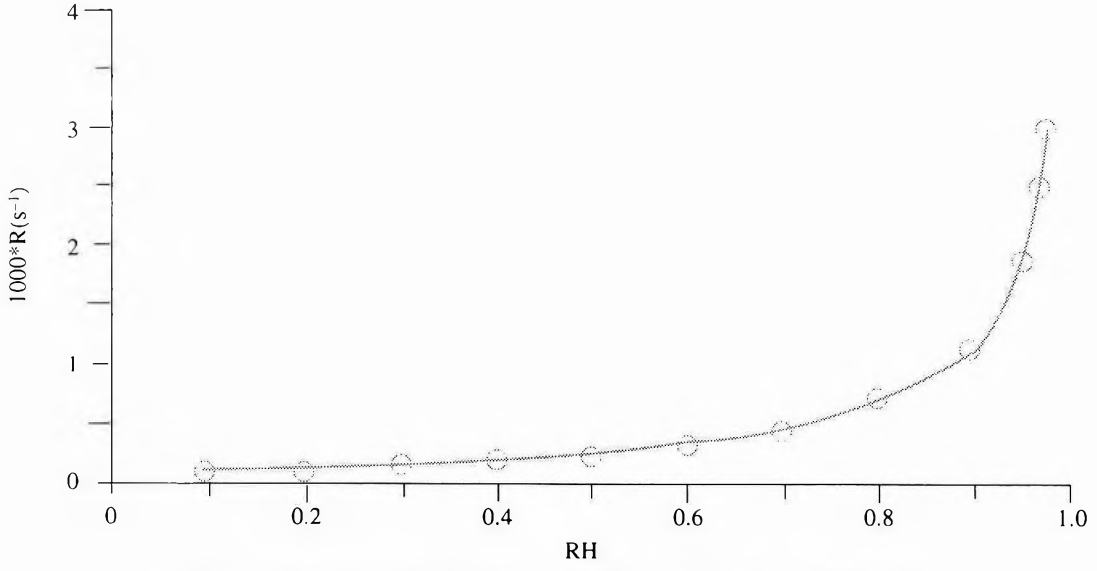

Figure 6. The desorption isotherm of natural rubber (after AURIA[5]).

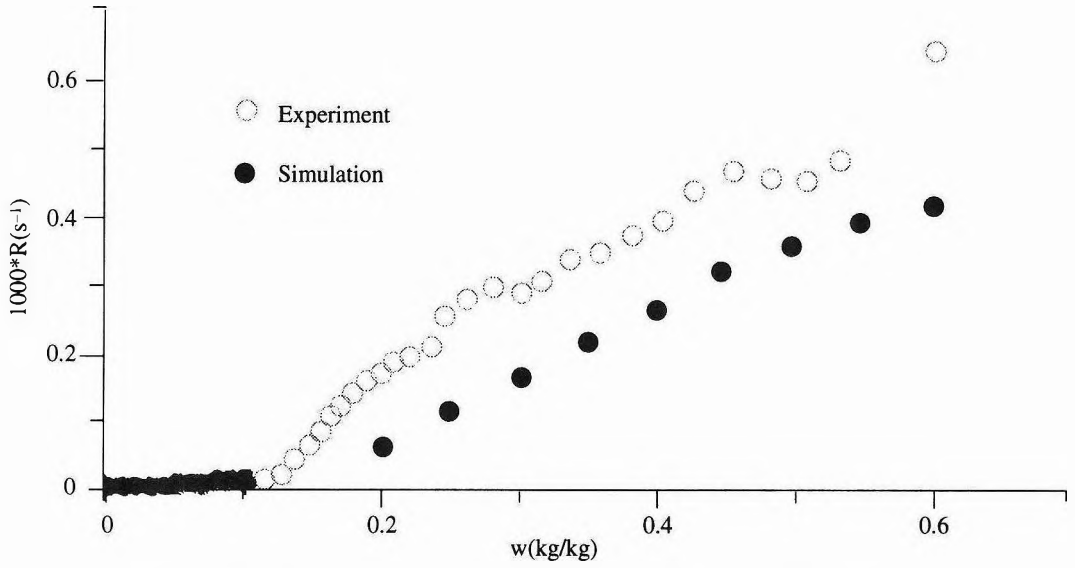

Figure 7a. Approximation of the drying rate at 60°C, 2.5 m/s, 60% RH.

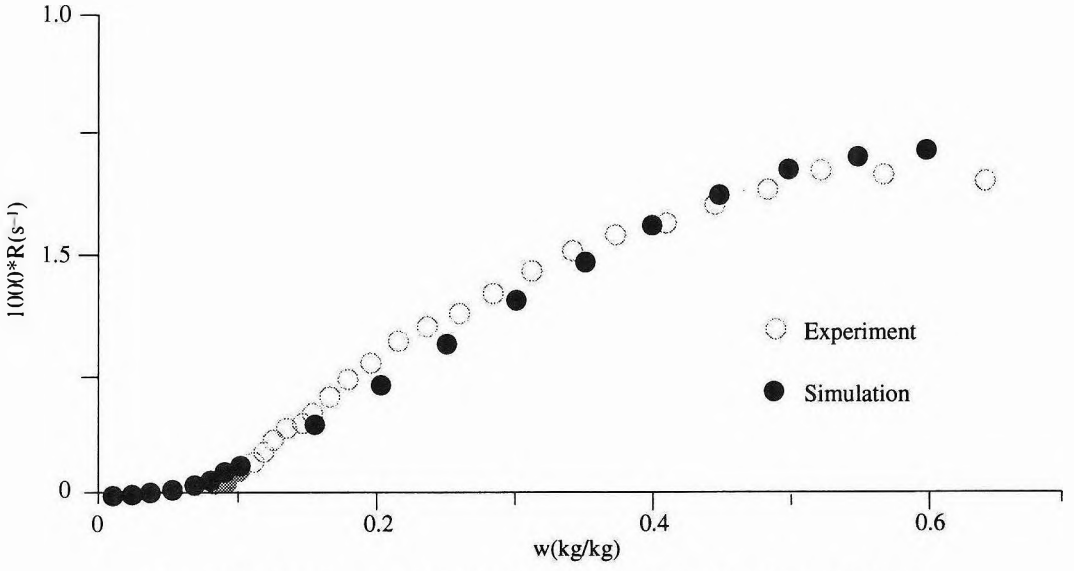

Figure 7b. Approximation of the drying rate at 100°C, 1.5 m/s, 20% RH.

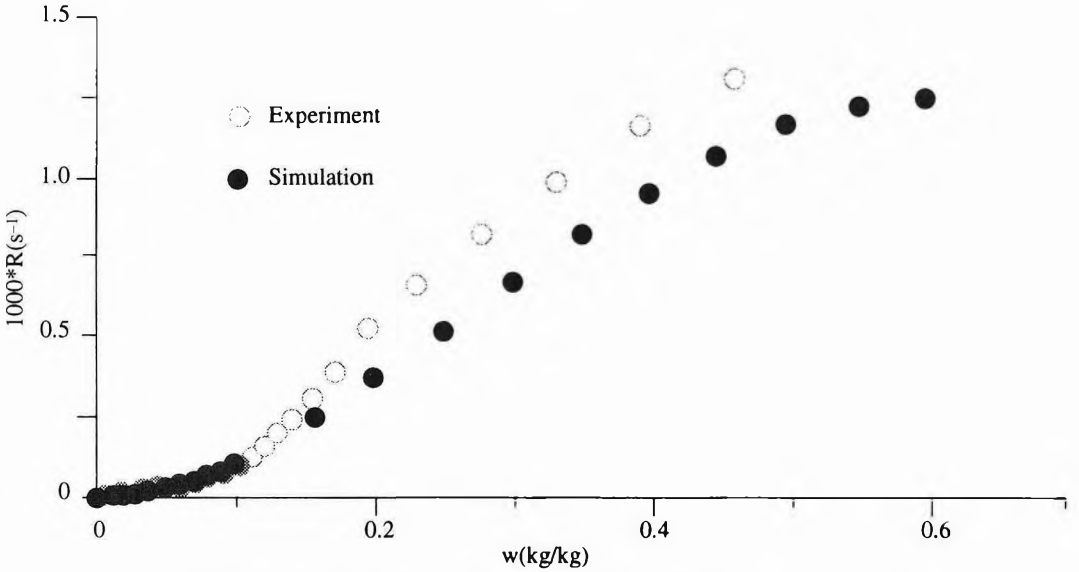

Figure 7c. Approximation of the drying rate at 112°C, 2 m/s, 4% RH.

the kinetics forms 80% of the drying time and is the range within which the greatest accuracy is required. When the water content is above 10%, divergence is marked in the tests at low temperatures that correspond to the initial raising of the temperature setting of the material in an industrial drier. The approximation of kinetics in the other tests can be considered to be satisfactory, given the variability of the material (*Figure 3*).

DETERMINATION OF THE ENERGY EXCHANGE COEFFICIENT

The coefficient of energy exchange h between air and granules is determined using the internal energy balance of the granules[7,8,12]. The equation is written:

$$(c_{pc} + w\,c_{pe})\frac{\partial}{\partial t}T_{\text{grain}} = \frac{h}{\rho c}(T_{\text{air}} - T_{\text{grain}}) - \{(c_{pc} + w\,c_{pe})\,v_{ce}^{k}\}\,T_{\text{grain}},\, k + R \{ - c_{pe}\,(T_{\text{air}} - T_{\text{grain}}) - L + \frac{R_g}{M_e}T_{\text{air}}\} \quad \ldots 3$$

where $\frac{\partial}{\partial t}$ = material derivative

c_{pc} = mass heat with constant pressure of rubber,
= 1880 J kg^{-1}K^{-1}

c_{pe} = mass heat with constant water pressure,
= 4220 J kg^{-1}K^{-1}

L = latent heat of vaporisation of water
= $2.54 \times 10^6 - 2.90 \times 10^3\,(T_{\text{air}} - 273)$

v_{ce}^{k} = settling rate of water + rubber

ρc = apparent voluminal mass of the dry rubber

R_g = perfect gas constant

M_e = molecular mass of water.

The settling rate v_{ce}^{k} is low in thin layers and the corresponding term can be ignored in the face of the others. This gives:

$$(c_{pc} + w\,c_{pe})\frac{\partial}{\partial t}T_{\text{grain}} = \frac{h}{\rho c}(T_{\text{air}} - T_{\text{grain}}) + R \{ - c_{pe}\,(T_{\text{air}} - T_{\text{grain}}) - L + \frac{R_g}{M_e}\,T_{\text{air}}\} \quad \ldots 4$$

This equation is used to determine h with knowledge of air and granule temperature and R in a thin layer test.

The internal temperature of granules was measured by making an incision in a granule and inserting a thermocouple. The granule closed and trapped the thermocouple. Measurement of the inter-granule temperature was by fitting small protective springs on thermocouples and placing them between the granules.

Air and granule temperatures are given by the average of three measurements.

Test Results

A series of twenty-four tests[12] was performed in a range of temperatures, velocities and water contents similar to those of the previous tests.

A typical example of the temperature curves recorded during these tests is shown in *Figure 8*. The plateau in the granule temperature curve corresponds to the phase change from water to water vapour.

These temperature curves can be used to find out T_{air} and T_{grain} values at any moment, together with the values of $\frac{\partial}{\partial t} T_{grain}$. R is deduced from the corresponding kinetics. It is also possible to determine h.

Figures 9a, *9c* and *9e* show the variation of h according to time at $T = 80°C$, 100°C and 120°C and for different values of V and RH. The large h values recorded at the start of the experiment resulted from the establishment of thermal equilibrium in the system. The infinite values of h at the end of the test result from the fact that the granule temperature moves towards the air temperature. The curves shown in *Figures 9b*, *9d* and *9f* are obtained when these extreme values are discarded.

Value of *h*

In all these tests, the values of h lie between 40 000 and 130 000 $Wm^{-3} K^{-1}$. Unlike the case of R, it was not possible to express h according to the drying parameters T, V and RH as their influence was fairly random. It is simply noted that at set values of V and RH, h decreases when the temperature rises, as shown in *Figure 10*.

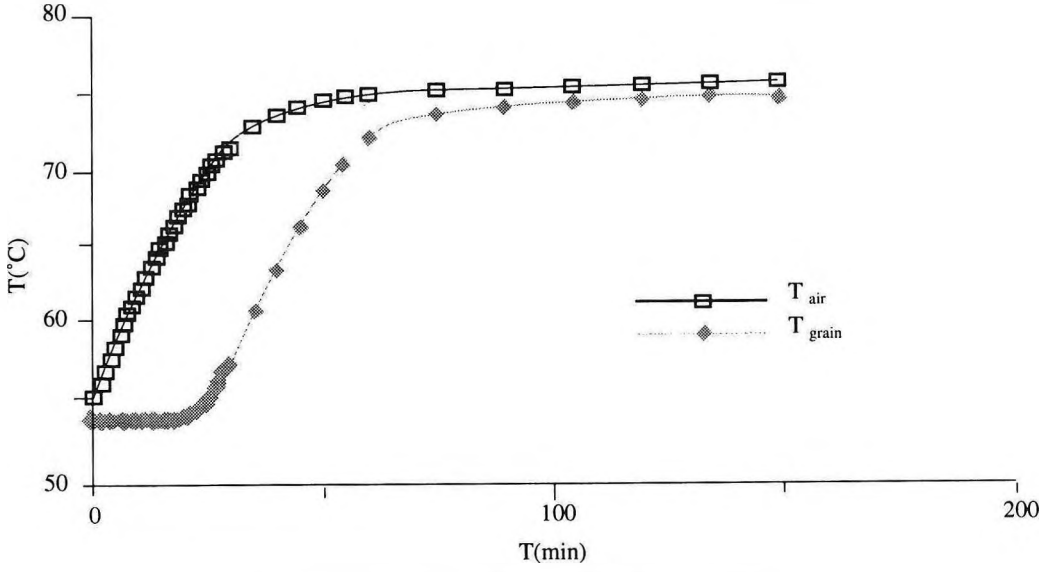

Figure 8. An example of variation of air and granule temperature (T=80°C; V=1.5m/s; RH=20%).

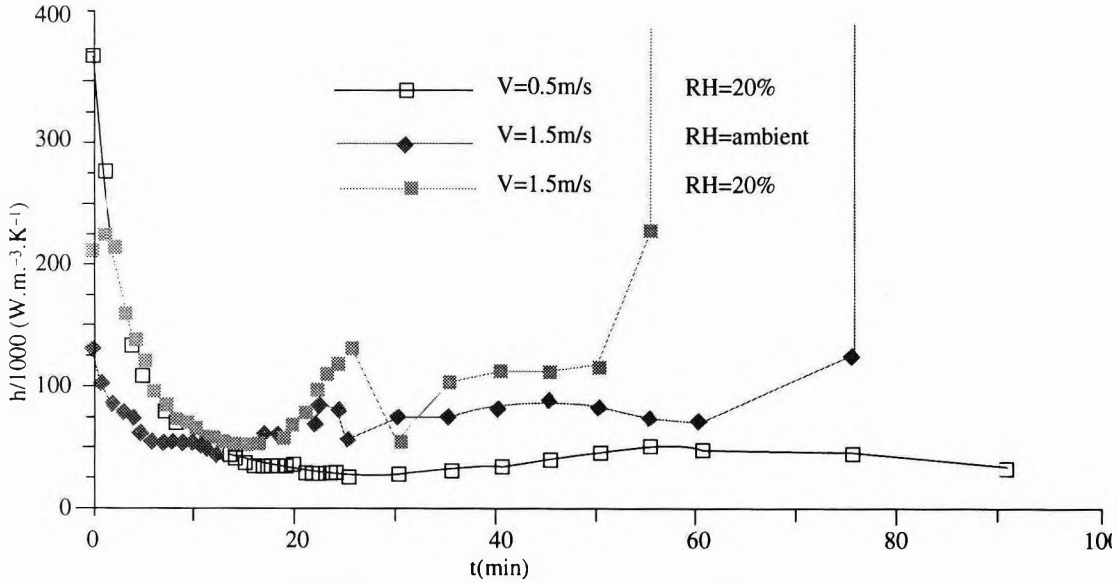

Figure 9a. Variations of h *at* T = *80°C (full curves).*

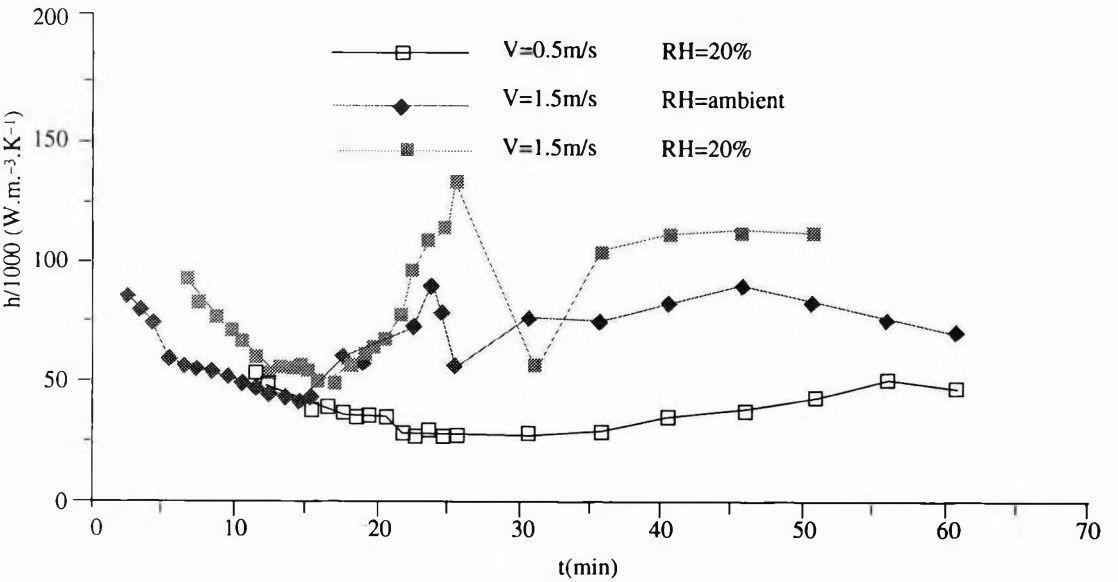

Figure 9b. Variations of h *at* T = *80°C (truncated curves).*

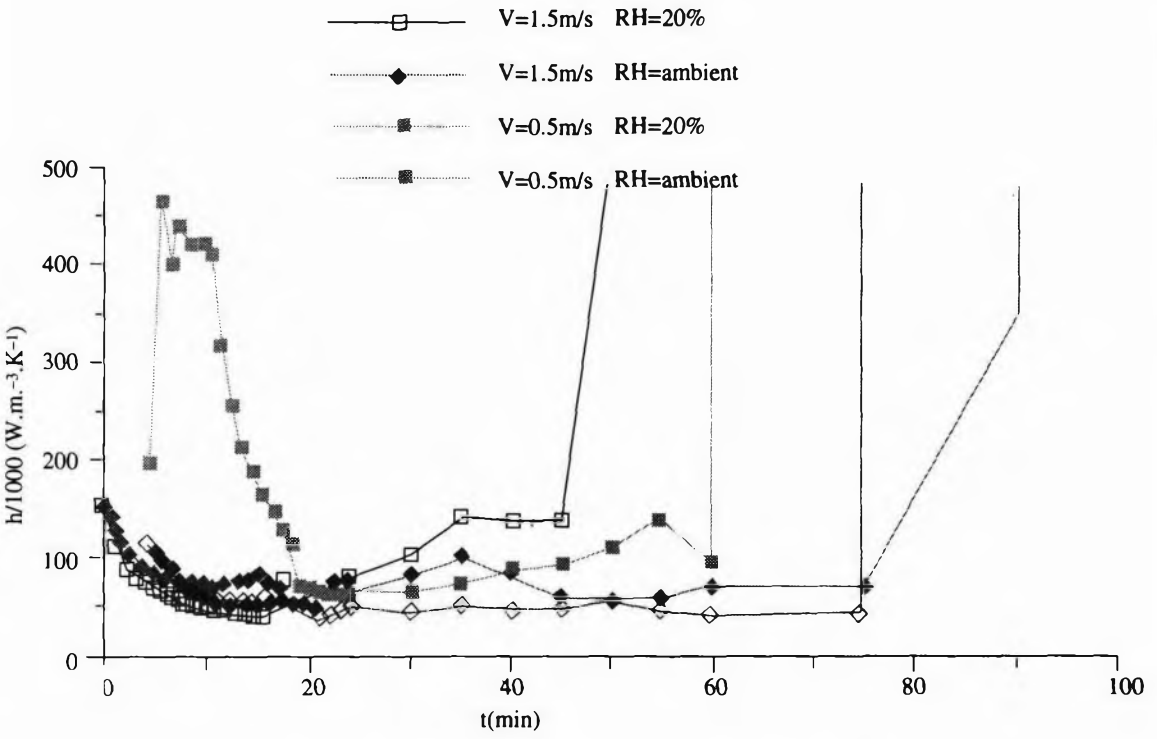

Figure 9c. Variations of h *at* T = *100°C (full curves).*

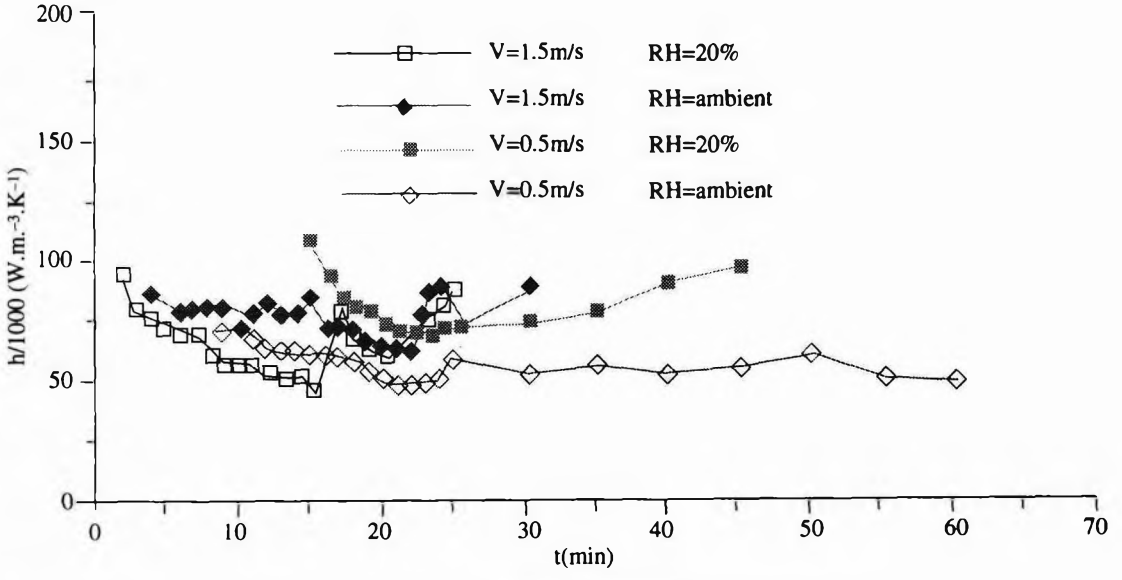

Figure 9d. Variations of h *at* T = *100°C (truncated curves).*

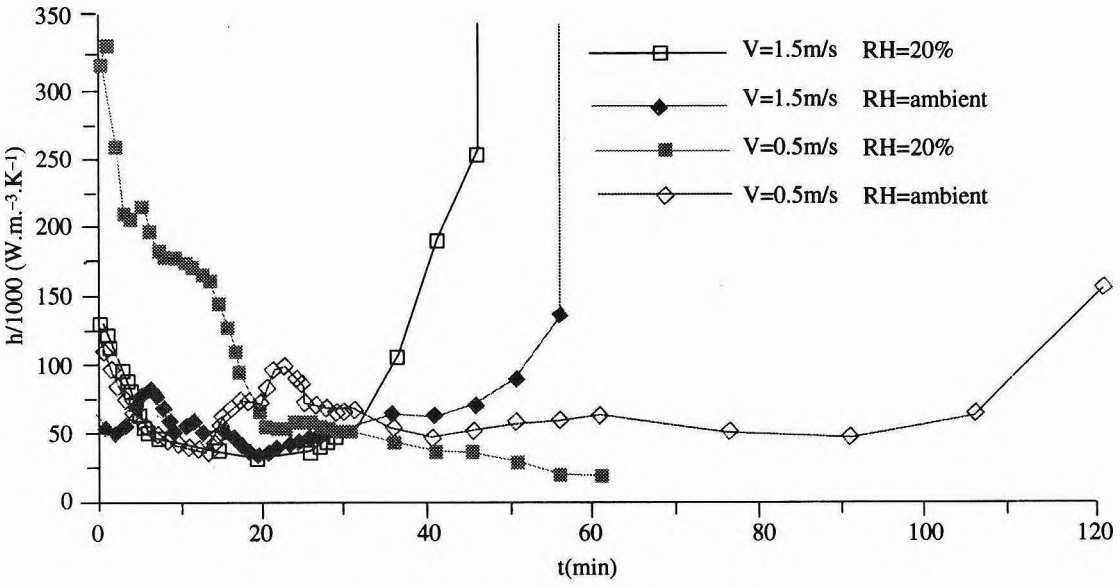

Figure 9e. Variations of h *at* T = *120°C (full curves).*

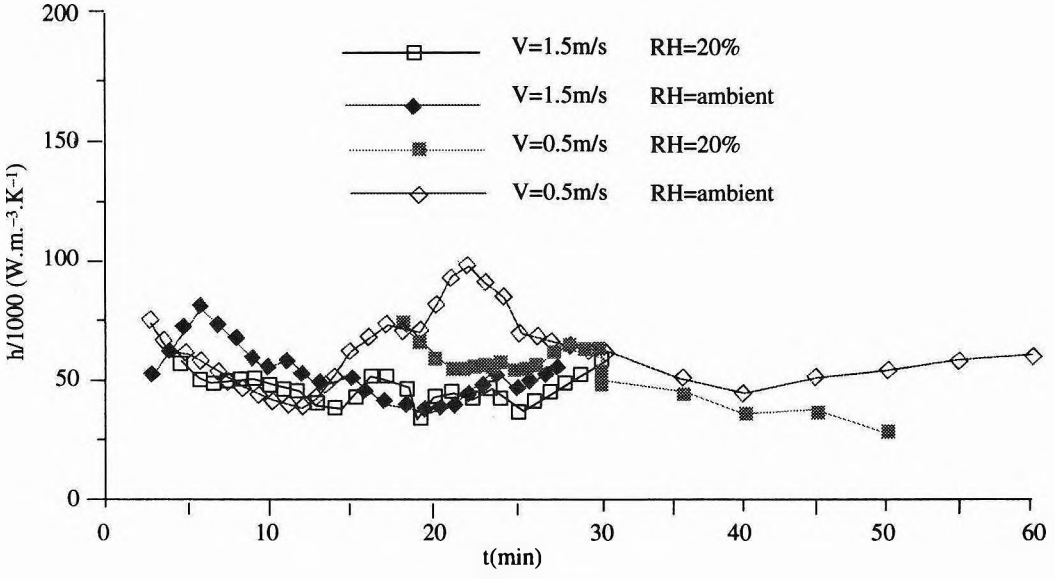

Figure 9f. Variations of h *at* T = *120°C (truncated curves).*

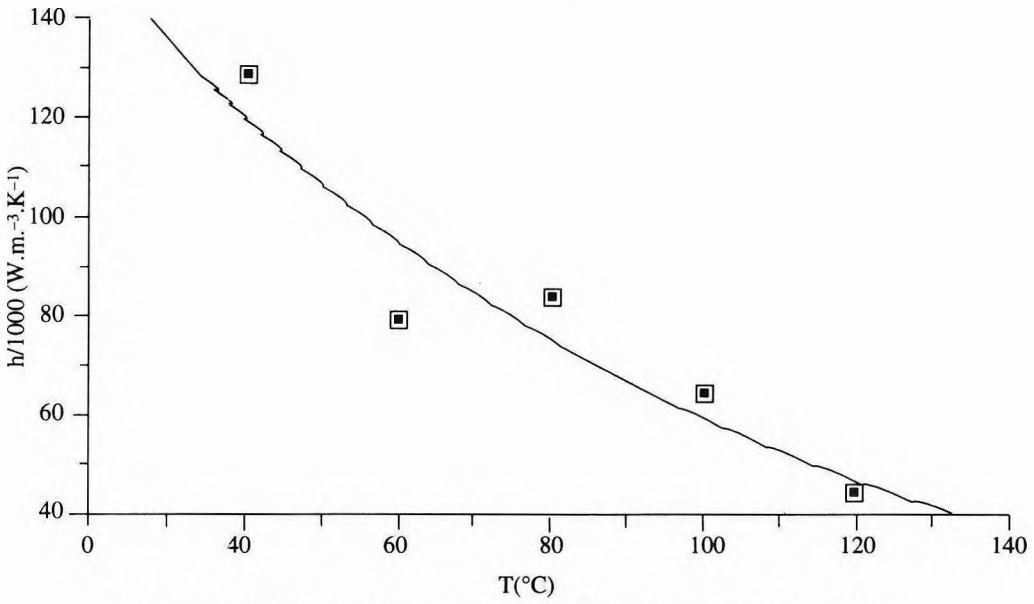

Figure 10. Variation of h *according to* T *at* V = *1.5 m/s and* RH = *20%.*

A study was performed to determine the influence of this parameter on the calculation of air and granule temperatures. Digital simulation of drying in thick layers performed for the purpose with values of *h* within the range mentioned above shows that movements of calculated temperatures are not very sensitive to *h*.

A fixed value of *h* was therefore chosen and set at 50 000W m^{-3} K^{-1}, whatever the test conditions.

CONCLUSION

Tests performed at a rubber production site using a portable laboratory drier were used to determine the matter and energy exchange coefficients during convective drying of natural rubber. These coefficients were used to activate a mathematical model giving the state of a granular medium (water content of the material, moisture content of the air, air and granule temperature and settling of the layer) according to the characteristics of the drying air and the direction of flow in each part of the drier.

Satisfactory validation of the model led to writing a simulation program for aid in the management and design of new rubber driers. Today, the optimisation of rubber drying using this model does not allow for the quality criteria that are increasingly important in sales. These criteria are the subject of ongoing research that should make it possible to establish links between drying conditions and rubber quality. These could subsequently be introduced in the model and thus complete the simulation program.

ACKNOWLEDGEMENTS

This research programme was financed by the Ministère de la Recherche et de la Technologie and was performed with assistance from the Centre de coopération Internationale en Recherche Agronomique pour le Développement - Cultures Pérennes (CIRAD–CP).

Date of receipt: September 1995
Date of acceptance: Febraury 1996

REFERENCES

1. SETHU, S. (1967) Through-circulation Drying of Particulate Natural Rubber I

Heveacrumb. *J. Rubb. Res. Inst. Malaysia*, **20(2)**, 65.

2. RIVASI, J. (1983) Contribution à l'étude des lois de séchage du caoutchouc sous forme de granulés. *Document CIRAD. CP : BP5035 34032* Montpellier Cedex1, France.

3. CAROMEL, G. (1984) Contribution à l'étude des lois de séchage du caoutchouc sous forme de granulés. *Document CIRAD.CP : BP 5035 34032* Montpellier Cedex1, France.

4. BUDIMAN, S. AND DALIMUNTHE, R. (1983) An effort to Improve the Drying of Crumb Rubber from Smallholders' Raw Materials. *Bulletin Perkaretan*, **2**.

5. AURIA, R. (1988) Contribution à l'étude de caoutchouc naturel: structure interne et transfert d'humidité lors du séchage. Thése de Doctorat de l'Université Montpellier II, Sciences et Techniques du Languedoc.

6. COUSIN, B. (1990) Séchage du caoutchouc naturel sous forme de granulés - Analyse théorique et expérimentale des processus internes. Thése de Doctorat de l'Université Montpellier II, Sciences et Techniques du Languedoc.

7. NAON, B. (1994) Séchage du caoutchouc naturel sous forme de granulés: cinétiques, modélisations, applications. Thése de Doctorat de l'Université Montpellier II, Sciences et Techniques du Languedoc.

8. NAON, B., SAIX, C., BERTHOMIEU, G. AND BENET, J.C. (1995) Modelling Convective Drying of Granular Materials: Application to Natural Rubber. *Drying Technology*, **13(3)**, 571.

9. PLATT, D., RUMSEY, T.R. AND PALAZOGLU, A. (1991) Dynamics and Control of Cross-flow Grain Dryers - Model Development and Testing. *Drying Technology*, **9(1)**, 27.

10. NAON, B., BERTHOMIEU, G., SAIX, C. AND BENET, J.C. (1994) Drying of Latex in Granule Form: Kinetics and Exploitations. IDS '94 *Australia, August 14, 1994*, **Vol.A**, 639.

11. NAON, B., BERTHOMIEU, G., BENET, J.C. AND SAIX, C. (1995) Improvement of Industrial Drying of Natural Rubber Through Analysis of Internal Transfers. *Drying Technology*, **13(8 & 9)**, 1807.

12. BENOIT, J.M. (1994) Séchage convectif de matériaux granulaires: application au caoutchouc naturel. *D.E.A. Mécanique des matériaux, structure, génie des procédés, Université Montpellier II, Sciences et Techniques du Languedoc.*

13. BUDIMAN, S. (1973) Water Removal from Natural Rubber Hydrogel. M.Sc. Thesis, Ohio State University.

14. AURIA, R. AND BENET, J.C. (1990) Transport de l'eau dans une feuille de caoutchouc naturel pendant la période de séchage à vitesse décroissante. *Int. J. Heat Mass Transfer*, **33(9)**, 1885.

15. AURIA, R., BENET, J.C., COUSIN, B. AND SAINTE BEUVE, J. (1991) Drying of Natural Rubber in Sheet Form — Internal Structure and Water Transfer. *J. nat. Rubb. Res.*, **6(4)**, 267.

16. COUSIN, B., BENET, J.C. AND AURIA, R. (1993) Experimental Study of the Drying of a Thick Layer of Natural Crumb Rubber. *Drying Technology*, **11(6)**, 1401.

J. nat. Rubb. Res. **10(4)**, 242–254

Acid-Catalysed Hydrolysis of Epoxidised Natural Rubber: Gel Formation During Latex Epoxidation

D.S. CAMPBELL*# AND P.S. FARLEY

The accumulation of a gel phase in the bulk products of epoxidation of polyisoprene latices is shown to be strongly dependent on both the proton acidity of the epoxidation medium and on the extent of epoxidation within the particles of the latex. Comparison of the degree of swelling of the gel phase in a hydrocarbon solvent and in a solvent which is capable of acting as a hydrogen bond acceptor demonstrates that the gelation is largely the result of secondary interactions between polymer chains and that the incursion of permanent inter-chain ether links must be minimal under the usual conditions of preparation of epoxidised natural rubber.

Epoxidation of unsaturated polymers has been widely investigated[1,2]. The chemical reaction is, at first sight, simple and has attractions of offering low reagent costs if a process can be based on hydrogen peroxide[3]. The epoxide ring can also be transformed to other oxygenated polymer modifications by secondary reactions[2].

This potential for subsequent reaction represents a constraint to large scale preparation of the parent epoxidised material[4]. The current process for production of epoxidised natural rubber (ENR) from natural rubber (NR) latex, using formic acid and hydrogen peroxide must minimise the secondary reactions in order to generate materials which offer good vulcanisate properties[4,5] and which have processing behaviour acceptable in factory operations[6]. The incursion of secondary reactions gives rise to an increase in Mooney viscosity of the dried rubber and an increase in its 'gel' content[6].

Secondary chemical reactions of epoxide groups can be considered as a spectrum of interactions with nucleophile-electrophile pairs[7]. In general, epoxide groups from isoprenic polymer units are more susceptible to the electrophilic influence than are those from butadiene units, but the interaction of the nucleophilic component remains relevant in determining the reaction products:

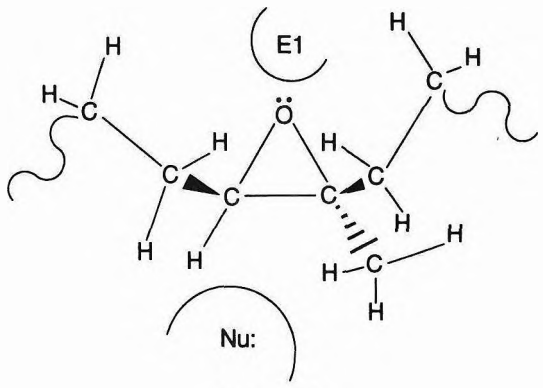

Scheme 1

In the context of the formic acid/hydrogen peroxide epoxidation process, the relevant electrophile is protic acid. Participation of water as nucleophile will result in formation of 1,2-diol (*i.e.* hydrolysis) but other oxygenated species can be involved. Thus interaction with the formate moiety of formic acid will generate hydroxyformate and interaction with adjacent epoxide rings will generate expanded cyclic ether structures[4,8]. This latter process is acid catalysed in epoxidised polyisoprenes but is base catalysed in epoxidised polybutadienes[9]. The nucleophilic attack can also take place at a hydrogen atom on carbon adjacent to the epoxide ring rather than a carbon atom of the ring itself[10,11].

*Malaysian Rubber Producers' Research Association, Brickendonbury, Hertford SG13 8NL, United Kingdom
#Corresponding author

If the nucleophile is on a separate molecular chain (*e.g.* an alcohol derived from the polymer by a previous hydrolysis reaction, or an epoxide ring) the reaction will result in the formation of a permanent ether linkage between the polymer chains. This process will have a profound effect on Mooney viscosity at very low extents of reaction and will quickly generate permanent gel. The reaction has been invoked as being directly responsible for the rapid increases in modulus that can occur on mixing of ENR and ageing of its vulcanisates if proper precautions are not taken to avoid acidic conditions[12]. Its incursion has been inferred in the production of raw rubbers when sufficient attention is not paid to controlling the bulk viscosity of the product[6,8].

Given this diversity of chemical reactivity, it is not surprising that the production of epoxidised natural rubbers requires good control of reaction conditions in order to meet processing specifications for the product[6]. It is also apparent that the balance of secondary reactions is intimately related to the local concentrations of reactants around the epoxide groups. Reaction in latex requires transfer of reagents from the aqueous phase into particles of rubber. The epoxidation step, and any secondary reactions, occur in a solvent-free rubber matrix which contains performic acid, formic acid, water and hydrogen peroxide at low concentrations. Solution chemistry of model compounds therefore has limited utility in guiding the optimisation of reaction conditions for the production process and in predicting the relative importance of the secondary reactions. Some close attention has already been given to the kinetics of consumption of hydrogen peroxide in this reaction system[13,14]. The present paper is concerned with the formation of gel fraction. It attempts to define more closely the conditions under which gelation occurs and the chemical structure of the gel phase.

EXPERIMENTAL

Epoxidations with Formic Acid and Hydrogen Peroxide

Latices were Malaysian high ammonia (HA) latex concentrate, deproteinised NR latex (DPNR latex, gel content 54%, 0.04% nitrogen on total solids) prepared by enzymic digestion of the HA concentrate[15] and synthetic polyisoprene latex, Maxprene IR-900 (Seitetsu Kagaku Co. Japan; gel content 0%, 92% *cis*-1,4-). The latices were stabilised with either Texofor FN 30 or Texofor A30 (ABM Chemicals) polyethylene oxide condensate stabilisers at a concentration of 3 p.p.h.r. and were allowed to equilibrate for at least 30 min before preparation of reaction mixtures. Formic acid (BDH Reagent grade, 90%, w/w, diluted with the distilled water required to adjust the final d.r.c. of the reaction mixture) was added slowly to the latex at the reaction temperature, followed by rapid addition of the hydrogen peroxide (Interox Chemicals, 60.7% w/v). Compositions of the reaction mixtures are summarised in *Table 1*.

Aliquots of reaction mixture (5 ml) were diluted to 100 ml with distilled water for estimation of residual hydrogen peroxide with cerium (IV) sulphate (BDH Convol, 0.05 *M*) and ferroin indicator or were coagulated in methylated spirits containing 2 *M* aqueous sodium hydroxide in stoichiometric excess over the formic acid in the sample. Coagulated samples were leached in distilled water and dried in vacuo at 50°C.

Reaction of Gel-free Epoxidised IR Latex with Formic Acid

Gel-free epoxidised latices were prepared at 0°C from stabilised Maxprene IR-900 (35 g, 0.32 mol isoprene unit) by addition of appropriate molar quantities of peracetic acid free from sulphuric acid (Interox, 38% w/w, redistilled) and allowing reaction to proceed to completion (24 h). Formic acid (BDH, Reagent grade, 90% w/w; 3.11 g, 19 mol %) was added and the latices were then heated at 60°C. The compositions of the reaction mixtures are summarised in *Table 2*. A reaction mixture at 30% d.r.c. and 40 mol % epoxidation was colloidally unstable at 60°C, due to the relatively high concentration of product acetic acid. Samples of rubber were recovered periodically by coagulation in methylated spirits containing aqueous sodium hydroxide, as described above.

TABLE 1. LATEX EPOXIDATION RECIPES

Reaction No.	HA	DPNR		IR-900		
		1	2	1	2	3
Latex d.r.c. (%)	59	53	–[a]	63	63	63
Reaction d.r.c. (%)	28.0	26.7	24.5	29.1	33.9	33.9
Reaction temp. (°C)	60	60	60	60	35	35
Formic acid (mol%)[b]	18.8	18.8	60.0	18.8	23.4	23.4
Hydrogen peroxide (mol%)[b]	76.7	77.1	49.8	76.3	36.9	73.7

[a] Epoxidation was carried out directly on the enzyme-digested HA latex without prior re-centrifugation.

[b] Mol per 100 mol of isoprene repeat unit. Initial molar concentrations in the aqueous phase of the reaction mixture are given by the expression:

mol % × d.r.c. (100 – d.r.c.) × 1.05/6.8

where d.r.c. is the reaction d.r.c., 1.05 is the average density for the aqueous phase in the reaction mixtures and 6.8 is derived from the repeat unit molecular weight of polyisoprene.

TABLE 2. REACTION MIXTURES FOR THE TREATMENT OF PRE-EPOXIDISED IR-900 LATEX WITH FORMIC ACID AT 60°C

Reaction No.	IR-900/4	IR-900/5	IR-900/6	IR-900/7	IR-900/8	IR-900/9	IR-900/10
Reaction d.r.c. (%)	18	18	18[a]	18[a]	30	30	30
Epoxide (mol %, (theoretical)	9.7	24.2	34.0	48.6	9.7	24.3	34.0
Epoxide (mol %, ^{1}H-NMR)	–	–	–	46.0	10.0	23.5	32.0
Formic acid (mol/l aq. phase)	0.65	0.65	0.65	0.65	1.23	1.23	1.23

[a] Reactions in duplicate

Equilibrium Volume Swelling Measurements

Accurately weighed samples of rubber (0.04 g – 0.08 g) were immersed in n-decane (BDH, Reagent grade, 2 cm^3) or di-n-butyl ether (BDH Reagent grade, 2 cm^3) and allowed to swell for 68 h at 25°C. The gel was collected on lens tissue, rinsed with fresh swelling agent and weighed, then dried in vacuo at 50°C to constant weight. No correction was made for sol rubber equilibrated in the swollen gel.

Gel Content and GPC Analysis

Gel contents of dried rubber samples were determined as part of a standardised procedure for gel permeation chromatographic (GPC) analysis. Redistilled, de-oxygenated tetrahydrofuran (THF, 8.0 cm^3) containing 2,6-di-tert-butyl-4-methyl phenol (BHT, 0.005% w/v) was added to an accurately weighed sample of rubber (0.03 g) in a 10 cm^3 volumetric flask. After 65 h at room temperature in the dark, the mixture was agitated and made up to volume. Discrete pieces of macro-gel were removed by filtration through lens tissue and the microgel was separated by centrifugation at 54 000 g for 60 min. A weighed aliquot (3 cm^3) was dried rapidly at 100°C and reweighed to give the weight of sol. Gel content was obtained by difference. GPC analysis of the solution was on a set of two 60 cm mixed-bed PL Gel columns (Polymer Laboratories) at a flow rate of 0.5 cm^3/min with UV detection at 215 nm. The hydrodynamic constants for NR were used in translating elution time to molecular weight. No provision was made for the modest change in these constants which occurs as the level of epoxidation increases.

RESULTS AND DISCUSSION

Reaction Rate for Epoxidation of Polyisoprene Latices

The rate of consumption of hydrogen peroxide in formic acid/hydrogen peroxide epoxidation of the polyisoprene latices was not markedly dependent upon the type of latex (*Figure 1*). The observation is consistent with the

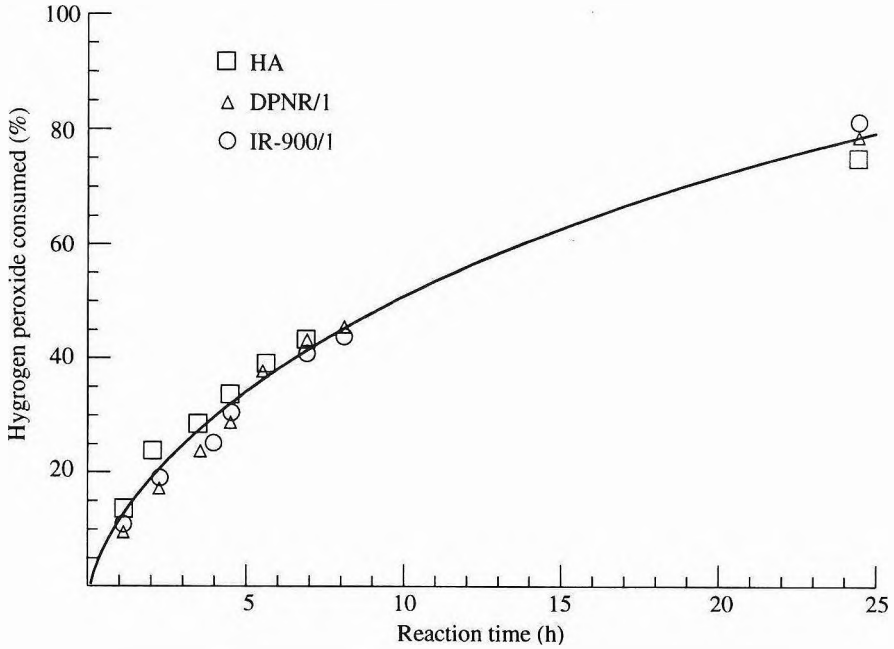

Figure 1. Conversion of hydrogen peroxide with time for reactions.

accepted kinetics[13,14], which indicate rate-determining formation of peroxyformic acid in the aqueous phase. The efficiency of conversion of hydrogen peroxide to epoxide was not determined directly for these three reactions. Previous work[16] has shown that efficiency is in the region of 85% provided the iron concentration in the latex is not in excess of 2 p.p.m. – 3 p.p.m. The slight tendency for the HA latex reaction to be faster at early reaction times, when compared with the DPNR and IR-900 latices may reflect a small amount of hydrogen peroxide decomposition caused by the natural iron content.

Table 3 illustrates the development of gel (as determined by the procedure for sample preparation prior to GPC analysis) as the reactions progress. The procedure did not distinguish between microgel that was formed during the epoxidation process, and macrogel which could only be formed after coagulation of the latex. Specific efforts were made to minimise gelation after sampling by coagulating samples directly into excess alkali. At intermediate gel contents, the scatter in the measurements is high and it is difficult to define the detailed response of the NR latices. The initial drop in gel content does appear to be real, as does the lower gel content for HA latex compared with DPNR latex at long reaction time. The IR-900 latex contained essentially no gel up to 6 h reaction but had a high gel content at long reaction time.

A more precise picture of the accumulation of gel was obtained from a further study of IR-900 latex (*Figure 2*). The reaction rate was manipulated (by adjustment of acid concentration, reaction d.r.c. and reaction temperature[14]) to allow more convenient sampling at intermediate stages of gelation. The two reactions were at identical dry rubber content and acid concentration but differed in the molar ratio of hydrogen peroxide to rubber double bonds (*Table 1*). Both reactions followed smooth conversion curves, similar to those in *Figure 1*. The times to 75% conversion of the hydrogen peroxide were 31 h and 46 h for the high and low peroxide concentrations, respectively. There was a well defined delay before the start of gel formation in each case. Although the reaction giving lower maximum epoxidation apparently formed gel more readily, the effect is a reflection of the longer time of exposure of the epoxide to acid conditions at the lower epoxidation rate. The times to the first detection of gel were 24 h and 46 h for the high and low peroxide loadings, respectively.

Figure 2 indicates that the gelation process is influenced by both reaction time and epoxide content but gives no measure of the expected influence of acid concentration in the aqueous phase. In a separate series of measurements (*Table 2*), samples of epoxidised IR-900 latex were prepared with peroxyacetic acid at low

TABLE 3. GEL FORMATION IN REACTIONS OF HA, DPNR AND IR-900 LATICES

Reaction time (h)	% gel in THF for reaction no.		
	HA	DPNR/1	IR-900/1
0	58	45	0
1	34	18	0
2	37	23	0
3	36	21	0 [a]
4	40	29	2
5	37	15	–
6	39	29	1
24	65	94	91

[a] Sampled at 3.5 h

temperature and were subsequently exposed to formic acid at 60°C. The gel contents in THF, for samples coagulated into excess alcoholic alkali, are recorded in *Figures 3* and *4*. The two series of experiments differed in the d.r.c. of the reaction mixtures and in the molar concentration of formic acid in the aqueous phase but not in the molar ratio of formic acid to isoprene units (or epoxide groups, at equal extents of epoxidation). At 10 mol% epoxidation, gelation was only detected at long reaction time. As the extent of the epoxidation was increased, gelation rate increased at constant acid concentration. At constant extent of epoxide, gelation rate increased with increasing acid concentration in the aqueous phase. The behaviour of material with 34 mol% epoxidation in 0.65 *M* acid (*Figure 3*) approximates to that of material with 24 mol% epoxidation in 1.23 *M* acid (*Figure 4*). At the highest extents of epoxidation, substantial gelation occurred at room temperature as the nominal 'zero time' samples were being prepared. It is inappropriate to attempt to interpret these results in terms of more formal rate constants for reactions of the epoxide groups. Percentage gel is not necessarily directly proportional to extent of chemical reaction because the generation of a second interaction between a pair of chains that are already linked does not increase the gel content.

The pattern of behaviour in *Figures 3* and *4* is entirely consistent with the observed induction periods for gel formation in *Figure 2* and with the technological observation that high Mooney viscosity and high gel content are specifically associated with ENR 50 preparation and not with ENR 25 preparations[6].

Crosslink Density in ENR Gel

The interpretation of 'gel content' is a matter of some complexity[17–20]. In addition to the mechanical differentiation between microgel and macrogel, there are known effects of solvent when measurements are carried out on parent

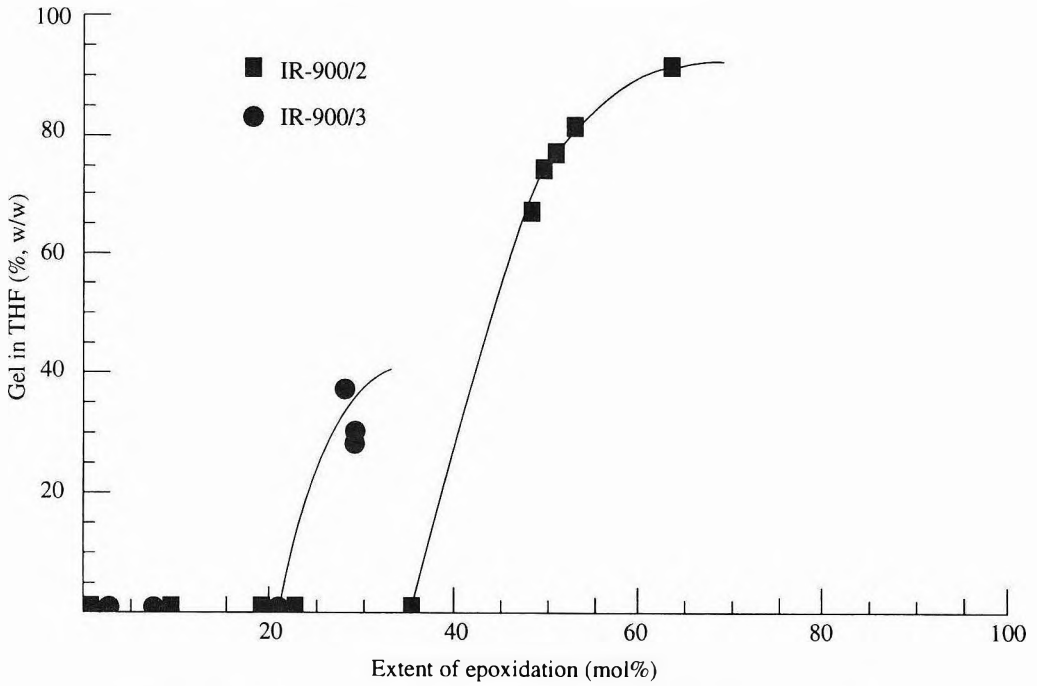

Figure 2. Gel content in THF versus *extent of epoxidation for reactions.*

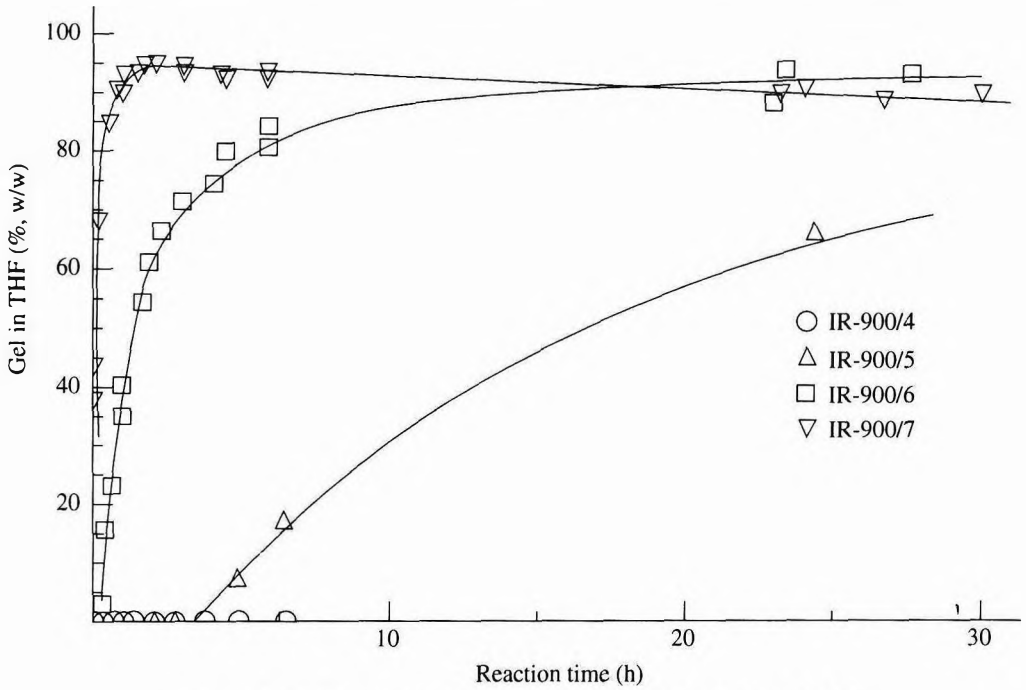

Figure 3. Gel formation in pre-epoxidised IR-900 latex at 60°C.

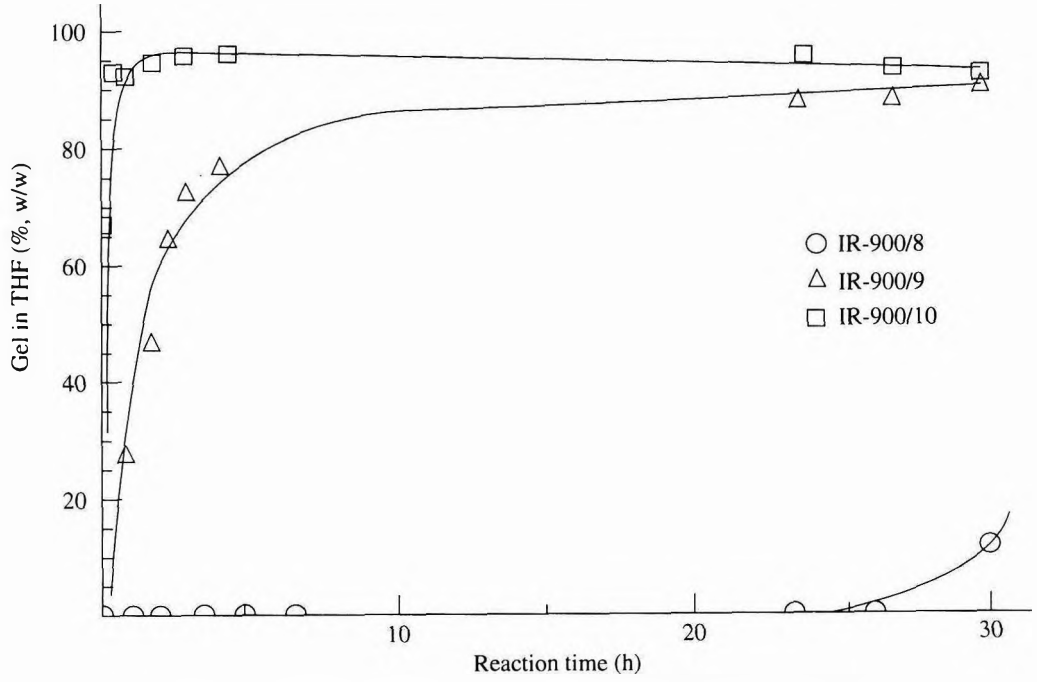

Figure 4. Gel formation in pre-epoxidised IR-900 latex at 60°C.

NR. For example, Baker[18] reports high gel contents in light petroleum for rubber from freshly tapped latex whereas Subramaniam[21] reports very low gel contents in tetrahydrofuran for similar, freshly tapped rubber. It is also known[18,19] that the presence of alcohols and carboxylic acids in the solvent can substantially affect the result. These effects are believed to arise from the disruption of specific secondary interactions (dipolar and hydrogen bonding) between polymer chains containing low concentrations of non-hydrocarbon structures[20]. The opportunity for secondary interactions can be expected to increase with increasing epoxidation during the preparation of ENR, particularly if ring-opening reactions of the epoxide groups occur.

In the present work, two contrasting indications of chain interaction were obtained by measuring the equilibrium volume swelling of samples of epoxidised rubber in n-decane and in di-n-butyl ether as a function of extent of epoxidation (*Figure 5*). The samples were prepared under conditions of exceptionally high formic acid concentration (reaction DPNR/2, *Table 1*) and attained >70% conversion of the hydrogen peroxide within 6 h at 60°C. Some coagulation occurred during the reaction under these conditions but coagulum was rejected from the samples taken for analysis. The two swelling solvents have similar solubility parameters (15.9 $MPa^{1/2}$ for n-decane[22] and 16.0 $mPa^{1/2}$ for di-n-butyl ether[23])[a] when classified as non-interacting solvents and the values are sufficiently close to that for NR (16.9 $MPa^{1/2}$)[24] to make them good swelling agents for NR. Di-n-butyl ether is a non-interacting solvent in the sense that it has a low dipole moment (1.17 D) and cannot act as a hydrogen bond donor. It can, however, act strongly as a hydrogen bond acceptor towards any hydroxylic material present on the polymer. It is this property which is the probable cause of the marked difference in behaviour of the two solvents in *Figure 5*.

An interpretation of the results in *Figure 5* in terms of the number of effective crosslink sites (or the molecular weight of the polymer chains between effective crosslinks) has to take into account the variation of the solubility parameter of the polymer as the extent of epoxidation increases[24]. The change in solubility parameter can be represented by the relationship:

$$\delta = (16.9 + 0.024 \times \text{mol\% epoxidation})\ MPa^{1/2} \quad ...1$$

which gives a range of 16.9 to 17.9$MPa^{1/2}$ for the materials represented in *Figure 5*. The data on which this relationship is based were obtained from measurements in solvents which were classified as non-interacting[24]. Many of them were, however, oxygenated hydrogen bond acceptors and should behave similarly to di-n-butyl ether when hydroxylic groups are present on the polymer chains. With this knowledge, it is possible to evaluate the Flory-Rehner solvent-polymer interaction coefficient (χ) at different levels of epoxidation from the relationship[23]:

$$\chi = 0.34 + (V_0/RT)(\delta_1 - \delta_2)^2 \quad ...2$$

where V_0 is the molar volume of the solvent, R is the gas constant, T the absolute temperature and δ_1 and δ_2 are the solubility parameters of the solvent and polymer, respectively. Effective crosslink density at different stages of the reaction can then be deduced, with due allowance for the change in χ, from the relationship[25]:

$$M_c = -\rho\, V_0 v_r^{1/3}/(\ln(1-v_r) - v_r - \chi v_r^2) \quad ...3$$

where M_c is the number-average molecular weight of the polymer chains between effective (tetrafunctional) crosslinks, ρ is the polymer density and v_r is the volume fraction of rubber in the swollen gel at equilibrium.

[a] An error has been perpetuated through editions of the *Polymer Handbook* for the solubility parameter of n-decane. The value given in the *Handbook* is not consistent with the values for other n-alkanes.

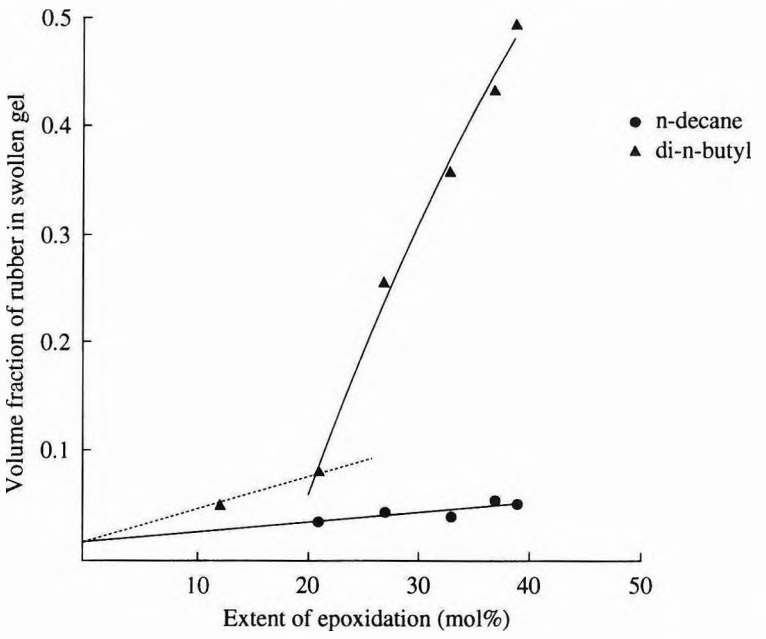

Figure 5. Equilibrium volume swelling of total polymer sample in n-decane and di-n-butyl ether as a function of extent of epoxidation. Reaction DPNR/2.

An attempt to apply these calculations to the data for volume swelling in di-n-butyl ether falls foul of difficulties with numerical precision at the very high degrees of swelling that are observed (*Figure 5*). A qualitative interpretation is that the value of M_c is of the order of 10^6 daltons throughout the range of samples; *i.e.*, there are only a very few effective crosslinks per polymer chain. The same calculations for swelling in decane give the results in *Figure 6*. Below 20 mol% epoxidation the estimate of effective crosslinking is of the same order as for di-n-butyl ether swelling and has the same high level of uncertainty. Thereafter, chain interactions which cannot be disrupted by the hydrocarbon solvent appear in increasing amounts.

The swelling results in decane demonstrate that the total density of interacting sites can reach the equivalent of full vulcanisation crosslinking in the range of epoxidation of interest in technological ENR usage. However, the swelling results in di-n-butyl ether show that, even under the forcing acid conditions used in the preparation of this series of samples, only about 1% of these interactions can be ascribed to permanent covalent crosslinking of the polymer chain. In considering these results, it is necessary to avoid the confusion that high gel content in THF (δ = 16.8 $MPa^{1/2}$; a hydrogen bond acceptor solvent), as determined in GPC measurements, reflects high levels of permanent covalent crosslink formation. Only one crosslink site per polymer molecule is required to produce 100% gel.

The conclusions reached in this section help to rationalise observations made by Lee and Porter[26] on the behaviour of solution-epoxidised NR and materials derived from it. These authors reported that samples of epoxidised NR recovered by precipitation from solution epoxidations could be readily re-dissolved immediately after precipitation but had high apparent gel contents if stored for some time before attempted re-dissolution. Re-dissolution of gelled material could, however, be greatly facilitated by addition of a trace of formic acid.

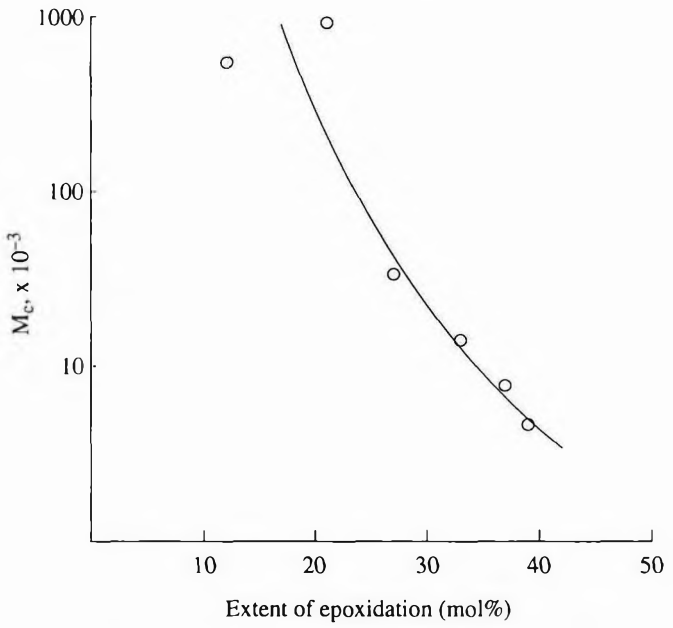

Figure 6. Apparent molecular weight between crosslinks at different extents of epoxidation from degree of swelling in decane. Reaction DPNR/2.

Small amounts of hydroxylation produced in solution are likely to be solvated either by intra-chain association or by low molecular weight solute molecules. Storage of the dry rubber will offer opportunity for rearrangement of these associations, and the formation of inter-molecular interactions which will only be disrupted if appropriate re-solvation conditions are provided. Formic acid will be an effective catalyst for redistribution of hydrogen bond interactions from inter-chain interactions back to intra-chain or polymer-small molecule interactions.

GPC Characterisation of Sol Rubber

Polymer molecular weight and molecular weight distribution are recognised as of high importance in the processing of raw polymers. There is therefore some temptation to use molecular weights as determined by GPC analysis in monitoring ENR production. The approach has little justification when formation of gel fraction is an inherent part of the production process because of the expected distortion of the sol molecular weight distribution by purely statistical factors governing the preferential incorporation of larger molecules into the gel network[27]. Although this distortion can be qualitatively appreciated for the NR latex epoxidation process, it is not easy to obtain direct experimental evidence to support it. In the course of the measurements on gelation of pre-epoxidised IR-900 latices it has been possible to obtain such evidence. The polyisoprene in Maxprene IR-900 has a strongly bimodal molecular weight distribution, with a low molecular weight component centred around 100 000 daltons. The molecular weight distribution of this component remains essentially unchanged during epoxidation and during the accumulation of gel fraction in the presence of formic acid. On the other hand the high molecular weight component, although unaffected by the epoxidation process as such, is lost almost entirely as the extent of gelation approaches 60% (*Figure 7*). The results are presented with the response at the maximum of the low molecular weight component normalised, *i.e.* it is assumed

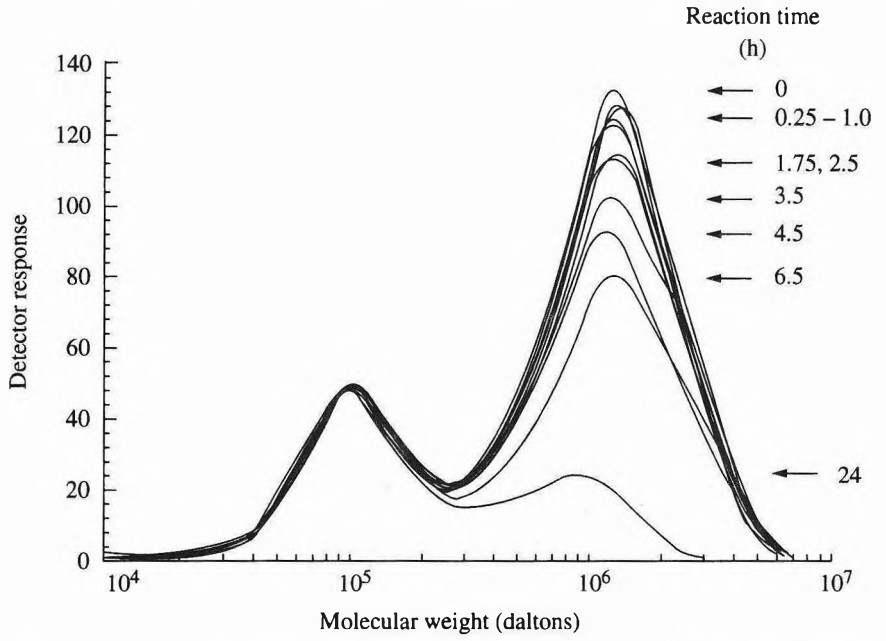

Figure 7. Molecular weight distribution of sol fraction at different reaction times for reaction IR-900/5.

that there has been no incorporation of this component into the gel. The justification offered for this assumption is that the shape of the distribution over this molecular weight range would be expected to change to a greater extent than it does if incorporation occurred. It is interesting that the depletion of the high molecular weight component becomes apparent before gel is detected in the sol-gel separation procedure. At an early stage in the process material is formed which is resistant to removal by centrifugation at 54 000 g but which does not pass through the GPC column.

Spectroscopic Characterisation of the Gelation Process

Several authors have discussed the NMR and IR characterisation of epoxidised polyisoprenes and of the secondary reaction products that are formed from them[8,13,28–31]. Within these discussions, the detection of ether crosslinks has received some passing comment. From the results presented in this paper, it becomes apparent that the likelihood of obtaining positive spectroscopic identification of ether crosslinks in the raw epoxidised rubbers prepared for technical use is very remote at the present time. At an Mc of the order of 1×10^6, only about 1 in 15 000 repeat units are involved as crosslink sites. On the other hand, secondary interaction sites can attain concentrations of 1 in 100 repeat units or higher and their identification is viable. In the present work, ^{1}H- and ^{13}C- NMR signals were observed in reaction products which were consistent with the published information for polymer-bound alcohol and cyclic ether groups but the signal intensities were low and for this reason no refinement of the assignments was made.

CONCLUSIONS

'Gelation' of NR during the process of latex epoxidation with formic acid and hydrogen peroxide is dependent on the extent of epoxidation, the concentration of acid and the time of exposure to the acid. In broad terms, the

gelation can be held responsible for increased bulk viscosity of the technical raw rubbers relative to NR, but a clear distinction must be drawn between the formation of measurable amounts of permanent ether crosslinks by acid catalysed inter-chain ring opening reactions of the epoxide and the occurrence of secondary (hydrogen bonding) interactions between the chains. The differentiation can be made by volume swelling measurements in a non-interacting (hydrocarbon) solvent and a hydrogen bond acceptor solvent (di-n-butyl ether). Permanent covalent crosslinks sites remain at the level of 1 in 15 000 repeat units even under forcing acidic conditions, whereas secondary interaction sites are as high as, or greater than conventional vulcanisate crosslink densities. High viscosity in poorly controlled preparations of ENR can be ascribed almost entirely to the secondary interactions which arise from hydroxylation associated with the different modes of epoxide ring opening.

ACKNOWLEDGEMENTS

The authors thank Dr A.D. Edwards of the Materials Characterisation Group, Tun Abdul Razak Laboratory, for his co-operation in obtaining the GPC information. Part of this work was performed in the course of post-graduate studies (by P.S.F.) for the award of the degree of PhD at Christopher Ingold Laboratories, University College London.

REFERENCES

1. GREENSPAN, F.P. (1964) Reactions of Unsaturated Polymeric Hydrocarbons, E. Epoxidation. *Chemical Reactions of Polymers (Fettes, E.M. ed.)*, New York: Interscience Publishers.

2. SCHULZ, D.N., TURNER, S.R. AND GOLUB, M.A. (1982) Recent Advances in the Chemical Modification of Unsaturated Polymers. *Rubb. Chem. Technol.*, **55**, 809.

3. GELLING, I.R. (1981) Epoxidised Natural Rubber. *Brit. Pat. No.2113692.*

4. GELLING, I.R. (1985) Modification of Natural Rubber Latex with Peracetic Acid. *Rubb. Chem. Technol.*, **58,** 86.

5. BAKER, C.S.L., GELLING, I.R. AND NEWELL, R. (1985) Epoxidised Natural Rubber. *Rubb. Chem. Technol.*, **58**, 67.

6. ABU BIN AMU AND SIDEK BIN DULNGALI (1989) Easy Processing Epoxidised Natural Rubber. *J. nat. Rubb. Res.*, **4**, 119.

7. BUCHANAN, J.G. AND SABLE, H.Z. (1972) Stereoselective Epoxide Cleavages. *Selective Organic Transformations, Vol.2 (Thyagarajan, B.S., ed.)*, New York: Wiley-Interscience.

8. PERERA, M.C.S., ELIX, J.A. AND BRADBURY, J.H. (1988) Furanized Rubber Studied by NMR Spectroscopy. *J. Polym. Sci., Pt. A, Polym. Chem.*, **26**, 637.

9. SCHULTZ, W.J., ETTER, M.C., POCIUS, A.V. AND SMITH, S. (1980) A New Family of Cation Binding Compounds: threo-αω-Poly(cycloalkane)diyl. *J.Amer. Chem. Soc.*, **102**, 7981.

10. CAMPBELL, D.S. (1973) Exchange Reactions as a Basis of Thermoplastic Behaviour in Crosslinked Polymers. *Br. Polym. J.*, **5**, 55.

11. LEE TONG KOOI (1980) Effect of Chemical Modification on the Low-temperature Crystallisation Behaviour of Natural Rubber. PhD Thesis, University of London.

12. GELLING, I.R. AND MORRISON, N.J. (1985) Sulfur Vulcanization and Oxidative Ageing of Epoxidised Natural Rubber. *Rubb. Chem. Technol.*, **58**, 243.

13. GAN, L.H. AND NG, S.C. (1986) Kinetic Studies of the Performic Acid Epoxidation of Natural Rubber Latex Stabilised by Cationic Surfactant. *Eur. Polym. J.*, **22**, 573.

14. CAMPBELL, D.S. (1989) The Relevance of Phase Heterogeneity in Epoxidations Using Formic Acid and Hydrogen Peroxide. *Proc. Int. Conf. Polym. Latex, III*, paper17. London: The Plastics and Rubber Institute.

15. SMITH, J.F. (1974) Treatment of Rubber. *Brit. Pat. No. 1366934.*

16. FARLEY, P.S., BANTHORPE, D.V. AND PORTER, M. (1992) Effect of Adventitious Iron on Epoxidation of Natural Rubber Latex. *J. nat. Rubb. Res.*, **7**, 157.

17. KEMP, A.R. AND PETERS, H. (1941) Fractionation and Molecular Weight of Rubber and Gutta Percha. *Ind. Eng. Chem.*, **33**, 1391.

18. BAKER, W.D. (1949) Microgel, a New Macromolecule. *Ind. Eng. Chem.*, **41**, 511.

19. BLOOMFIELD, G.F. (1954) Studies in *Hevea* Rubber, Part II. The Gel Content of Rubber in Freshly Tapped Latex. *J. Rubb. Res. Inst. Malaya*, **13**, 18.

20. ALLEN, P.W. AND BRISTOW, G.M. (1963) The Gel Phase in Natural Rubber. *J. Appl. Polym. Sci.*, **7**, 603.

21. SUBRAMANIAM, A. (1975) Molecular Weight and Other Properties of Natural Rubber: A Study of Clonal Variations. *Proc. Int. Rubb. Conf., Kuala Lumpur*, Vol. IV, p.3. Kuala Lumpur: Rubber Research Institute of Malaysia.

22. GORDON, J.L. (1964) Cohesive Energy Density. *Encyclopedia of Polymer Science. (Mark, H.F., Gaylord, M.G. and Bikales, N.M., eds.)*, Vol. 3, p.833. New York: John Wiley and Sons.

23. GRULKE, E.A. (1989) Solubility Parameter Values. *Polymer Handbook, 3rd Edition (Brandrup, J. and Immergut, E.M., eds.)*, p.VII/519. New York: John Wiley and Sons.

24. GELLING, I.R., TINKER, A.J. AND HAIDZIR BIN ABDUL RAHMAN (1991) Solubility Parameters of Epoxidised Natural Rubber. *J. nat. Rubb. Res.*, **6(1)**, 20–9.

25. FLORY, P.J. (1953) *Principles of Polymer Chemistry*. New York: Cornell University Press.

26. LEE, T.K. AND PORTER, M. (1979) Effect of Chemical Modification on the Crystallisation of Unvulcanized Natural Rubber at Low Temperatures. *Proc. Int. Rubb. Conf., Venice*, p.991.

27. ZHU, S. AND HAMIELEC, A.E. (1993) Kinetics of Network Formation *via* Free Radical Mechanisms - Polymerization and Polymer Modification. *Makromol. Chem., Macromol. Symp.*, **69**, 247.

28. NG, S.C. AND GAN, L.H. (1981) Reaction of Natural Rubber Latex with Performic Acid. *Eur. Polym. J.*, **17**, 1073.

29. BURFIELD, D.R., LIM, K.L., LAW, K.S. AND NG, S. (1984) Analysis of Epoxidised Natural Rubber. A Comparative Study of DSC, NMR, Elemental Analysis and Direct Titration Methods. *Polymer*, **25**, 995.

30. DAVEY, J.E. AND LOADMAN, M.J.R. (1984) A Chemical Demonstration of the Randomness of Epoxidation of Natural Rubber. *Brit. Polym. J.*, **16**, 134.

31. BRADBURY, J.H. AND PERERA, M.C.S. (1985) Epoxidation of Natural Rubber Studied by NMR Spectroscopy. *J. Appl. Polym. Sci.*, **30**, 3347.

J. nat. Rubb. Res. **10(4)**, 255–265

Determination of Dithiocarbamyl Compounds in Natural Latex Concentrate

CHOOI SIEW YUEN*

The carbon disulphide evolution procedure of determining dithiocarbamyl compounds was modified to a simple and practical method of assessing thiram (TMTD) and other dithiocarbamyl preservatives in natural latex concentrate.

TMTD and its breakdown product ZDMC (zinc dimethyldithiocarbamate) were detected by thin layer chromatography in the TMTD/ZnO (TZ) dispersion, but only TMTD was apparently observed in LA/TZ latex concentrate. It was proposed that for practical purposes of process control in the production of LA/TZ latex, the TMTD, existing either alone or with its breakdown product ZDMC, could be assessed as an overall amount of TMTD.

With the use of tetramethylthiuram disulphide and zinc oxide (TMTD/ZnO) system of preservation of low ammonia (0.2%) natural latex concentrate (LA/TZ) and field latex in the Malaysian rubber plantation industry, a method of analysis of TMTD is needed for process control to ensure correct addition, and for the monitoring of its residue in aged LA/TZ latex concentrate.

It has been reported that TMTD in the TMTD/ZnO (TZ) dispersion, and the LA/TZ latex concentrate breaks down to zinc dimethyldithiocarbamate (ZDMC). The ZDMC in the latex breaks down further to dimethylamine, ammonium thiocyanate, thiourea and zinc sulphide (the major product)[1].

Numerous methods for the determination of the individual dithiocarbamyl compounds are reported as reviewed by Lowen and Pease[2]. The method of carbon disulphide (CS_2) evolution has generally been recommended[2–9]. The dithiocarbamates when reacted with an acid give quantitative evolution of carbon disulphide which is converted to the xanthate and assessed by titration with iodine[2–4,9], or converted back to a dialkyl-dithiocarbamate, which is then assessed as a copper complex by spectrophotometric measurement[2,5–7]. A rather complex digestion-evolution-absorption train of apparatus is recommended by the Association of Official Analytical Chemists (AOAC) for their determination[9].

The method reported by Hillton and Newall[8] has been simplified and developed for the determination of the amount of TMTD and other dithiocarbamyl compounds in latex concentrate. The modified method uses a simple quickfit distillation set and a water-bath. The evolved carbon disulphide is flushed out, using a small volume of vaporised methanol, into an absorbing methanolic diethylamine solution to reform into the diethyldithiocarbamate. The colour formed between this compound and cupric acetate solution is assessed colorimetrically.

EXPERIMENTAL

Apparatus

A quickfit distillation apparatus, provided with a coil-condenser, a dropping funnel and an elongated adaptor-receiver, was used. Silicone grease was used at the joints for gas tight fitting.

Spectrophotometric measurements were made on a Bausch & Lamb 340 Spectronic 20 colorimeter using 1.9 cm tubes.

*Guthrie Research Chemara, Jalan Sungei Ujong, 70990 Seremban, Malaysia

Reagents

Analar methanol, phosphoric acid (BDH, SG 1.75), diethylamine (redistilled) and cupric acetate (BDH) were used. Used methanol was treated with sodium hydroxide pellets over-night and distilled in a vacuum rotary evaporator. The recovered methanol was acidified with phosphoric acid and fractionated (65°C – 66°C) over a 60 cm Vigreux column for re-use.

Commercial technical grade tetramethylthiuram disulphide (TMTD), tetrapentamethylenethiuram disulphide (RPTD), zinc diethyl dithiocarbamate (ZDC) and zinc dimethyldithiocarbamate (ZMDC) were recrystallised twice with chloroform-methanol mixture. High ammonia (HA) latex concentrate (0.8% ammonia, 61% dry rubber content) and field latex (0.2% – 0.5% ammonia, 30% dry rubber content) were used as matrices.

TMTD Standard Solution

25 mg of recrystallised tetramethylthiuram disulphide (m.p. 155°C – 156°C) was first dissolved in chloroform (2 ml) in a small beaker, washed with methanol into a 250 ml volumetric flask and made to the mark to give a 100 µg per ml stock solution. 1 ml – 7 ml of this solution were used for standardisation.

Standard Solutions of Other Dithiocarbamates

The same concentration (25 mg/250 ml methanol) as the TMTD standard solution was similarly prepared for each dithiocarbamate.

Diethylamine Solution

0.5 ml of redistilled diethylamine was diluted to 100 ml with methanol.

Cupric Acetate Solution

0.1 g of cupric acetate was dissolved in 100 ml of distilled water.

Calibration Procedure for the Determination of TMTD

Standard TMTD solution (1 ml – 7 ml) was pipetted into a round bottom flask (250 ml) and phosphoric acid (1 ml) was added prior to distillation. The flask was fitted to the stil-head of the quickfit distillation apparatus and placed over a boiling water-bath. A quickfit dropping funnel containing 15 ml methanol stoppered the opening of the still-head.

A 50 ml volumetric flask containing 15 ml of the 0.5% diethylamine was placed at the elongated adaptor-receiver end such that the tip of the latter just immersed below the surface of the diethylamine solution. The aqueous methanol mixture was heated 25 – 30 min for the decomposition of TMTD to CS_2.

At the end of the period 15 ml of methanol were dropped into the flask while having the receiver flask lowered momentarily to expose the tip of the adaptor-receiver. The vaporising methanol flushed the system of evolved CS_2.

As more methanol condensed the receiver flask was lowered maintaining the immersion of the tip of the adaptor-receiver. When most of the methanol (15 ml) had distilled over (5 – 10 min) the receiving flask was finally lowered from the receiver to allow the rinsing of the condenser and the latter by the methanol condensate. At the end of the distillation these two parts were again rinsed with methanol from a wash bottle.

Colour Development and Measurement

5 ml of the 0.1% aqueous cupric acetate was pipetted into the 50 ml volumetric flask and the volume made to the mark with methanol. The mixture was well shaken. A golden yellow to dark brown colour developed.

After 20 min to allow colour development the solution was filtered through cotton wool into a 1.9 cm Spectronic 20 colorimeter tube. The

absorbance was measured at 430 nm. The colour was observed to be stable even after 24 h.

All determinations were duplicated.

Calibration Procedure for the Determination of TMTD in the Matrix of Latex Concentrate

Calibration was carried out as before with 1 ml – 7 ml of the standard TMTD solution. HA latex concentrate (3g) was accurately weighed into a quickfit round bottom flask (250 ml). The flask was slowly rotated around an axis along its neck to form a thin latex film. Methanol (5 ml) was introduced to coagulate the film. Using a spatula the coagulum was detached from the flask wall and placed in a loosely folded lump at the bottom of the flask. 1 ml of phosphoric acid was pipetted into the flask for decomposition—distillation and the determination proceeded as described in the above calibration procedure.

Calibration of Other Dithiocarbamyl Compounds

RPTD was calibrated like TMTD, with and without the matrix of latex concentrate. ZDMC and ZDC were calibrated without a matrix of latex.

Repeatability and Recovery Studies

The precision of the method for each dithiocarbamyl compound was studied by carrying out duplicated determinations. Aged LA/TZ latices were used to assess the repeatability of the method for TMTD (*Table 1*). This also gave a study of the breakdown of TMTD in natural latex concentrate. Recovery tests were carried out by adding known amounts of each dithiocarbamyl standard solution to the latex concentrate, field and skim latices, with or without existing known amount of the dithiocarbamyl compound.

TABLE 1. REPEATABILITY STUDY OF METHOD USING 3 G LA/TZ LATEX CONCENTRATE SAMPLES OF VARIOUS AGES

Storage (weeks)	Amount of TMTD (μg) in 3 g samples LA/TZ latex concentrate		
	Sample		
	A	B	C
0	205	356	531
	202	358	536
	(204)	(357)	(534)
3	151	301	420
	148	296	416
	(150)	(299)	(418)
7	94	198	275
	96	194	284
	(95)	(196)	(280)
12	28	74	35
	29	70	37
	(29)	(72)	(36)

Figures in parenthesis denote mean

Effect of Latex Non–rubbers on TMTD Determination

To examine whether the rubber or the non-rubbers affect the determination of TMTD, a sample of HA latex concentrate (3 g) was coagulated with methanol (5 ml). The coagulum was removed, rolled and washed with water to remove as much of the trapped serum as possible. Determinations were carried out with 2 ml of the TMTD standard solution in the presence of the serum, coagulum, and purified rubber (derived from field latex that had been purified of its non-rubbers sequentially with detergent and water washing and partitioned by ultra-centrifugation), respectively. The absorbance readings are shown in *Table 2*.

To show whether there was interference from the decomposition distillate of the non-rubbers, a blank determination *a* of 5 g HA latex concentrate, and a determination *b* of 4 ml TMTD standard solution, were carried out as usual. In both cases the distillate-diethylamine mixtures were made to 50 ml without the addition of the cupric acetate solution. 20 ml of distillate-diethylamine mixture *a* were added to 20 ml that of *b*, and 5 ml cupric acetate solution were added for colour development. The mixture was made to 50 ml with methanol. Similarly, another 20 ml of distillate-diethylamine mixture *b* were reacted with 5 ml cupric acetate solution and made to 50 ml. The colour intensities of both mixtures were determined as usual and compared.

To examine the effect of the amount of non-rubbers in the latex, increasing amounts (1 g – 5 g) of HA latex concentrate were added to the determination of 2 ml standard TMTD solution. The absorbance readings at 430 nm were measured and plotted against the amount of latex used (*Figure 1*).

Thin Layer Chromatography of TMTD in LA/TZ Latex Concentrate and TZ Dispersion

Latex concentrate (200 g) was swollen in chloroform (200 ml) for 1h. Methanol was added until coagulation occurred. The chloroform-methanolic serum was decanted off and filtered through a Whatman No.1 paper. The filtrate was evaporated to dryness under vacuum at 50°C. The residue was re-dissolved in a small volume of chloroform and a small volume was spotted on a thin-layer plate of alumina together with reference spots of TMTD and ZDMC. The plate was developed in a solvent mixture of hexane : benzene : acetone (volume 20:2:5)[9], and then sprayed with 0.1% aqueous-methanolic cupric acetate after drying. TMTD and ZDMC present formed yellow brown spots. For the TZ dispersion a chloroform extract was concentrated and spotted on the TLC plate.

TABLE 2. ABSORBANCE READINGS OF 200 µg TMTD DETERMINED IN THE PRESENCE OF DIFFERENT MATRICES

Matrix	Absorbance
3 g HA latex concentrate	0.296
Methanolic serum from 3 g HA latex concentrate	0.285
Coagulum from HA latex concentrate	0.244
Soap purified rubber by ultra-centrifugation	0.218
TMTD only	0.203

RESULTS AND DISCUSSION

Breakdown of TMTD in Latex and TZ Dispersion

Thin layer chromatographic results of the chloroform extracts of commercially prepared TZ dispersions, both fresh (within 1-week-old) and old (6 weeks' old), showed a yellow brown spot of TMTD ($Rf = 0.50$) followed by a ZDMC spot ($Rf = 0.15$). This was not consistent with the reported observation that the TMTD in the dispersion decomposes within 30 min to essentially ZDMC[1]. TMTD was detected in the extracts of commercial LA/TZ latices but not ZDMC. The absence of ZDMC could probably be due to its breakdown during the extraction and concentration process[1]. For all practical purposes of monitoring the effective amount of preservative in the dispersion or latex, TMTD alone or in the company of its breakdown product ZDMC, could be expressed as an overall amount of TMTD.

Effect of Non–rubbers on TMTD Determination

Figure 2 shows a linear relationship of absorbance *versus* TMTD (μg) for the determination of TMTD. The regression equation (A) is given in *Table 3*. When the recoveries of TMTD, added to HA latex concentrate, were computed using this equation, an average recovery of 140% was observed (*Table 4*).

It was apparent that some volatile fractions or decomposition product fractions from the non-rubbers interfered with the determination, as was evidenced by the results in *Table 2*. The table shows that the absorbance reading of 200 μg TMTD, determined in the presence of soap purified rubber, was the lowest and was close to that for TMTD alone.

The study of the colour development using a mixture of the distillates from the blank determination of HA latex concentrate and that of TMTD, showed similar absorbance reading with the distillate from TMTD. This observation indicated that the interference was inherent in the decomposition stage of TMTD by phosphoric acid in the presence of non-rubbers.

The results from the determination of 2 ml standard TMTD solution, in the presence of increasing amounts of HA latex, showed that the optimum enhancement of absorbance reading was reached when 3 g of latex was present (*Figure 1*). The assessment of TMTD in latex concentrate was therefore empirically resolved by using a calibration in the matrix of 3 g HA latex concentrate shown in *Figure 2* as (b). The regression equation is shown in *Table 3* as *Compound b*.

Determination of Other Dithiocarbamyl Compounds

RPTD, a tetraalkylthiuram disulphide, like TMTD also required a calibration of the method in the matrix of HA latex concentrate for its assessment in latex. The calibration regression equation without a matrix is shown as *Compound c* in *Table 3*, while the calibration regression equation in the matrix of latex concentrate is given as *Compound d* in *Table 3*.

The analysis of the dialkyldithiocarbamates, ZDC and ZDMC, in latex was not interfered with by the non-rubbers. Equations for *Compounds e* and *f* (*Table 3*) give their respective calibration regression relationships.

Repeatability

A good repeatability of the method, with an SD = ± 3 μg, for the determination of TMTD in latex is shown in *Table 1*. For the other dithiocarbamyl compounds a repeatability within an SD = ± 4 μg was observed.

Recovery

Tables 5 and *6* show the recovery results of TMTD from 3 g LA/TZ latex concentrate and field latex, respectively. The recovery range in both cases was between 95% – 104%. This was achieved using latices from different production lots, showing that the variable non-rubbers content in the concentrate latices (1.4% – 1.8%) and field latices (2.0% – 2.5%) did not significantly affect the analysis.

TABLE 3. REGRESSION EQUATIONS FOR THE STANDARDISATION OF RPTD, ZDC, AND ZDMC DETERMINATION

Compound	Regression equation	Correlation coefficient (r)
a. TMTD	$A = \frac{1.013\,C}{10^3} - 0.006$	0.9998
b. RMTD (in the matrix of 3 g HA latex conc.)	$A = \frac{1.305\,C}{10^3} - 0.032$	0.9996
c. RPTD	$A = \frac{0.742\,C}{10^3} - 0.001$	0.9996
d. RPTD (in the matrix of 3 g HA latex conc.)	$A = \frac{0.980\,C}{10^3} - 0.009$	0.9987
e. ZDC	$A = \frac{1.014\,C}{10^3} - 0.020$	0.9992
f. ZDMC	$A = \frac{1.073\,C}{10^3} - 0.014$	0.9992

A = Absorbance; C = Amount of compound in µg

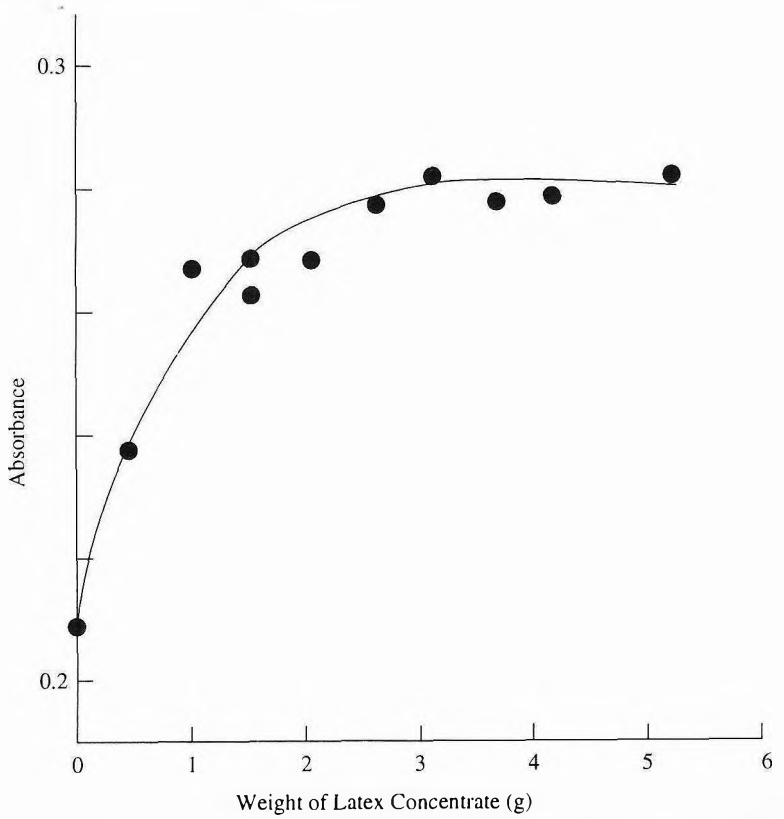

Figure 1. Effect of non-rubbers in latex on the analysis of TMTD.

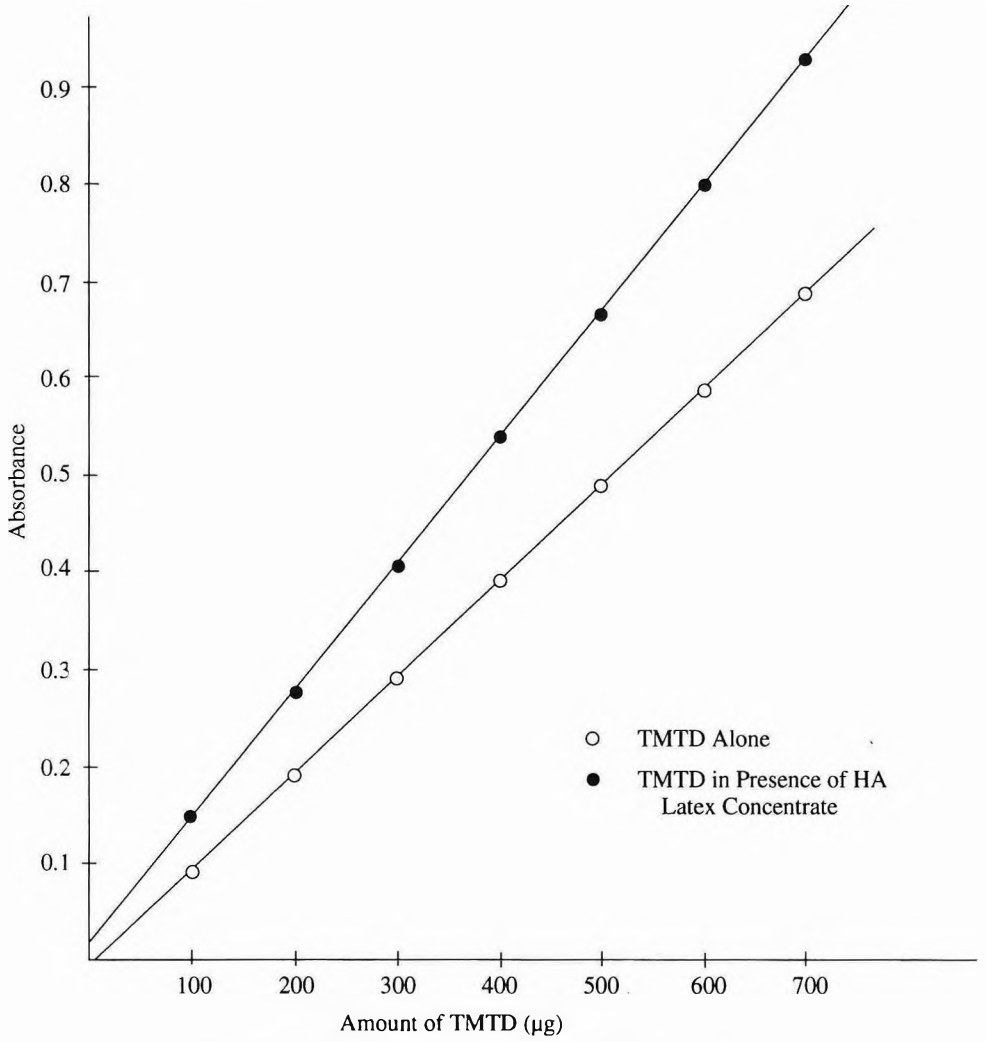

Figure 2. Calibration graphs for the analysis of TMTD.

TABLE 4. PERCENTAGE RECOVERIES OF TMTD FROM 3 G HIGH AMMONIA LATEX CONCENTRATE[a]

TMTD added to latex concentrate (μg)	TMTD recovered (μg)	Recovery (%)
100	158	158
200	298	149
300	430	143
500	683	137
700	944	135

[a]Using regression equation for *Compound a* in *Table 3*.

TABLE 5. RECOVERY OF TMTD ADDED TO 3 G LA/TZ LATICES

TMTD present (μg)	TMTD added (μg)	Total TMTD found (μg)	TMTD recovered (μg)	Recovery (%)
30	100	129	99	99
204	102	301	97	95
204	305	522	318	104
204	508	706	502	99
250	300	550	300	100
332	25	358	26	104
332	75	405	73	97
364	250	605	241	96

TABLE 6. RECOVERY OF TMTD ADDED TO 3 G LA/TZ FIELD LATICES

TMTD present (μg)	TMTD added (μg)	Total TMTD found (μg)	TMTD recovered (μg)	Recovery (%)
0	100	97	97	97
0	305	307	307	101
21	200	221	200	100
232	301	542	310	103

In the case of skim latex where the water content is around 96%, low recovery was observed due to the water affecting the colour intensity. However, if the volume of distillate and reagents was made to 100 ml with methanol instead of 50 ml, recoveries of over 90% were obtained when the amount of TMTD in the 3 g skim latex sample was 300 μg and above, as shown in *Table 7*.

Tables 8 and *9* show the recoveries of the other dithiocarbamyl compounds from latex to be in the 91% – 106% range.

Rate of Breakdown

Table 1 showed that the TMTD in the LA/TZ latex was unstable and decreased rapidly within 12 weeks to less than 20% of the initial amount[1]. A latex film, from 3 g LA/TZ latex concentrate, when stored for a number of days on the laboratory bench, was found to lose its TMTD content more rapidly than latex concentrate (*Table 10*).

CONCLUSION

The TMTD in the LA/TZ latex concentrate and the dispersion has been shown to break down to

ZDMC, which subsequently decomposes further as reported, but the detection of TMTD in the dispersion and the apparent absence of the break-down product ZDMC in the latex concentrate need further verification with reported observation[1]. For all practical purposes of process control in the determination of the TMTD content in the production of LA/TZ latex concentrate and its TZ dispersion, the TMTD, either alone or in the company of its break down product ZDMC, could be assessed as an overall amount of TMTD.

The carbon disulphide evolution method reported for the assessment of individual dithiocarbamyl compounds in latex affords a simple and practical procedure for the monitoring of such preservative addition in the production of latex concentrate. The interference from the non-rubbers in the determination of TMTD in latex was empirically resolved by carrying out the calibration in a matrix of HA latex concentrate.

TABLE 7. RECOVERY OF TMTD ADDED TO 3 G SKIM LATICES

TMTD added* (μg)	TMTD recovered (μg)	Recovery (%)
100	60	60
200	161	81
300	279	93
400	403	101
500	501	100
700	702	100

*Added to skim latex containing no TMTD

TABLE 8a. RECOVERY STUDIES ON THE DETERMINATION OF ZDC AND ZDMC IN HA LATEX CONCENTRATE

ZDC added* (μg)	ZDC recovered (μg)	Recovery (%)
	(Mean)**	
100	160	106
300	305	102
500	506	101
700	704	101

*Amount of ZDC added to 3 g latex concentrate containing no ZDC

**Mean of 2 tests, ± 4 μg ZDC

TABLE 8b. RECOVERY STUDIES ON THE DETERMINATION OF ZDC AND ZDMC IN HA LATEX CONCENTRATE

ZMDC added* (µg)	ZMDC recovered (µg)	Recovery (%)
	(Mean)**	
100	104	104
200	198	99
300	290	97
500	475	95
700	710	101

*Amount of ZMDC added to 3 g latex concentrate containing no ZMDC

**Mean of 2 tests, ± 4 µg ZMDC

TABLE 9. RECOVERY STUDY ON THE DETERMINATION OF RPTD IN AMMONIA PRESERVED LATEX CONCENTRATE AND FIELD LATEX

Sample	RPTD present (µg)	RPTD added (µg)	Total RPTD found (µg)	RPTD recovered (µg)	Recovery (%)
Concentrate	228	109	337	99	91
	228	217	445	211	97
	228	326	554	318	97
Field latex	0	105	97	97	94
	0	210	205	205	98
	0	315	312	312	99
	0	530	532	532	100

TABLE 10. EFFECT OF STORAGE OF LA/TZ LATEX CONCENTRATE FILMS ON TMTD CONTENT

Storage (days)	TMTD content (µg)	
	In latex film from 3 g LA/TZ latex concentrate	In 3 g LA/TZ latex concentrate
0	512	514
12	44	511

ACKNOWLEDGEMENT

The author thanks the Controller, Research and Development of Kumpulan Guthrie Berhad, for permission to publish this paper, and Dr A. Subramaniam, previously with the Rubber Research Institute of Malaysia, for the very constructive comments.

Date of receipt: October 1995
Date of acceptance: March 1996

REFERENCES

1. LOADMAN, M.J.R. AND TIDD, B.K. (1988) Chemical Analysis, *Natural Rubber Science and Technology (Roberts, A.D. ed.)*, 991 & 1033 – 1034. Oxford: Oxford University Press.

2. LOWEN, W.K. AND PEASE, H.L. (1964) Analytical Methods for Pesticides, Plant Growth Regulators and Food Additives *(Zweig, G. ed.), Vol.3,* 69.

3. CALLAN, T. AND STRAFFORD, N. (1924) *J. Soc. Chem. Ind.*, **43**, 1T.

4. PATTERSON, J.D. (1950) *J. Assoc. Off. Agr. Chem.*, **33**, 788.

5. CALLAN, T., HENDERSON, J.A.R. AND STRAFFORD, J. (1932) *J. Soc. Chem. Ind.*, **51**, 193T.

6. MEZONNET, R., BERGES, P. AND CUSTOT, F. (1974) *Anal. Abstr.*, **27**, 3648.

7. GORDON, C.F., *et al.* (1967) *J. Assoc. Off. Chem.*, **50(5)**, 1102.

8. HILLTON, C.L. AND NEWALL, J.E. (1958) *Rubber Age*, **83(6)**, 981.

9. OFFICIAL METHODS OF ANALYSIS OF THE ASSOCIATION OF OFFICIAL ANALYTICAL CHEMISTS (1984) 14th Ed. pp. 139 – 140 & 144.

10. VEKSHTEIN, M. SH. AND KLISENKO, M.A. (1971) *Anal. Abstr.*, **20**, 4071.

J. nat. Rubb. Res. **10(4)**, 266–275

Genotypic Variation in Non-steady State Photosynthetic Carbon Dioxide Assimilation of Hevea brasiliensis

A. NUGAWELA*#, S.P. LONG** AND R.K. ALUTHHEWAGE*

Under natural conditions, leaves of Hevea *plants often experience either continuous or fluctuating light levels. Thus, in this study three* Hevea brasiliensis *genotypes were compared for their response to such light environments, simulated in the laboratory. It is evident that genotypes differ in their ability to maintain steady CO_2 assimilation rates throughout the day, under constant saturating light. Similar differences were apparent in the ability to maintain the induction states under low light levels. Further, carbon losses could result due to the undershoot in CO_2 assimilation rate when light levels are suddenly reduced. Genotypic differences in such non-steady state behavior of CO_2 assimilation may contribute to differences in productivity.*

The rate of latex production in the latex vessels of *Hevea brasiliensis* Muell. Arg. (rubber tree) has been related to the supply of sucrose in the adjacent sieve tubes[1]. This suggests that economic yield in this crop may be closely linked to photosynthetic rate, the primary source of sucrose. This possible link has promoted examination of the potential of selecting higher yielding clones by screening for higher photosynthetic capacity[2–4]. However, previous studies of the relationship between photosynthesis and yield have failed to find any strong correlation[2–4]. These previous studies were concerned with steady-state light saturated rates of CO_2 uptake. However, this is not the only factor governing the daily rate of CO_2 assimilation by the whole canopy. Canopy size and organisation, light limited rates of photosynthesis, and non-steady state responses will all influence canopy rates. The present study concerns the last of these points: non-steady state responses. Light in a crop canopy changes continuously[5]. A mature *Hevea brasiliensis* plantation could receive either continuous high light during clear skies, continuous low light or fluctuating light levels during cloudy conditions. Even on days with clear skies light received by the leaves in the lower canopy could be highly variable and continually changing. For example, 50% – 80% of the light received in the under storey habitats of tropical forests is in the form of sun-flecks[6–8]. In a mature *Hevea brasiliensis* plantation, fluctuating light levels are common within and at the canopy surface and hence an understanding of the response of CO_2 assimilation by leaves to fluctuating light levels will be important in explaining variation in canopy rates of CO_2 gain. Given the rapid changes in light that will occur within a tree canopy in the field, any differences in the rapidity of adaptation between genotypes would have implications for canopy photosynthesis. Interspecific differences in photosynthetic responses to fluctuating light levels are reported for other species by Chazdon and Pearcy[9]. CO_2 assimilation rates and stomatal conductances at any given light level have been found higher earlier in the day than later, even though light levels may be the same[10]. There may be genotypic differences in the ability to maintain the initial steady-state CO_2 assimilation rates throughout the day under saturating light.

This study examines the possibility that non-steady state responses of CO_2 assimilation differ between *Hevea brasiliensis* genotypes.

*Sri Lanka Rubber Research Institute, Dartonfield, Agalawatta, Sri Lanka
**Department of Biology, University of Essex, Colchester CO4 35Q, United Kingdom.
#Corresponding author

Variation in rate with both continuous saturating light and during step changes in the light levels are investigated. *Hevea brasiliensis* is particularly appropriate for such a study since its cultivars are clones providing genetically identical replicates.

MATERIALS AND METHODS

Plant Material

Budded stumps of clones RRIC 100, RRIM 600 and PB 86 were grown in cement pots (diameter 45 cm). Manuring was done as recommended by the Rubber Research Institute of Sri Lanka[11]. When plants had grown to the 2–3 whorl stage, leaflets from the uppermost mature whorl were used for CO_2 assimilation rate measurements.

CO_2 Assimilation Rate Measurements

The response of the CO_2 assimilation rates of *Hevea brasiliensis* to continuous and fluctuating light were measured under controlled conditions in an open gas exchange system[12]. Atmospheric air from roof level (30 m) was drawn into the system through a 25 litre tank to buffer short term fluctuation in atmospheric CO_2 concentration, by a gas handling system (Series WA 161, ADC Ltd.. UK). A variable amount of air was passed through a magnesium perchlorate column to maintain a relative humidity of 65%. The flow rates of analysis and reference air streams were controlled and maintained at 500 ml min^{-1}, *via* a gas handling system (Series WA 161, ADC Ltd., UK). Flow meters were calibrated against a bubble flow meter[12].

A leaf section chamber (LSC, ADC Ltd., UK) was modified for use with the attached leaves. The area of the leaf exposed to light was constant at 10 cm^2. The leaf temperature was measured with a copper-constantan thermocouple pressed against the lower surface of the leaf and monitored with an electronic thermometer (Series 2001, Copper-Constantan, Comark Electronics Ltd., UK). The temperature in the leaf chamber was maintained at 30°C ± 1.5°C. A quartz-iodide light source (Model 250H, Scholly Fiberoptik, Denzlingen, Germany) was used to illuminate the leaf chamber. Photosynthetic photon flux density (IP) at the position of the leaf was varied by interposing neutral density filters in the light path. This was determined with a quantum sensor (LI-190SR, LI-Cor Ltd., Lincoln, Nebraska, USA) placed below the chamber window in the position normally occupied by the leaf. The CO_2 assimilation rate (A), stomatal conductance (gs) and internal leaf CO_2 concentration (c_i) were determined using the equations described by Long and Haellgren[12].

Response to Continuous Saturated Light

Three potted plants from each of the clones RRIC 100, RRIM 600 and PB 86 were taken and a leaflet from the upper most mature whorl was used from each plant for measurements. The A, gs and c_i were monitored under controlled conditions with saturating light, *i.e.* 1600 µmol m^{-2} s^{-1}, from 0700 h – 1700 h. These times were chosen to correspond to daylight hours and to avoid compliations that might result from any endogenous rhythm of stomatal opening.

Reponse to Short Term Variation in light

The speed with which the different genotypes responded to step increases in light (Ip), *i.e.* 200 – 400, 400 – 600, 600 – 900, 900 – 1600 µmol $m^{-2}s^{-1}$ and the equivalent step decreases were examined. Light levels were changed soon after steady rates were apparent. The undershoot in CO_2 uptake, commonly observed when light level is reduced (*Figure 1*) was also examined[13]. Three potted plants from each of the genotypes PB 86, RRIC 100 and RRIM 600, were selected for the study. Measurements were made using attached leaflets, under controlled conditions, using the open gas exchange system described earlier.

Leaves from the same plants used in the above study were allowed to attain steady state CO_2

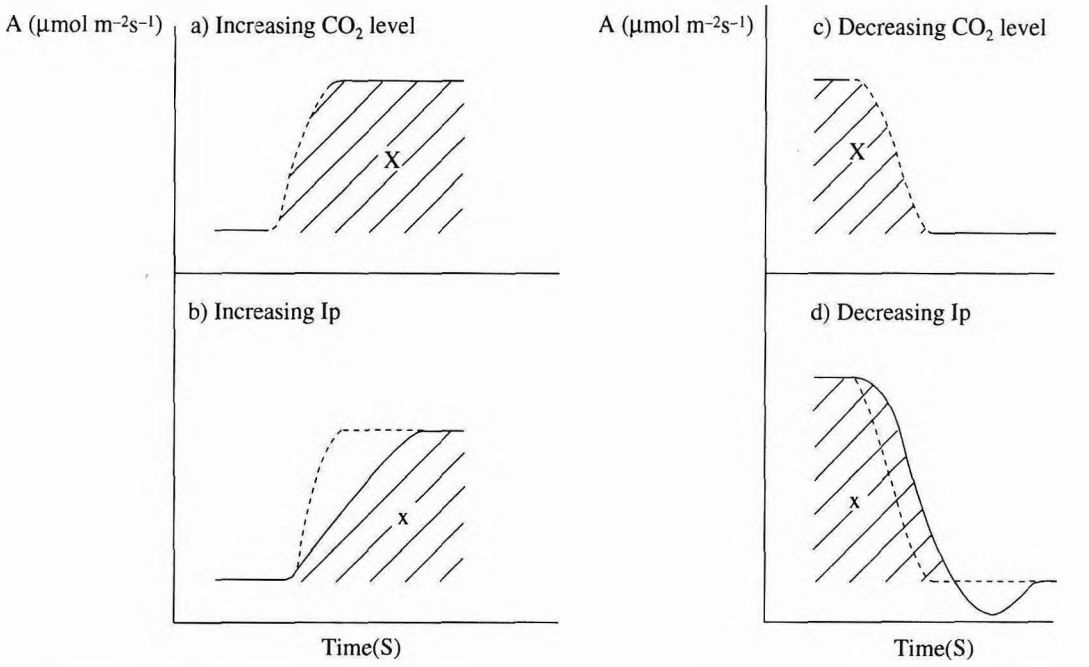

(a) Illustrates the time taken for the gas exchange system to respond fully to an increase in the CO_2 concentration across the chamber, produced artificially by introducing a flow of CO_2 rich air.

(b) Illustrates the increase in A with time following an increase in photon flux on a leaf in the chamber. By subtracting the area under curve up to steady-state rates following the increase in light level (area x) from system control (area X) the actual loss of CO_2 molecules fixed per unit area in μmol m^{-2}, can be computed. The percentage of this is given by:

$(X-x)/X$

(c) Similarly illustrates a simulated decrease in CO_2 assimilation produced by introducing a supply of CO_2-free air into the chamber. Note that there is no undershoot of the artificially simulated decrease in CO_2 uptake rate. The area under the curve up to a steady response illustrates the system response time.

(d) Illustrates the kinetics of change in A for a leaf with a step decrease in photon flux. The loss of potential CO_2 fixation over the period taken to attain steady-state rates since decrease in photon flux was calculated as explained above for a step increase.

Figure 1. Calculation of the loss of potential CO_2 assimilation due to the time taken for the leaf to adjust its photosynthetic rate to a new photon flux.

uptake at 600 μmol $m^{-2}s^{-1}$ and then the light level was lowered to 100 μmol $m^{-2}s^{-1}$ for different lengths of time, *i.e.* 30 s, 1 min, 2 min, 5 min, 10 min, 30 min and 60 min before returning Ip to 600 μmol $m^{-2}s^{-1}$. The speed with which the steady state photosynthesis was reached when returned to 600 μmol $m^{-2}s^{-1}$ was compared between the genotypes. Steady-state photosynthesis was considered to have been obtained if *A* varied less than 1% over a two minute period.

An apparent lag in the response of the leaf to a step change in light could be caused by the time taken to replace the air in the I.R.G.A. analysis cell in addition to the time required for physio-

logical adjustment by the leaf. To correct for this system error, a step change in CO_2 differential was produced by a gas diluter (Series GD 600, ADC Ltd., UK). The time taken for the system to respond fully to a 1 p.p.m. increase or decrease in CO_2 was 1.5 s and 2.5 s, respectively. The computations of CO_2 uptake loss due to the actual lag in response to light fluctuations and the undershoot in CO_2 assimilation rates when lowering light levels were made as described in *Figure 1*.

RESULTS

Response to Continuous Saturated Light

In all three clones, *A* reached a maximum within the first hour *i.e.* 0700 h – 0800 h, remained steady for a period before starting to decline slowly. The rate of decline in *A* from the maximum was least in clone RRIC 10 (*Table 1* and *Figure 2*). The *gs* changes in parallel despite the constant environmental conditions. The c_i remained unchanged during most of the period but began to increase slightly later in the day (*Figure 2*).

Response to Short Term Variation in Light

In all three clones, leaves in which photosynthesis had been fully induced responded rapidly to step changes in light. Nevertheless, a loss in CO_2 uptake is evident due to the rate of CO_2 assimilation (*A*) declining during the transient to a level below the steady-state *A* that is attained at the lower light level. The amount of CO_2 loss due to this undershoot in the rate of CO_2 assimilation, when calculated as a percentage (as described in *Figure 1*) is similar for all step-wise decreases in light in all genotypes (*Table 2*). The actual amount of potential CO_2 uptake lost decreased with decreasing magnitude of the step change in light (*Table 3*). The losses of potential CO_2 uptake are significantly different between clones ($F = 5.39$, $p < 0.05$) (*Table 2*), the losses being greatest in clone RRIC 100. The percentage losses are 5.8, 6.1 and 10.6 for clones PB 86, RRIM 600 and RRIC 100, respectively.

When a leaf in which photosynthesis is fully induced at 600 µmol $m^{-2}s^{-1}$ is exposed to short durations, *i.e.* 30 s, 1 min, and 2 min of low light (100 µmol $m^{-2}s^{-1}$) before returning to 600 µmol $m^{-2}s^{-1}$, the CO_2 assimilation rate increased almost instantly and regained the original steady-state value within 30 – 40 s. Exposing to low light for 5 min or more resulted in a lag in the response to increased to light (*Figure 3*). The resulting loss in CO_2 uptake increased with

TABLE 1. THE INITIAL AND MEAN VALUES OF CARBON DIOXIDE ASSIMILATION RATE, STOMATAL CONDUCTANCE AND INTERNAL LEAF CARBON DIOXIDE CONCENTRATION OF PB 86, RRIC 100 AND RRIM 600[a].

Clone	*A*(i)	*A*(m)	*gs*(i)	*gs*(m)	c_i(i)	c_i(m)
RRIM 600	13.5	10.1	0.29	0.21	255	255
PB 86	13.4	10.8	0.29	0.25	256	258
RRIC 100	13.3	12.1	0.35	0.30	269	264

[a] The gas exchange parameters were monitored under controlled conditions, *i.e.* Ip = 1400 µmol $m^{-2}s^{-1}$, Temperature = 30°C and a vapour pressure deficit (VPD) of >1.2 kPa, using attached leaves of pot plants.

A (µmol $m^{-2}s^{-1}$) = Carbon dioxide assimilation rate
gs (µmol $m^{-2}s^{-1}$) = Stomatal conductance
c_i (µmol mol^{-1}) = Leaf carbon dioxide concentration
(i) = Initial value (0800 h)
(m) = Mean values (0800 h – 1700 h)

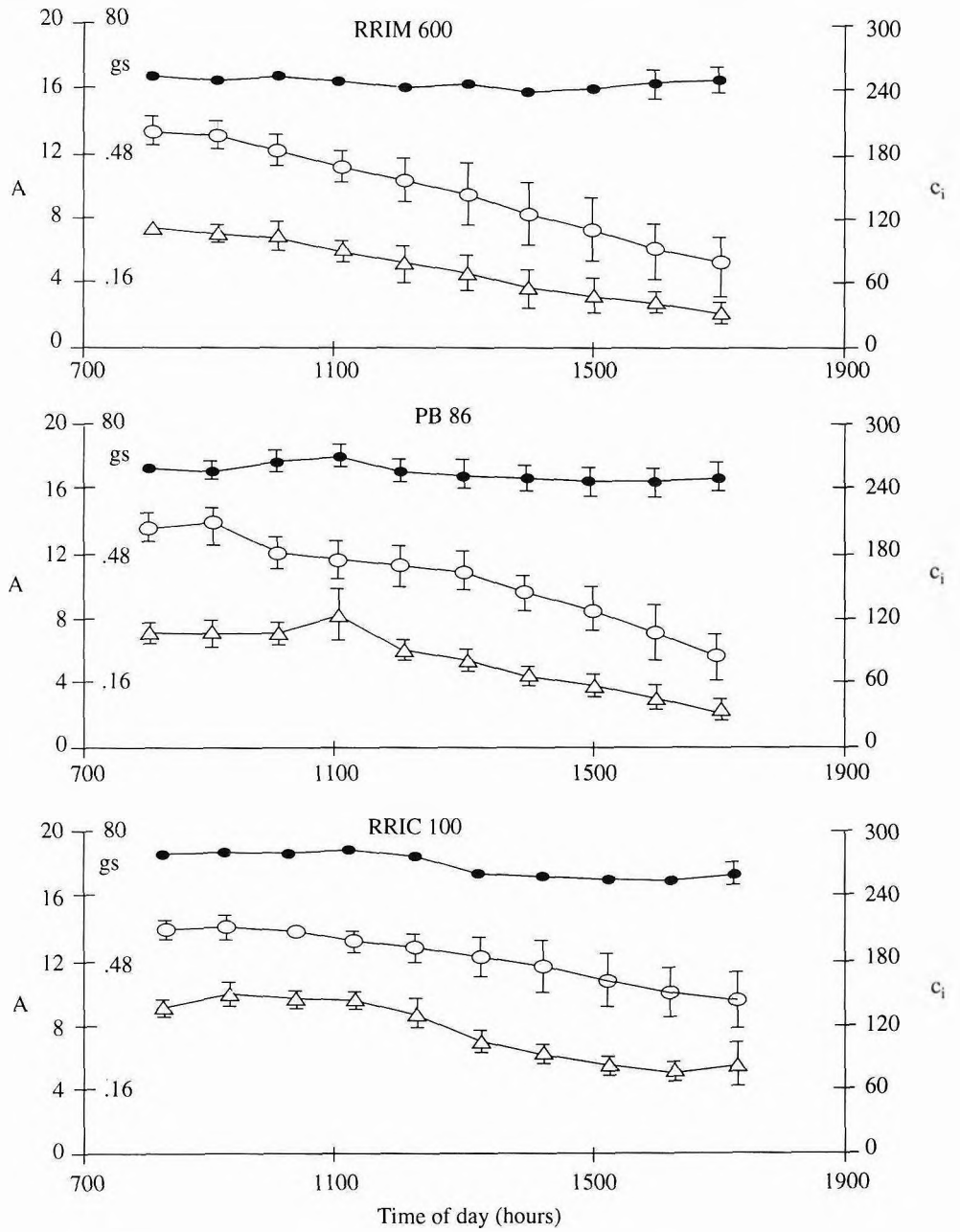

Figure 2. The variation in gas exchange parameters, i.e. *CO_2 assimilation rates,* A (○: *μmol $m^{-2}s^{-1}$*), *internal leaf CO_2 concentrations,* c_i (●: *μmol $m^{-2}s^{-1}$*) *and stomatal conductances,* gs (Δ: *μmol $m^{-2}s^{-1}$*) *of* Hevea brasiliensis *clones RRIM 600, PB 86 and RRIC 100 during the day. Measurements were made under controlled conditions,* i.e. *Ip = 1400 μmol $m^{-2}s^{-1}$, temperature = 30°C and a vapour pressure deficit (VPD)> 1.2 kPa using leaflets detached at different times, during the day from field grown plants. Each point is the mean of four observations and the vertical bars indicate the standard error of the mean.*

TABLE 2. THE PERCENTAGE LOSS IN POTENTIAL CO_2 UPTAKE CALCULATED BY COMPARING THE LOWER CO_2 ASSIMILATION RATES IN THE TRANSIENT PERIOD WITH AN IDEAL INSTANT RESPONSE TO A STEADY-STATE DURING STEP-WISE DECREASE IN LIGHT LEVELS IN GENOTYPES PB 86, RRIC 100 AND RRIM 600. THE TWO WAY ANALYSIS OR VARIANCE DETAIL

Source	Degree of freedom	Mean square	F ratio
Step changes	3	37.1	2.31^{ns}
Clones	2	86.6	5.39*
Step changes × clones	6	50.8	3.16*
Error	24	16.1	–

^{ns}Not significant at $P = < 0.05$

*$P = < 0.05$

TABLE 3. THE ACTUAL LOSS IN CO_2 UPTAKE CALCULATED BY COMPARING THE LOWER CO_2 ASSIMILATION RATES IN THE TRANSIENT PERIOD WITH AN IDEAL INSTANT RESPONSE TO A STEADY-STATE DURING STEP-WISE DECREASES IN LIGHT LEVELS[a]

Step change in *Ip* (μmol $m^{-2}s^{-1}$)	Actual CO_2 loss (μmol m^{-2})
1600–900	19.10
900–600	9.42
600–400	5.43
400–200	0.84

[a] Each value given is the mean of nine observations, three from each of the genotypes PB86, RRIC100 and RRIM 600.

Significance **
L.S.D. (5%) 6.1
**$P = < 0.01$

TABLE 4. THE CLONAL DIFFERENCE IN THE LOSS IN CO_2 UPTAKE CALCULATED BY COMPARING THE LOWER CO_2 ASSIMILATION RATES IN THE TRANSIENT PERIOD WITH AN INSTANT RESPONSE TO A STEADY-STATE DURING INCREASES IN LIGHT LEVEL[a]

Clone	% loss in CO_2 uptake
PB 86	19.8
RRIC 100	33.9
RRIM 600	42.9

[a] 100 to 600 μmol $m^{-2}s^{-1}$ (Each value given is the mean for low light periods of 5, 10, 30 and 60 min).

Significance *
L.S.D. (5%) 12.7
*$P < 0.05$

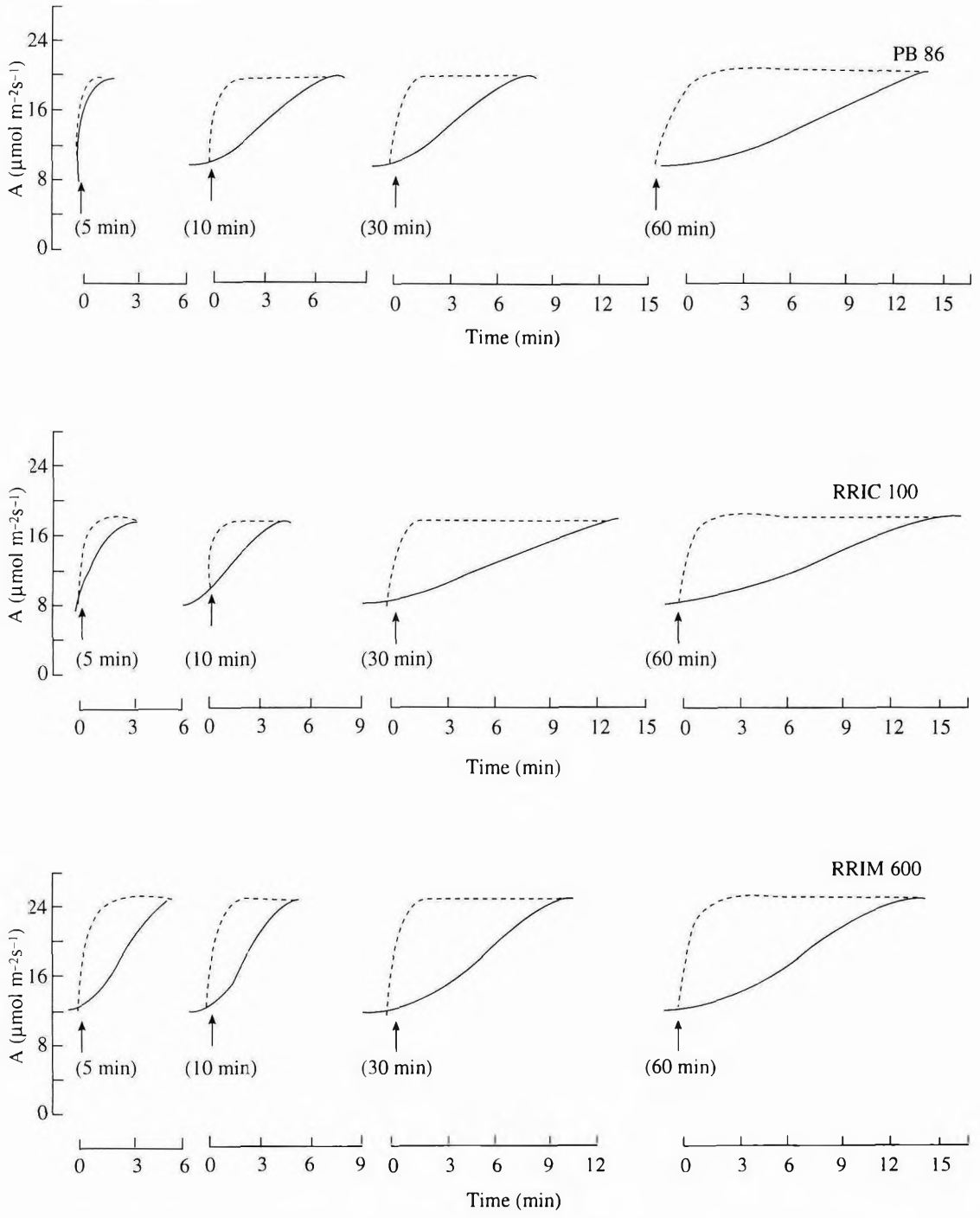

Figure 3. Induction of photosynthesis at high light (600 µmol $m^{-2}s^{-1}$), after being in low light (100 µmol $m^{-2}s^{-1}$) for different periods of time, as indicated. The dotted lines represent the IRGA response for similar depletions in CO_2 levels, created physically.

increasing time in the low light. The CO_2 uptake losses, estimated for the clone PB 86, RRIC 100 and RRIM 600, were significantly different ($F = 9.38$, $p < 0.05$) (*Table 4*) with clone PB 86 showing the smallest loss of CO_2 uptake.

DISCUSSION

The results showed that significant differences in non-steady state rates of leaf photosynthesis can occur between different clones of one crop species. When diurnal variation in gas exchange parameters of attached leaves of *Hevea brasiliensis* were monitored under constant and optimal conditions, CO_2 assimilation rates (A) and stomatal conductances (gs) showed a constant rate for the first two hours and then declined at a more-or-less constant rate throughout the remainder of the photoperiod (*Figure 2*). A similar pattern has been reported for wheat[14], Eucalyptus spp.[15] and for tree species in the mediterranean regions[15–16]. In these studies and in the present study c_i remained unchanged. This indicates that a restricted supply of CO_2 due to decreased gs may not be responsible for decreases in A. Furthermore, the steady values c_i obtained even when there was decreasing gs suggests the inability of the leaf to utilise the CO_2 entering the leaf, for photosynthesis. By measuring CO_2 assimilation rates at a c_i of 350 mol mol^{-1}, at different times during a cloudless day, Kuppers *et al.*[15] found it to decline with time of day. It can be concluded therefore that the decline in A is due to an increase in the mesophyll limitations rather than to an increase in the stomatal resistance. Parallel increase in gs may be due to less demand for CO_2 as a result of increase in the mesophyll limitations and to increase efficiency in water use. The inhibition of mesophyll activity responsible for lowered CO_2 assimilation rates is speculated to result either from an end product inhibition[14] or the involvement of a hormone, ABA[10,15,16]. Recently it has been shown that decline in CO_2 assimilation due to ABA, may be caused by an increase in the stomatal limitations[17]. In the past this was discounted as the cause for ABA induced lower CO_2 assimilation rates, because c_i remained constant despite of the decline in A. However, it is now known that an apparent constant c_i can be obtained yet stomata become increasingly limiting if closure occurs in patches[17]. If stomata closure occurs in patches, unconnected *via* the intercellular spaces, both gs and A will decline in similar magnitude but c_i will remain apparently unchanged as per the equation used in determining it. Further, the clones seems to differ inthe pattern in which A declines with time of day. Decline is least marked in clone RRIC 100 when compared with clones PB 86 and RRIM 600 (*Figure 2* and *Table 1*). Earlier studies on comparative gas exchange rates indicate that clone RRIC 100 has a lower mean daily CO_2 assimilation rate than the other two clones[18]. This would make development of feed-back inhibition slower in this genotype if capacity for translocation is similar. Alternatively, this genotype may have a higher capacity for metabolism of photosynthate to sucrose and a higher translocation rate of sucrose so decreasing the potential for feed-back inhibition.

The results also indicate the limitations of screening crop genotypes for increased photosynthetic capacity based on A_{sat} measurements at one point in time. At the beginning of the photoperiod steady-state A_{sat} does not differ significantly between genotypes. However, by the end of the photoperiod, A_{sat} in RRIM 600 was only 60% of the rate in RRIC 100 (*Figure 2*).

In leaflets in which photosynthesis had been fully induced, the rate of CO_2 uptake responded rapidly to step-wise increases and decreases in light, in all three clones. Similar rapid response to light-flecks by leaves in which photosynthesis is fully induced are reported by Chazdon and Pearcy[9].

Nevertheless, in all three clones when light levels were lowered, step-wise, an undershoot in A was apparent before reaching the steady state rate of the subsequent low light level. Similarly, an undershoot in CO_2 assimilation rate following a reduction in light level has been reported for *Alocasia macrohiza* and *Toona australis*, two Australian rainforest species[13]. The lower A following a reduction in Ip represents a loss of CO_2 uptake. For the *Hevea brasiliensis* clones studied, the estimated percentage loss of CO_2 uptake caused by a reduction in Ip is independent

of the magnitude in the change of the light level. Nevertheless, the actual loss of CO_2 uptake varies with the magnitude in change of light level (*Table 3*). The lower CO_2 assimilation rates, following step-wise lowering of light levels resembles the post-illumination CO_2 burst in C3 species. Post-illumination CO_2 burst is considered to reflect the photorespiratory activity of the leaf in the preceding light period and has been used as a measure of the photorespiratory rates of leaves[19]. The genotypic differences in the loss of CO_2 uptake were significant (*Table 2*).

When *Hevea brasiliensis* leaves in which photosynthesis was fully induced at 600 µmol $m^{-2}s^{-1}$ are exposed to low light for periods longer than 5 min, it resulted in an apparent loss in the induction state of the leaves, *i.e.* the capacity of the leaf to utilise high light levels. The loss of induction state was proportional to duration in low light (*Figure 3*). Leaves in low light, *i.e.* 100 µmol $m^{-2}s^{-1}$, for 60 min needed *ca.* 10 min – 15 min. of high light for photosynthesis to be fully induced again. The ability to maintain the state of induction varies with species. *Alocasia macrorhiza* required more than 60 min of continuous exposure to low light conditions, *i.e.* 10 µmol $m^{-2}s^{-1}$ to lose the induction state[9]. The ability to maintain relatively high states of induction during long periods of low light will enable the leaf to utilise periods of high light, *e.g.* as sun-flecks, more effectively. The CO_2 uptake loss due to the lag in reaching steady-state rates is significantly less in PB 86 (*Table 4*). To illustrate the possible significance of the losses under non steady-state conditions, the loss of potential CO_2 fixation by sun leaves due to the loss in induction state from a low light period, *e.g.* if the light level dropped to 100 µmol $m^{-2}s^{-1}$ from 600 µmol $m^{-2}s^{-1}$ for 30 min due to cloud cover was estimated. The amounts are 1215, 1727 and 1920 µmol m^{-2} for genotypes PB 86, RRIC 100 and RRIM 600 respectively, and this emphasises the importance of the non steady-state responses and genotypic differences. The induction requirement for maximum photosynthetic rates is an intrinsic feature of photosynthesis. The processes that occur during induction are poorly understood, but it is believed that induction is primarily associated with photochemical reaction[20].

There is evidence to show that *Hevea brasiliensis* clones differ in their ability to maintain CO_2 assimilation rates under constant saturating light. Further, it is evident that the genotypes differ in their response to fluctuating light. Thus, it is apparent that significant difference in non-steady state CO_2 assimilation rates exist amongst the *Hevea* genotypes studied. These differences may also contribute to the genotypic differences in productivity.

ACKNOWLEDGEMENT

The authors wish to acknowledge the Food and Agricultural Organisation of the United Nations for funding this project.

Date of receipt: February 1995
Date of acceptance: September 1995

REFERENCES

1. TUPY, J. (1985) Some Aspects of Sucrose Transport and Utilization in Latex Producing Bark of *Hevea brasiliensis*. *Biol. Planta (Prugue)* **27(1)**, 51.

2. SAMSUDDIN, Z., TAN, H. AND YOON, P.K. (1985) Variations, Heritabilities, Correlations of Photosynthetic Rates, Yield and Vigour in Young *Hevea* Seedling Progenies. *Proc. Int. Rubb. Conf. 1985 Kuala Lumpur,* **3**, 137.

3. CEULEMANS, R., GABRIELS, R., IMPENS, I., YOON, P.K., LEONG, W. AND NG, A.P. (1984) Comparative Study of Photosynthesis in Several *Hevea brasiliensis* Clones and *Hevea* Species under Tropical Field Conditions. *Trop. Agric.*, **6(14)**, 273.

4. NUGAWELA, A. AND ALUTHHEWAGE, R.K. (1988) Clonal Differences in Growth and Gas Exchange Parameters of Young *Hevea* Buddings and their Relation to

Field Performance. *Proc. Colloque. Hevea 88, IRRDB, Paris.* 451.

5. ORT, D.R. AND BAKER, N.R. (1988) Consideration of Photosynthetic Efficiency at Low Light as a Major Determinant of Crop Photosynthetic Performance. *Plant Physiol. and Biochem.* **26(4)**, 555.

6. BJORKMAN, O. AND LUDLOW, M.M. (1972) Characterization of the Light Climate on the Floor of a Queensland Rainforest. *Carnegie Inst. Washington Year Book*, **71**, 85.

7. Pearcy. R.W. (1983) The Light Environment and Growth of C3 and C4 Species in the Understorey of a Hawaiian Forest. *Oecologia (Berlin)*, **58**, 19.

8. CHAZDON, R.L. AND FETCHER, N. (1984) Photosynthetic Light Environments in a Lowland Tropical Rain Forest of Costa Rica. *J. Ecol.* **72**, 553.

9. CHAZDON, R.L. AND PEARCY, R.W. (1986) Photosynthetic Responses to Light Variation in Rain Forest Species. 1. Induction Under Constant and Fluctuating Light Conditions. *Oecologia (Berlin)* **69**, 517.

10. KUPPERS, M., MATYSSEK, R. AND SCHULZE, E.D. (1986) Diurnal Variations of Light Saturated CO_2 Assimilation and Intercellular Co_2 Concentration are not Related to Leaf Water Potential. *Oecologia*, **69**, 477.

11. YOGARATNAM, N. (1980) Fertilizers to Rubber. In *Advisory Circular No. 85, Rubber Research Institute of Sri Lanka.* Colombo: Ceylon Printers Ltd.

12. LONG, S.P. AND HAELLGREN, J.E. (1985) Measurement of CO_2 Assimilation by Plants in the Field and the Laboratory. *Techniques in Bioproductivity and Photosynthesis (J.Coombs, D.O.Hall, S.P. Long and J.M.O. Scurlock eds.* 62. Oxford: Pergamon Press.

13. CHAZDON, R.L. AND PEARCY, R.W. (1986) Photosynthetic Responses to Light Variation in Rain Forest Species. 2. Carbon Gain and Photosynthetic Efficiency During Light Flecks. *Oecologia (Berlin)*, **69**, 524.

14. AZCON-BEITO, J. (1983) Inhibition of Photosynthesis by Carbohydrates in Wheat Leaves. *Plant Physiol.* **73**, 681.

15. KUPPERS, M., WHEELER, A.M., KUPPERS, B.I.L., KIRSCHBAUM, M.U.F. AND FARQUHAR, G.D. (1986) Carbon Fixation in Eucalyptus in the Field. *Oecologia*, **70**, 273.

16. BURSCHKA, C., LANG, O.L. AND HARTUNG, W. (1985) Effect of Abscisic Acid on Stomatal Conductance and Photosynthesis in Leaves of Intact *Arbutus unedo* Plants under Natural Conditions. *Oecologia.* **67**, 593.

17. DOWNTON, W.J.S., LOVEYS, B.R. AND GRANT, W.J.R. (1988) Stomatal Closure Fully Accounts for the Inhibition of Photosynthesis by Abscisic Acid. *New Phytol.* **108**, 263.

18. NUGAWELA, A. (1989) Gas Exchange Characteristic of *Hevea* Genotypes and their Use in Selection for Crop Yield. Thesis submitted to the University of Essex for the Degree of Doctor of Philosophy.

19. LUDLOW, M.M. AND JARVIS, P.G. (1971) Photosynthesis in Sitka Spruce *(Picea sitchensis).* 1. General Characteristics. *J. App. Ecol.* **8**, 925.

20. EDWARDS, G. AND WALKER, D. (1983) *C3, C4 Mechanisms and Cellular and Environmental Regulation of Photosynthesis*, 542. Berkeley: University of California Press.

J. nat. Rubb. Res. **10(4)**, 276–282

An Economic Analysis of the Commencement Time for Tapping Rubber by Smallholders in Imperata *Areas of Indonesia*

P.G. GRIST*# AND K. M. MENZ*

A bioeconomic model for estate rubber is modified to apply to conditions facing Indonesian smallholders in low fertility Imperata *areas. The economic component of the model is updated using prices and costs prevailing in South Sumatra in 1995. The modifications to the model are briefly described, then used to analyse the decision of when tapping should commence. It is shown that smallholders who tap prior to recommended minimum tapping girths are acting logically. Early commencement of tapping is consistent with maximising economic returns over the life of the plantation, even though there is a sacrifice in terms of total rubber yield.*

Bioeconomic modelling is a powerful tool for analysing issues of this type, where the undertaking of long run biophysical experiments is prohibitively expensive.

Smallholder rubber production in many parts of Indonesia is characterised by poor growing conditions (low fertility soils and a high level of competition with weeds such as *Imperata*), and poor plant stock (genetic material). These poor growing conditions lead to low growth rates of trees planted by smallholders. The recommended rubber tree girth for tapping to commence is 45 cm[1] (under good growing conditions), but smallholders commonly commence tapping at girths around 40 cm, down to nearly 30 cm[2]. The preference for early tapping comes from the desire to obtain income as soon as possible. Due to their low income levels, smallholders are more likely than estates to have a preference for earlier tapping.

In this paper, an analysis is made of the economic trade-offs that are involved in the timing of the decision by smallholders to commence tapping. In undertaking this analysis, a modified version on the BEAM rubber agroforestry model is used. The designers of the BEAM model encouraged subsequent users to adapt and apply the model to particular situations of interest. This has been done with a focus on the smallholder rubber producing sector of Indonesia which is often characterised by low tree growth rates. The work reported is part of a broader ranging study on the prospects for tree growing in *Imperata* areas of Southeast Asia.

The BEAM Rubber Agroforestry Model

The BEAM rubber agroforestry model, RRYIELD[3], was developed by the University of Wales, Bangor. It is one of a series of bioeconomic agroforestry models[4]. The latex yield, timber and intercrop output can be determined for a number of bioclimatic, topographical and silvicultural regimes. The model was designed to represent conditions in rubber estates (*i.e.* it was not designed to represent smallholder conditions). The RRYIELD model is linked to an economic model RRECON[5], which determines the economic returns from the rubber plantation. These models are useful as extension tools — supplying farmers with information on the viability of rubber intercropping systems.

*Centre for Resource and Environmental Studies, The Australian National University, Canberra ACT 0200, Australia
#Corresponding author

The models can also provide information on the best combination of inputs for efficient use of resources such as labour and land. They are also useful for research — enabling 'experiments' to be conducted over both time and space. Such experiments would otherwise be prohibitively expensive.

The RRYIELD model was modified to represent smallholders in poor growing conditions (such as *Imperata* areas), and improve the model specifications. A summary of the modifications is given below. A full description of the modifications, and the reasoning behind them, is given in more detail elsewhere[6].

Modifications to the Model

The most pervasive variable within the model is tree girth. It provides a building block for many of the functions in the BEAM model. Girth features as a variable in equations for height, canopy width and wood volume (and also latex in the modified model).

Girth itself is a function of tree age, density and site conditions[4]. The function that relates these variables to girth is based on information from DeJonge[7] and Westgarth and Buttery[8] (referring to a *tapped* tree in an estate situation). Tree age and density provide the general shape of the function, while changing site conditions shift the girth function vertically[4].

Girth calculation. From the girth function, girth increment is calculated annually, then added to the previous year's girth. This allows *annual* changes in the parameters of the girth equation to be represented. (This was not possible in the original BEAM model).

Girth/tapping relationships. The girth at which tapping commences is a key element affecting the output of a rubber plantation. An assumption, underlying the girth equation in the original version of the BEAMR RYIELD model, is that tapping *will commence* at a girth of 45 cm (commonly recommended as the tapping commencement girth in estates).

The option to choose when tapping commences was added to the model. The approach taken in modifying the model was to subtract from, or add to, girth increment, according to whether tapping occurs before or after 45 cm. Tapping prior to 45 cm will reduce girth increment, compared to that determined in the original BEAM model. Tapping after 45 cm will increase girth increment compared to that determined in the original BEAM model.

The estimates of relative changes in girth increment, as a result of tapping, were derived from a study by Templeton[9]. For a small sample of RRIM 600 and RRIM 500 clones, Templeton calculated the girth increment of a tapped tree as a percentage of the girth increment of an untapped tree (58.7%). This is the only *direct* relationship between tapping and girth increment that was found in the literature.

However, support for the magnitude of this difference can be obtained by combining information from Simmonds[10] and Shorrocks *et al.*[11] Simmonds established, for tapped and untapped trees, the difference in annual dry shoot weight increment. Shorrocks *et al.* provided a relationship to translate this difference in annual dry shoot weight increment into a girth increment.

From Simmonds:

$$W = W_p (1-k) \qquad \ldots 1$$

where: W = annual dry shoot weight increment in a tapped stand

W_p = annual dry shoot weight increment in an untapped stand

k = proportion of dry shoot weight increment partitioned towards latex

$1-k$ = dry shoot weight increment unrealised because some of the assimilates are partitioned towards latex.

Simmonds found the annual dry shoot weight increment of a tapped tree to be about half (*i.e.* $k = 0.49$) the annual dry shoot weight increment of an untapped tree.

In order to convert this difference in dry shoot weight increment to a difference in girth increment, the Shorrocks *et al.*[11] equation was used. Transposing this equation, such that girth is the dependent variable:

$$G = 8.51862\ W^{0.36} \qquad \ldots 2$$

where: G = girth (cm)
W = dry shoot weight (kg).

By combining the above two relationships, the effect of tapping on tree girth was calculated. Annual girth increment was found to be reduced by 50% through tapping. This reduction approximates, and is thus supportive of the relationship found by Templeton, (*i.e.* the girth increment of a tapped tree is 58.7% the girth increment of an untapped tree). Thus the Templeton relationship was chosen for calculating changes in girth increment, as a result of commencing tapping at different times.

Inverting the Templeton relationship (*i.e.* 1/0.587 = 1.7), it is found that the girth increment of an untapped tree is 170% of the girth increment of a tapped tree. Thus for untapped trees the girth increment equation, in the modified BEAM model, is multiplied by 1.7. This is done every year that a tree is not tapped after reaching a girth of 45 cm.

Conversely, when a tree is tapped prior to reaching 45 cm, the reduction in girth increment (as a result of tapping) is 41.3% (*i.e.* 1 - 0.587 = 0.413) of the girth increment derived in the original BEAM model. This figure is subtracted from the girth increment in the original BEAM model for every year that a tree is tapped prior to reaching a girth of 45 cm.

These modifications to the model provide the option to choose tapping commencement time. Subsequently, the economic and biophysical consequences of various tapping commencement times can be assessed.

Latex Yield

The original BEAM latex yield equation has a constant factor of 2000. This is then converted into the latex yield per hectare *via* a series of indices. The key adjustment index is for planting material, altering the yield relative to the clone RRIM 600. The index for wildlings (trees from unselected seedlings used by smallholders) is expected to be significantly lower than the latex yield of trees used by estate farmers (such as RRIM 600). This conclusion is supported by Barlow and Murharminto[12], who suggest an average rubber yield of approximately 600 kg/ha/year for non-project smallholder producers in Indonesia. Thus, in calibrating the model to represent the smallholder situation, this index ('inadj' in the latex yield equation) was reduced to one third of the original value in BEAM.

Other factors which affect the latex yield include tree density, tree age and site condition. Changes in the density of the rubber plantation will effect both: the number of trees available to be tapped, thus the amount of latex collected, per hectare; and, the rubber yield per tree, due to the change in the level of competition between trees.

The age index reflects the relatively lower latex yields achieved in the early years of tapping. The site index reflects the effect of environmental factors on the growth rate of the tree and thus on latex yield. Full details are available in the original BEAM documentation[4].

The overall *shape* of the BEAM latex yield equation seems to accord with information from scientific literature and producer surveys. However, the equation did not explicitly represent yield as a function of girth and therefore cannot capture the effects of some important management practices. Many studies have shown that there is a strong

relationship between latex yield and girth of rubber trees[1,13,14,15].

The BEAM latex yield equation was modified to directly include the *girth variable*. While maintaining the original shape of the latex yield function, a relationship between latex yield and *girth* was estimated. All other components of the latex yield equation remain the same. Thus, a variable expression (30 × girth, where girth is in cm) was substituted for the original constant value (2000). The new latex yield equation became:

$$\text{Latex Yield} = 30 * \text{girth} * \frac{\exp(\text{tapping year}/0.5)}{1 + \exp(\text{tapping year}/0.5)} * \frac{(\text{site index})}{100} * \text{inadj} * \frac{(\text{density})^{0.7}}{400} \quad \ldots 3$$

where: girth = tree girth in cm
tapping year = number of years since tapping commenced
site index = an index of the climate and soil characteristics and their impact on latex yield, for a given site
inadj = index of planting stock
density = number of trees per hectare.

Experiments with the Model

Using the modified model, described above, and in more detail elsewhere[6], a number of simulation experiments were performed. These involved changing tapping commencement girth (and by implication, the year that tapping commenced). The corresponding changes to the monetary present value of income streams were noted. In arriving at the present value figures, different discount rates were used. This enabled a test of sensitivity of the conclusions to these changes in discount rates. The planting density in all experiments was 400 trees/ha. A site index of 75 was used to represent an average site index for smallholders in *Imperata* areas of Indonesia. Cost and revenue factors, necessary to calculate economic returns in the model, were obtained from the Palembang region of South Sumatra in 1995.

RESULTS

Tree Girth at Tapping Commencement

The presentation of results begins with outputs from model runs, using a real discount rate of five percent (*Figure 1*). From an economic viewpoint, the optimal girth for commencement of tapping was found to be 35 cm,

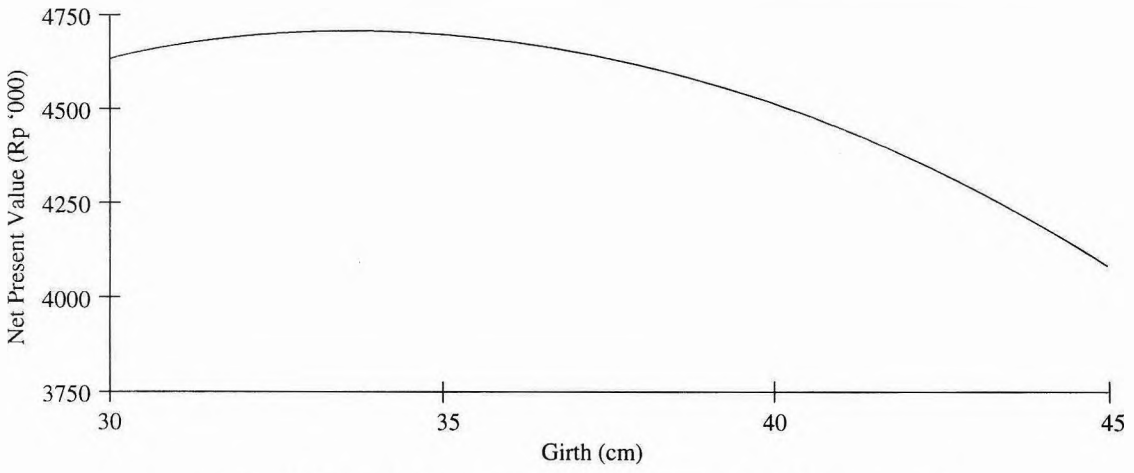

Figure 1. NPV from different tapping commencements (5% discount rate).

which for the smallholders under consideration here is equivalent to a tree age of 10 years. With commencement of tapping at 35 cm girth, total income (in present value terms) is maximised. If tapping commences at less than 35 cm, tree growth, and latex flows are reduced, outweighing the early returns from latex. Alternatively, if tapping commences after 35 cm, the faster tree growth, and increased latex yields, are insufficient to offset delays in the receipt of income.

The balance of revenue flows is influenced by the choice of discount rate. As discount rates increase, optimal tapping commencement is at lower girths. This is in line with the intuitive result — higher discount rates enhance the value of income flows in early years. The net effect of these forces on the girth at tapping commencement is shown in *Figure 2*.

The difference in economic returns between tapping commencement at a girth of 35 cm and other girths such as 30 cm and 40 cm (equivalent to years 8 and 13 respectively) is in the order of 5%, as shown in *Figure 1*. Although not shown here, the model results were consistent in this regard over a range of discount rates (*i.e.* the sensitivity of the present value of income streams to changes in the girth at tapping commencement is not great and is usually under 10%). Given this low sensitivity, short term demands for cash are likely to speed up commencement of tapping.

Economic *versus* Physical Optimum

Choosing the best girth for tapping commencement involves a trade-off between tree growth and commencement of income receipts. Maximum revenue (in present value terms) occurs when tapping commences at 35 cm, but maximum *latex yield* occurs when tapping commences at 45 cm. Faster tree growth, resulting from delayed tapping, will provide a greater total latex yield over the life of the tree. A comparison of the total latex yield from different girth at tapping commencement is presented in *Table 1*.

The sensitivity of total latex yield to different tapping commencement girths, is substantial, but the resulting net present values of income flows do not differ as much. For example, total latex yield increases 30% by allowing tree girth to increase from 30 cm to 45 cm prior to commencement of tapping. Thirty percent is well above the corresponding percentage change in net present value of income (*Figure 1*).

The difference between the total latex yield and its present monetary value is embodied in the discount factor applied to future income

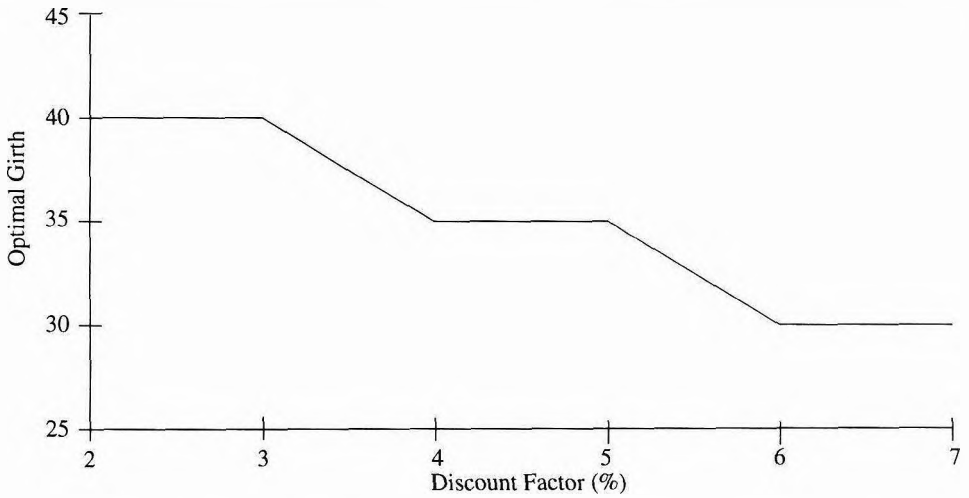

Figure 2. Optimal girth for tapping to commence (various discount rates).

TABLE 1. AGE, NPV AND LATEX YIELD FOR VARIOUS TAPPING COMMENCEMENTS

Age (years)	Girth of tree at tapping commencement (cm)	Latex yield over the life of the plantation ('000 ka/ha)	NPV (Rp '000 @ 5%)
8	30	10.2	4600
10	35	11.6	4700
13	40	12.9	4500
16	45	13.3	4100

streams. In the case examined here, cash costs are assumed to be negligible. Therefore present value is simply total latex yield multiplied by its per unit value, then discounted.

CONCLUSION

For trees managed under a low intensity smallholder regime, commencement of rubber tapping at 45 cm girth gives the maximum latex yield over the life cycle of the plantation. However, advice to smallholders to delay tapping to 45 cm in order to increase total latex yields will be contrary to their economic interests. Earlier tapping, at 35 cm, gives a greater economic return in today's dollars and is consistent with the short term demands for cash flow typical of smallholders.

Bioeconomic modelling is a powerful tool for analysing issues of this type, where the undertaking of long run biophysical experimentation is prohibitively expensive. Indeed maintenance of appropriate treatment controls for an experiment of this type would be virtually impossible, irrespective of cost. The BEAM rubber agroforestry model is a convenient and efficient tool for analysing relatively complex bioeconomic issues. The modified BEAM model and documentation is available from the authors.

ACKNOWLEDGMENTS

This work was conducted under the auspices of the project entitled: *Improving Smallholder Farming Systems in* Imperata *Grassland Areas of Southeast Asia: A Bioeconomic Modelling Approach.* The project has received substantial funding assistance from the Australian Centre for International Agricultural Research (ACIAR) and the Center for International Forestry Research (CIFOR).

Date of receipt: November 1995
Dta of acceptance: March 1996

REFERENCES

1. DIJKMAN, D.J. (1951) *Thirty Years of Research in the Far East.* Miami: University of Miami Press.

2. GOUYON, A. AND NANCY, N.C. (1989) Increasing the Productivity of Rubber Smallholders in Indonesia: A Study of Agro-economic Constraints and Proposals. *Proc. Rubb. Res. Inst. Malaysia Rubb. Grow. Conf. Malacca 1989.*

3. THOMAS, T.H., WILLIS, R.W., BEZKOROWAJNYJ, P.G., SANGKUL, S. AND NG, A.P. (1993) *RRYIELD:* A Bioeconomic Agroforestry Model. *The BEAM Project School of Agricultural and Forest Sciences, University of Wales, Bangor, Gwynedd, UK.*

4. THOMAS, T.H., WILLIS, R.W., BEZKOROWAJNYJ, P.G., SANGKUL, S. AND NG, A.P. (1993) A Compendium of Technical Overviews for the BEAM Spreadsheet Models: TANZMOD, RRYIELD, POPMOD and ROWECON4. *The BEAM Project, School of Agricultural and Forest Sciences, University of Wales, Bangor, Gwynedd, UK.*

5. WILLIS, R.W., THOMAS, T.H., WOJTKOWSKI, P.A., BEZKOROWAJNYJ, P.G., SANGKUL, S. AND NG, A.P. (1993) RRECON: *A* Bioeconomic Agroforestry Model. *The BEAM Project School of Agricultural and Forest Sciences, University of Wales Bangor, Gwynedd, UK.*

6. GRIST, P.G., MENZ, K.M. AND THOMAS T.S. (1995) A Modified Version of the BEAM Rubber Agroforestry Model: Smallholders in Indonesia. Imperata *Project Paper 1995/3, CRES, ANU Canberra.*

7. DEJONGE, P. (1961) Tapping of Young Rubber. *Plrs' Bull. Rubb. Res. Inst. Malaysia No. 56*, 149.

8. WESTGARTH, D.R. AND BUTTERY, B.R. (1965) The Effect of Density of Planting on the Growth, Yield and Economic Exploitation of *Hevea brasiliensis* Part1: The Effect on Growth and Yield. *J. Rubb. Res. Inst. Malaysia,* **19**, 62.

9. TEMPLETON, J.K. (1969) Partitioning of Assimilates. *J. Rubb. Res. Inst. Malaysia,* **21**, 259.

10. SIMMONDS, N.W. (1981) Some Ideas on Botanical Research on Rubber. *Trop. Agric.* **59**, 2.

11. SHORROCKS, N.W., TEMPLETON, J.K. AND IYER, G.C. (1965) Mineral Nutrition, Growth and Nutrient Cycle of *Hevea brasiliensis* III. The Relationship Between Girth and Dry Shoot Weight. *J. Rubb. Res. Inst. Malaysia,* **19**, 85.

12. BARLOW, C. AND MUHARMINTO (1982) The Rubber Smallholder Economy. *Bull. Indon. Econ. Stud.*, **18**, 86.

13. ONG, S.H. (1981) Correlations Between Yield, Girth and Bark Thickness of RRIM Clone Trials. *J. Rubb. Res. Inst. Malaysia,* **29**, 1.

14. NARAYANAN, R. AND HO, C.Y. (1973) Clonal Nursery Studies in *Hevea* II. Relationship Between Yield and Girth. *J. Rubb. Res. Inst. Malaysia,* **23**, 332.

15. NGA, B.H. AND SUBRAMANIAM, S. (1974) Variation in *Hevea brasiliensis* I. Yield and Girth Data of the 1937 Hand Pollinated Seedlings. *J. Rubb. Res. Inst. Malasyia,* **24**, 69.

ERRATA

Changes in some Physiological Latex Parameters in Relation to Over-exploitation and the Onset of Induced Tapping Panel Dryness

*[J. nat. Rubb. Res., Volume **10(3)**, page 189]*

The y-axis should be calibrated from 0 to 140 Invertase units and not as shown.

ORDER FORM

JOURNAL OF NATURAL RUBBER RESEARCH

Please send to

The Secretary
Editorial Committee
Journal of Natural Rubber Research
Rubber Research Institute of Malaysia
P.O. Box 10150
50908 Kuala Lumpur, Malaysia

Name: .....
(Please print)

Address: .....
.....
.....
.....

No. of copies required: .....

Volume/Issue: .....
.....
.....
.....
.....

Form of remittance: Cheque/Bank Draft/Postal Order/Money Order No. .....
payable to 'Rubber Research Institute of Malaysia' (please include bank commission, if applicable). Amount: RM/US$ .....

Date: ..... Signature: .....

Journal Price

	Local	Abroad
Per issue	RM30	US$15
Per volume (4 issues)	RM100	US$50

Postage (other countries only)

	Surface mail	Airmail
Per issue	US$2	US$6
Per volume (4 issues)	US$8	US$25

JOURNAL OF NATURAL RUBBER RESEARCH

·ope

The **Journal of Natural Rubber Research** publishes results of research and authoritative reviews on all aspects of natural bber.

Contributions are welcome on any one of the following topics: Genetics, Breeding and Selection; Tissue Culture and egetative Propagation; Anatomy and Physiology; Exploitation: Tapping Systems and Stimulation; Agronomic Practices d Management; Nutrition and Fertiliser Usage; Soils: Classification, Chemistry, Microbiology, Use and Management; iseases and Pests; Economics of Cultivation, Production and Consumption and Marketing; Mechanisation; Biochemistry d Biotechnology; Chemistry and Physics of Natural Rubber; Technology of Dry Rubber and Latex; Natural Rubber ·ocessing and Presentation, Product Manufacture, End-uses and Natural Rubber Industrialisation; Tyres; NR and SR ends; and, Effluent Treatment and Utilisation.

The Editorial Committee, in accepting contributions for publication, accepts responsibility only for the views expressed members of the MRRDB and its units.

:st Paper Award

Papers submitted to each volume of the **Journal** will be considered for the annual **Best Paper Award** which carries a cash ize of 1000 ringgit and a certificate. The decision of the Editorial Committee and publisher of the **Journal** on the award ll be final.

ıbmission of Articles

General. Manuscripts should be submitted double-spaced throughout on one side only of A4 (21.0 x 29.5 cm) paper and nform to the style and format of the **Journal of Natural Rubber Research.** Contributions, to be submitted in four copies ıe original and three copies) should be no longer than approximately ten printed pages (about twenty double-spaced ɔewritten pages). Intending contributors will be given, on request, a copy of the journal specifications for submission of pers.

Title. The title should be concise and descriptive and preferably not exceed fifteen words. Unless absolutely necessary, ientific names and formulae should be excluded in the title.

Address. The author's name, academic or professional affiliation and full address should be included on the first page. All rrespondence will be only with the first author, including any on editorial decisions.

Abstract. The abstract should precede the article and in approximately 150-200 words outline briefly the objectives d main conclusions of the paper.

Introduction. The introduction should describe briefly the area of study and may give an outline of previous studies with pporting references and indicate clearly the objectives of the paper.

Materials and Methods. The materials used, the procedures followed with special reference to experimental design and alysis of data should be included.

Results. Data of significant interest should be included.

Figures. These should be submitted together with each copy of the manuscript. Line drawings (including graphs) should in black on white drawing paper. Alternatively sharp photoprints may be provided. The lettering should be clear. Half-ıe illustrations may be included. They should be submitted as clear black-and-white prints on glossy paper. The figures ould be individually identified lightly in pencil on the back. All legends should be brief and typed on a separate sheet.

Tables. These should have short descriptive titles, be self-explanatory and typed on separate sheets. They should be as ncise as possible and not larger than a Journal page. Values in tables should include as few digits as possible. In most cases, ɔre than two digits after the decimal point are unnecessary. Units of measurements should be SI units. Unnecessary breviations should be avoided. Information given in tables should not be repeated in graphs and *vice versa.*

Discussion. The contribution of the work to the overall knowledge of the subject could be shown. Relevant conclusions ould be drawn, and the potential for further work indicated where appropriate.

Acknowledgements. Appropriate acknowledgements may be included.

References. References in the text should be numbered consecutively by superscript Arabic numerals. At the end of the .per, references cited in the text should be listed as completely as possible and numbered consecutively in the order in which ey appear in the text. No reference should be listed if it is not cited in the text. Abbreviations of titles of Journals should llow the **World List of Scientific Periodicals.**

Reprints. Twenty-five copies of Reprints will be given free to each author. Authors who require more reprints may obtain em at cost provided the Chairman or Secretary, Editorial Committee is informed at the time of submission of the manuscript.

orrespondence

All enquiries regarding the **Journal of Natural Rubber Research** including subscriptions to it should be addressed to the ɔcretary, Editorial Committee, Journal of Natural Rubber Research, Rubber Research Institute of Malaysia, P.O. Box 10150,)908 Kuala Lumpur, or 260 Jalan Ampang, 50450 Kuala Lumpur, Malaysia.


INSTITUT PENYELIDIKAN GETAH
RUBBER RESEARCH INSTITUTE